UNIVERSITAT POLITÈCNICA DE CATALUNYA

DOCTORAL THESIS

Structural damage monitoring based on machine learning and bio-inspired computing

---

Author:
Jaime VITOLA OYAGA

Advisors:
Dr. Francesc POZO MONTERO
Dr. Diego A. TIBADUIZA BURGOS

**UNIVERSITAT POLITÈCNICA
DE CATALUNYA
BARCELONATECH**

UPC

CoDAlab - Control, Dynamics and Applications
Department of Civil and Environmental Engineering

Barcelona, Spain
October, 2020

Abstract

Structural damage monitoring based on machine learning and bio-inspired computing

by Jaime VITOLA OYAGA

Advisors: Dr. Francesc POZO MONTERO - Dr. Diego A. TIBADUIZA BURGOS

For a few decades, systems for supervising structures have become increasingly important. This evolution has gone from, the strategies had as a goal only the detection of damages. Furthermore, now monitoring the civil or military structures permanently and offering sufficient and relevant information helping make the right decisions. The SHM is applicable, carrying out preventive or corrective maintenance decisions, reducing the possibility of accidents, and promoting the reduction of costs that more extensive repairs imply when the damage is detected early. The current work focused on three elements of diagnosis of structural damage: detection, classification, and location, either in metallic or composite material structures, given their wide use in air, land, maritime transport vehicles, aerospace, wind turbines, civil and military infrastructure. This work used the tools offered by machine learning and bio-inspired computing. Given the right results to solve complex problems and recognizing patterns. It also involves changes in temperature since it is one of the parameters that influence real environments' structures. Information of a statistical nature applied to recognizing patterns and reducing the size of the information was used with tools such as PCA (principal component analysis), thanks to the experience obtained in works developed by the CoDAlab research group. The document is divided into five parts. The first includes a general description of the problem, the objectives, and the results obtained, in addition to a brief theoretical introduction. Chapters 2, 3, and 4 include articles published in different journals. Chapter 5 shows the results and conclusions. Other contributions, such as a book chapter and some papers presented at conferences, are included in appendix A. Finally, appendix B presents a multiplexing system used to develop the experiments carried out in this work.

Resumen

Monitorización de daños en estructuras basada en machine learning y computación bio-inspirada

Por Jaime VITOLA OYAGA

Directores: Dr. Francesc POZO MONTERO - Dr. Diego A. TIBADUIZA BURGOS

Desde hace algunas décadas los sistemas para supervisar estructuras han tenido cada vez más relevancia. En esta evolución se ha pasado de estrategias que tenían como meta sólo la detección de fallas a otras que buscan monitorizar permanentemente las estructuras bien sean éstas civiles o militares, ofreciendo información suficiente y pertinente que incide positivamente en el momento de tomar buenas decisiones, dentro de las cuales cabe destacar por ejemplo, las orientadas a realizar mantenimientos preventivos o correctivos si es del caso, reduciendo la posibilidad de accidentes, además de propiciar la disminución de costos que implican las reparaciones más extensas cuando el daño se logra detectar de manera temprana. El presente trabajo se enfocó en tres elementos de diagnóstico de daños en estructuras, siendo estos en particular la detección, clasificación y localización, bien sea en estructuras metálicas o de material compuesto, dado su amplio uso en vehículos de transporte aéreo, terrestre, marítimo, aeroespacial, aerogeneradores, infraestructura civil y militar. Se utilizaron las herramientas que ofrecen el aprendizaje automático (machine learning) y la computación bio-inspirada, dados los buenos resultados que han ofrecido en la solución de problemas complejos y el reconocimiento de patrones. Involucranto cambios de temperatura dado que es uno de los parámetros a los que se ven enfrentadas las estructuras en ambientes reales. Se utilizó información de naturaleza estadística aplicada al reconocimiento de patrones y reducción del tamaño de la información con herramientas como el PCA (análisis de componentes principales), gracias a la experiencia lograda en trabajos desarrollados por el grupo de investigación CoDAlab.

El documento está dividido en cinco capítulos. En el primero se incluye una descripción general del problema, los objetivos y los resultados obtenidos, ademas de un breve introducción teórica. Los Capítulos 2,3 y 4 incluyen los artículos publicados en diferentes revistas. En el Capítulo 5 se realiza una presentación de los resultados y conclusiones. En el Anexo A se incluyen otras contribuciones tales como un capítulo de libro y algunos trabajos presentados en conferencias. Finalmente en el anexo B se presenta el diseño de un sistema de multipliexación utilizado en el desarrollo de los experimentos realizados en el presente trabajo.

Acknowledgements

The current thesis is the result of the work of many people. I would like to express my gratitude to my advisors: Francesc Pozo Montero and Diego Alexander Tibaduiza Burgos, for their permanent orientation to guide this work.

I also like to extend my gratitude to to all the members of CoDAlab research group, Miguel Angel Torres, Maribel Anaya Vejar, for their collaboration.

To Santo Tomas University, in special to Electronics Engineering Faculty and the MEM research group, thank you very much for the support in all these years of work.

God, for being present on every path that I have traveled in my life. All my friends, parents and family. To my wife Laly, to be patient and accompany me in every step I have taken in my life.

Contents

List of Figures

List of Tables

List of Abbreviations

k-**NN**	*k*-nearest neighbors algorithm
PCA	Principal Component Analysis
PZT	Lead-zirconate-titanate
SHM	Structural Health Monitoring
CFRP	Carbon fibre-reinforced plastic.
db8	Daubechies.
DWT	discrete wavelet transform.
h-NLPCA	Hierarchical non-linear principal component analysis.
ML	Machine learning.
MLP	Multilayered perceptron.
mm	Millimetres.
MSE	Mean square error.

Chapter 1

Introduction

Contents

1.1 Introduction

The Structural Health Monitoring (SHM) has a wide field of application in civil and military constructions, and its goal is to evaluate structures but avoiding any change in its characteristics [1.1], to determine its conditions, and obtain judgment elements that can qualify the health or functionality, with the interest of issuing a concept about the risks that its use may bring.

Even more, with the data collected in the time, the system can historically follow up on the changes in the structure, facilitating its evaluation or opening the possibility of studying the gradual deterioration of the structure, being able to predict its wear associated and extrapolate its useful life. [1.2].

Motivation

One of the most important motivations for SHM is safety, because reducing the risks associated with the use of structures, the damages, natural wear, deterioration for lack of maintenance, can increase the probability of accidents [1.3]. SHM also brings with it other associated benefits such as can positively impact decisions around maintenance processes, reduction of maintenance times, or times in which the structures are not operational [1.4],which redounds in economic benefits[1.5, 1.6].

Finally and not least, SHM has decidedly led to the development of smart materials and structures, that promise to facilitate and make monitoring more efficient [1.7].

The original proposal of Rytter [1.8], established four levels for the identification of damage in structures, the first that is the detection only foresee whether or not the damage is present, the second the location in which is determined the position the third that classification that can particularize the type of damage, and the last determination of severity, a fifth element that would be the prognosis that gives aspects of judgment on the stability of the structure and its time of safe use [1.9].

The field of application is very wide; also the types of materials like, timber structures [1.10], composite [1.11], metallic [1.12], concrete (bridges [1.13] and buildings [1.14]), for recent structures [1.15] but also contributes to the preservation of historical structures[1.16], static structures [1.17] or in movement [1.18], on the earth [1.19], air [1.20], sea [1.21], and the space [1.7].

1.2 Objectives

1.2.1 General objectives

Develop a damage monitoring system that integrates the detection, location, and classification of these in metal structures or composite material, using machine learning and bio-inspired computing techniques.

1.2.2 Specific objectives

1. Study and evaluate the use of Machine Learning in structural damage monitoring applications.

2. Verify the most relevant techniques of bioinspired computing in the monitoring of damage to structures.

3. Develop a methodology for the detection of damage in structures.

4. Develop a methodology for the classification of damage in structures.

5. Develop a methodology for the location of damage in structures.

6. Perform experimental laboratory tests with scaled structures to validate the effectiveness of the methodologies subject to different temperature levels and, if necessary, do the corresponding compensation.

1.3 General results and contribution

To fulfill the proposed objectives, study about machine learning and bio-inspired algorithms was performed, this study includes the use and review of some techniques for data reduction, digital signal processing, and physics of wave propagations, also structural health monitoring theory. The results were presented in three journal articles, a book chapter, and various scenarios, such as five conferences and workshops. These made it possible to disclose the developments associated with each objective in the following way.

Below is a brief review of each of the objectives achieved.

Study and evaluate the use of Machine Learning approaches in structural damage monitoring applications.

The use of machine learning in structural health monitoring is a novelty approach; in the actuality are applied to a variety of techniques of this field to find solutions to the main problems in civil and military structures. In particular, the support machines, decision trees, k-nearets neighbor were reviewed, offering some better results than others, depending on the different types of tasks and preprocessing.

Verify the most relevant techniques of bioinspired computing in the monitoring of damage to structures.

The problems that SHM faces are mostly complex and complicated to address, which is why it uses different approaches to find a solution; one of them is to imitate the way nature faces its challenges. Bioinspired algorithms are analogies in hardware and software of biological systems; some of the most popular are artificial neural networks that seek to behave like their natural similes. In the current work, this strategy was applied in discrete classification solutions and also in continuous solutions (regression) of location.

Develop a methodology for the detection of damage in structures.

Determining the presence or not of a damage in a structure is the lowest category or level I of information according to Rytter's damage identification levels [1.8]. The solutions in SHM are circumscribing with the safety, but also with the maintenance; it is there that being able to rule

out the presence or not of the damage becomes extremely important. Several methodologies were developed to determine the presence or not of damage with the use of some machine learning and bio-inspired computing strategies. Since it is a subproblem of classification, it was developed in union with the following objective.

Develop a methodology for the classification of damage in structures.

In the classification of damages, not only information about the presence of the damage is provided, in this case, the damage must be related to a category, in the current work some activities covering this and the previous item were developed. The methodologies involve the application of machine learning techniques and bioinspired algorithms, in particular neural networks, decision trees, nearest neighbors, vector support machines, and some modifications that seek to improve accuracy such as boosting, bagged trees. These techniques were applied on composite material, aluminum plate. It is important to indicate that Principal Component Analysis and Hierarchical Nonlinear Principal Component Analysis were used for data reduction.

- A sensor data fusion system based on k-nearest neighbor pattern classification for structural health monitoring applications Authors Jaime Vitola, Francesc Pozo, Diego Tibaduiza, Maribel Anaya, Publication date: 2017, Jse desarraron algunas actividades que cubren este y el anterior item.ournal: Sensors MDPI, Volume: 17, Issue: 2, Pages 14 Publisher Multidisciplinary Digital Publishing Institute.

- Data-Driven Methodologies for Structural Damage Detection Based on Machine Learning Applications Authors: Jaime Vitola, Maribel Anaya Vejar, Diego Alexander Tibaduiza Burgos, Francesc Pozo Publication date: 2016/12/14, Book: Pattern Recognition-Analysis and Applications: Publisher: IntechOpen

- A damage classification approach for structural health monitoring using machine learning Authors Diego Tibaduiza, Miguel Ángel Torres-Arredondo, Jaime Vitola, Maribel Anaya, Francesc Pozo, Publication date: 2018, Journal: Pages 18 Publisher Hindawi.

- Damage classification based on machine learning applications for an unmanned aerial vehicle Authors: Maribel Anaya Vejar, Hernan Ceron, Jaime Vitola Oyaga, Diego Alexander Tibaduiza Burgos, Francesc Pozo Montero Publication date: 2017, Conference: IWSHM 2017: 11th International Workshop on Structural Health Monitoring: Stanford, California: September 12-14, 2017: proceedings book, Pages: 2042-2049.

- Non-linear damage classification based on machine learning and damage indices Authors: Diego Tibaduiza, Miguel Angel Torres, Jaime Vitola Oyaga, Maribel Anaya Vejar and Francesc Pozo Montero Publication date: 2017, Conference: IWSHM 2017: 11th International Workshop on Structural Health Monitoring: Stanford, California: September 12-14, 2017: proceedings book, Pages: 2042-2049.

- A machine learning methodology for structural damage classification in structural health monitoring Authors: Francesc Pozo Montero, Diego Alexander Tibaduiza Burgos, Maribel Anaya Vejar, Jaime Vitola Oyaga Publication date: 2017, Conference: SMART 2017: ECCOMAS Thematic Conference on Smart Structures and Materials: Madrid, Espanya: June 5-8, 2017: proceedings book. Pages: 698-708.

- Structural Damage detection and classification based on Machine learning algorithms Authors: Jaime Vitola Oyaga, Diego Alexander Tibaduiza Burgos, Maribel Anaya Vejar, Francesc Pozo Montero Publication date: 2016, Conference: Proceedings of the 8th European Workshop on Structural Health Monitoring

Develop a methodology for the location of damage in structure.

The location of damages offers an additional level of information, can deliver the place exact or area depending on the resolution of the methodology, the sensors quantity, and type, the noise level, and others. This work uses a lamb wave exploration mechanism and neural networks and decision trees that support this objective, this was presented in the following conference.

- Damage Localization Methodology using Pattern Recognition and Machine Learning Approaches Authors: Maribel Anaya Vejar, Hernan Ceron, Jaime Vitola Oyaga, Diego Alexander Tibaduiza Burgos, Francesc Pozo Montero Publication date: 2017, Conference: IWSHM 2017: 11th International Workshop on Structural Health Monitoring: Stanford, California: September 12-14, 2017: proceedings book, Pages: 2042-2049.

Perform experimental laboratory tests with scaled structures to validate the effectiveness of the methodologies subject to different temperature levels and, if necessary, do the corresponding compensation.

Since the structures are subject to temperature changes by the direct action of the environment, determining the immunity of the methodologies to these conditions is very important given that parameters such as attenuation, the signal-to-noise ratio, and others strongly affect the surface waves. Placement the pieces understudy in a climatic chamber, tests were carried out with temperature changes in steps of five Celcius degrees, verifying that the flexibility of the algorithms used in the present work with adequate training that starts from presenting the conclusive examples can absorb these changing conditions.The results were presented at the publication related below.

- Distributed piezoelectric sensor system for damage identification in structures subjected to temperature changes Authors Jaime Vitola, Francesc Pozo, Diego Tibaduiza, Maribel Anaya, Publication date: 2017, Journal: Sensors MDPI, Volume: 17, Issue: 6, Pages 18 Publisher Multidisciplinary Digital Publishing Institute.

1.4 Theoretical Background

An SHM system has two well-differentiated elements; one of them is the acquisition hardware or measurement system that is in charge of collecting, organizing, and storing the information depending on the type of variable or variables to be monitored. And the second is the processing system that extracting the data of interest depending on the pursuit objective. It is essential to mention that some systems can be transmitting various kinds of data, directly the sensors data, data processed in some grade, only processed data, and pure data no processed when the processing is remote.The other is the processing system for this exit two

The other system is the processing unit, for which there is a wide variety of possibilities such as microprocessors[1.22], microcontrollers[1.23], embedded systems [1.24], programmable logic devices [1.25], Graphic unit processors (GPUs) [1.26], Digital signal processors (DSP)[1.22], and distributed systems [1.27].

These systems using algorithms that make use of methodologies that seek to answer the questions for which SHM systems are designed and answer the most relevant questions that can be had around a method to know the state of a structure, being these: Is there damage? Where is it located? What type of damage is it? Is it severe? And finally, how much useful life does it have and under what conditions? [1.28, 1.9].

There are two perspectives; the first includes the creation of a mathematical model called model-based, and the second is the data-driven based, on the last one is not build a model, but instead, used algorithms like pattern recognition in order to find an answer the questions [1.29].

The present work makes use of a measurement system with active piezoelectric sensors to explore the surface of metal or composite structures using surface lamb wave, with a data-driven approach. For processing reduces information using principal component analysis (PCA) Hierarchical Non-Linear Principal Component Analysis h-NLPCA, also Wavelets in order to extract characteristics and after use machine learning algorithms included bioinspired algorithms, specifically artificial neural networks (ANN) to detect, classify and localize damages in metallic and composite material structures.

1.4.1 SHM measurement system

The SHM measurement system is a set of elements that allows obtaining information of a feature or attribute of a component or structure under observation, giving it a quantitative or qualitative value that qualifies it. Search a correspondence between the granted values and the described properties. Also, it is essential to note that the human being is part of the measurement system, and can contribute positively but also be a source of errors, even fully automatic systems. In general, systems for monitoring damage to structures have one of the two architectures presented below. In the first, only sensors are added to the structure and took the

information. It is the case, for example, of some types of bridge monitoring in which the sensors obtain information on the mechanical frequencies present in it, and by searching for Small changes in these frequencies and their comparison can derive their health state. Second, there are the excitation signal systems with excitation signal, from the signal obtained, can infer how the structure responds to it. In this case, analyzing the return information seeks to identify the presence or not of a particular situation [1.30].

The most relevant elements of the basic model of a structural health monitoring system with excitation signal are:

- The excitation system that fulfills the function of generating some stimulus, mechanical, thermal, magnetic, light, or others to show the damage, is subdivided into:

  - Signal generator: can be an arbitrary wave or a conventional signal generator. It is responsible for delivering the signal form necessary for the transducer to produce the relevant stimulus.

  - Signal conditioning system: it is a mechanism that can include amplification and impedance coupling, fulfills the function of acting as a link between the generation system and the sensor or transducer.

  - Transducer: is the mechanism that takes the signal delivered by the previous system and translates it into a stimulus signal for the part under inspection.

- The acquisition system, which fulfills the function of obtaining the information, is composed of:

  - Signal conditioning system: it is a mechanism that can include amplification, filtering, and impedance coupling, fulfills the function of obtaining the signal of interest in the least distorted way possible and the best conditions.

  - Digitization system: it fulfills the function of converting the analog signal to a digital one. This digital version is interpretable by the processing systems.

- The processing system, which interprets the output signal based on the input signal and its interaction with the object under study, can be analog or digital, in the same way, it could include storage, presentation, and transmission. Portability and computational load management considerations they are pertinent elements to this system; in the digital case, they can build with microprocessors [1.31], microcontrollers [1.32], programmable logic devices [1.33] or digital signal processors [1.34].

1.4.2 Lamb waves

During the last decades, the use of lamb waves plate-like structures has been of great interest to the SHM, given its characteristics such as presenting low attenuation in metallic structures and the ability to detect small damages, the low cost of its implementation.[1.35].

Based on the work of Lord Rayleigh, Horace Lamb published his discovery in 1917, due to the complexity of the equations that describe them, it was not until the 50s and 60s that new works made their application feasible [1.36].

The lamb waves are superficial waves that propagate in thin plates, with dispersive characteristics. This waves are susceptible to the surface state; they attenuate increased with the imperfections found in his propagation path.

Following the development in [1.36] and [1.37], in these works using the displacement potentials method, founded on Helmholtz decomposition, the equation that describes the behavior of a lamb wave in a homogeneous plate is 1.1 :

$$\frac{tan(qh)}{tan(ph)} = \frac{4k^2 qp\mu}{(\lambda k^2 + \lambda p^2 + 2\mu p^2)(k^2 - q^2)} \tag{1.1}$$

Making the corresponding replacements shown in equations 1.2 and 1.3:

$$p^2 = \frac{\omega^2}{c_L^2} - k^2 \tag{1.2}$$

$$q^2 = \frac{\omega^2}{c_T^2} - k^2 \tag{1.3}$$

In which ω is circular frequency,λ wavelength, and k is the wavenumber and is defined by 1.4 :

$$k = \frac{2\Pi}{\lambda} \tag{1.4}$$

c_L is the wave velocity of longitudinal mode and is defined by:

$$c_L = \sqrt{\frac{2\mu(1-\nu)}{\rho(1-2\nu)}} \tag{1.5}$$

c_T is the wave velocity of transversal mode and is defined by:

$$c_T = \sqrt{\frac{\mu}{\rho}} \tag{1.6}$$

Performing the appropriate manipulations with the interest of separate into two equations that only consider the symmetric case and the antisymmetric case:

$$\frac{tan(qh)}{tan(ph)} = -\frac{4k^2 qp}{(k^2 - q^2)^2} \tag{1.7}$$

$$\frac{tan(qh)}{tan(ph)} = -\frac{(k^2 - q^2)^2}{4k^2qp} \tag{1.8}$$

The resulting equations are known as the Rayleigh-Lamb equations for symmetric 1.7 mode for antisymmetric mode 1.8.

The figure 1.1 shows the antisymmetric wave mode in this mode predominant radial movement of particles adapted of [1.36].

FIGURE 1.1: Antisymetric wave mode

Figure 1.2 shows the antisymetric wave mode.

FIGURE 1.2: Antisymetric wave mode

1.4.3 Piezoelectric sensors in SHM system

Piezoelectric sensors build to take advantage of the effect of piezoelectricity, this word comes from the Greek word piezo which means pressure [1.38]; this effect is presented in some crystals when mechanical stress is applied to them, generating a potential difference and their ends. This reciprocal effect also occurs when the electric field is applied to some crystals and these deform. The piezoelectrics are widely applied in SHM systems and using a wide range of frequencies, although recently they have aroused much interest in the generation of energy [1.39]. In SHM, there are two types of ultrasonic systems that use piezoelectric sensors, first is the pulse-echo; in this, the same probe is actuator and sensor. The second scheme is through-transmission; a transmission probe generates the signal and sends to the inspection piece, and a sensor receives the signal and gives it to the digitalization system [1.40].

The piezoelectric materials can be found naturally in nature such as quartz crystals and others, but there are also ferroelectrics such as lithium nitrate which, after being subjected to polarization, acquire this property [1.38].The commercials ones generally are piezoceramic like Pb(Zr–Ti)O3 lead zirconate titanate (PZT) [1.41], .

In piezoelectric sensors application to explore damage to structures, these sensors are usually attached to the structures under study, since they are easy to install. However, in other cases, they are built into the material and are part of the structure. Similarly, some works address the possibility of damage to them and their impact on the values provided for monitoring, in this case, study debonding and breaking sensors problem [1.42, 1.43].

1.4.4 Bio-inspired computing

The bio-inspired computing aims at providing a toolbox of theories and methods for the human being to develop solutions to complex problems that other, more traditional approaches can not solve [1.44]. However, it is also important to mention that the algorithms are not only inspired by biology but also algorithms based on physics, chemistry, and mathematics [1.45]. And just as nature has many mechanisms to solve problems and achieve species survival, bio-inspired computing also has them such as evolutionary algorithms, neural networks, collective intelligence algorithms (emergent systems), immune systems, cellular automata, to name just a few. Recognizing that many of its searchings can be close to machine learning [1.46]. The development of better and more powerful processors and the most recent introduction of graphic processing units (GPUs) have also facilitated this type of processing to be made possible since something that characterizes them is their high computational load[1.47].

1.4.4.1 Artificial Neural Networks

The artificial neural networks (ANNs) are a bio-inspired model, emulating the brain-behavior, given their goods skills resolving complex problems. The ANNs are suitable for classification, forecasting, clustering, and others.

Neural networks are a broad topic with many implications as complex as the biological mechanism that they have as a reference, elements such as topology, the form of connections, the type of learning, the way it associates the input and output information. Finally, how represented the input and output information are elements that define the applications of the network[1.48].

The ANNs journey is long, starting with the perceptron, introduced by Frank Rosenblatt in 1957, through the developments made by Bernard Widrow and Marcial Hoff, Stephen Grossberg, James Anderson, Kunihiko Fukushima, Teuvo Kohonen, John Hopfield, and so many others enthusiast have developed a broad spectrum of neural networks which have equally ample field of application.

- First: the synaptic weights (Wij) are multiply for the K different inputs sources; this adjusts the among of stimulus that the neuron assumes.

- Second: Vi is determined by adding these values, including the offset or bias (bi).

- Third: the resulting value Vi enters a transfer or activation function f that determines the final output of the neuron Yi.

Figure 1.3 shows the model of a neuron; this has various process stages [1.49], This model is very similar to the perceptron proposed by Rosenblatt in 1958; the principal difference is the activation function; in the perceptron is a hard limit function [1.50].
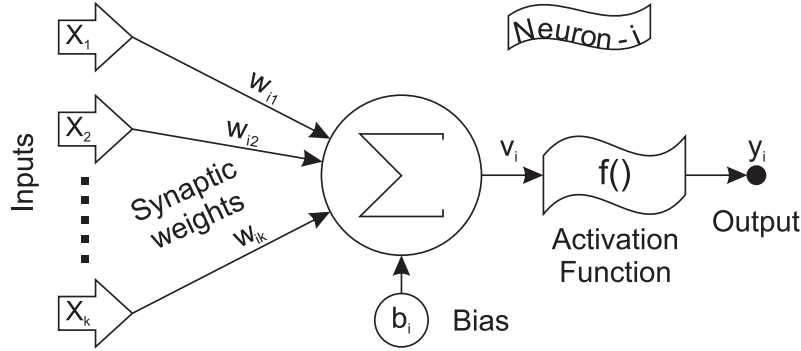
FIGURE 1.3: Neuron model

The output of the neural network is the ecuation 1.9.

$$y_i = f\left(\sum_{j=1}^{m} w_{ij}x_{ij} + b_i\right) \tag{1.9}$$

The transfer functions or activation functions depend on the architecture and the problem to be solved, among the most used are the hard limit or binary equation 1.10, and the sigmoid functions like shows in equation 1.11 and equation 1.12 [1.51].

$$y_i = \begin{cases} 1 & \text{if } \left(\sum_{j=1}^{m} w_{ij}x_{ij} + b_i\right) \geq 0 \\ 0 & \text{if } \left(\sum_{j=1}^{m} w_{ij}x_{ij} + b_i\right) < 0 \end{cases} \tag{1.10}$$

$$y_i = \frac{1}{1 + e^{-\left(\sum_{j=1}^{m} w_{ij}x_{ij} + b_i\right)}}, \rightarrow y_i \in [0,1] \tag{1.11}$$

$$y_i = \frac{e^{\left(\sum_{j=1}^{m} w_{ij}x_{ij} + b_i\right)} - e^{-\left(\sum_{j=1}^{m} w_{ij}x_{ij} + b_i\right)}}{e^{\left(\sum_{j=1}^{m} w_{ij}x_{ij} + b_i\right)} + e^{-\left(\sum_{j=1}^{m} w_{ij}x_{ij} + b_i\right)}}, \rightarrow y_i \in [-1,1] \tag{1.12}$$

Although the artificial neuron is a simple tool, when it is interconnected with other neurons in the network, it reveals its robustness. The architecture of ANNs is three kinds, the first the networks with one layer named feed-forward, the second with various layers named multi-layer -forward and the third the recurrent, in its has feedback connections. The figure shows a neural network composed of three layers, one input, one output, and one hidden, even though they may be more than one hidden.
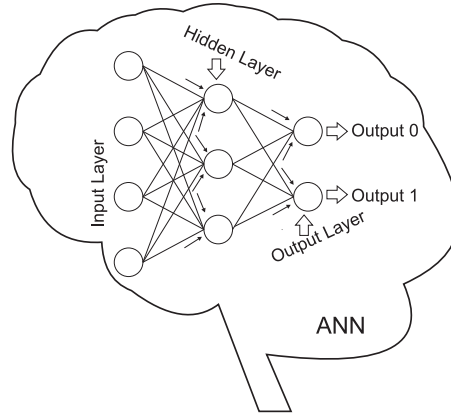
FIGURE 1.4: Artificial Neural Network

The learning process is the mechanism to modify the synaptic weights in the search to the target,

$$\Delta\vartheta_{kj}\left(n+1\right) = \eta\left(\sum_{p=1}^{P}\delta_k^p y_j^p\right) + \alpha\Delta\vartheta_{kj}\left(n\right) \tag{1.13}$$

1.4.5 Machine learning

Arthur L. Samuel gave one of the more extended definitions of machine learning: equip computers with the capacity to learn without programming them explicitly [1.52]. Figure 1.5 shows the classification of machine learning.

Machine learning is a set of algorithms that, through a series of strategies, allows them to emulate human intelligence and his learning ability, acquiring information from the medium to abstract it, and make future decisions[1.53]. It has a wide field of application in pattern recognition, optimization, control, manufacturing, and it is vast even more when including data mining, in which case, machine learning is applied to large databases[1.54].

The process of learning in machines has two approaches:

- Supervised learning. For this type, is necessary the data input and the data output or target, the knowledge is adjusted or tuner using pairs of two kinds of data (input and output), the result can be a classification or a regression.

- Unsupervised learning, only is necessary input data; the information is grouped in conjuntos per affinities and interpreted from this only information.

The types of problems that can be solved using machine learning techniques can be extensive; however, a classification can cover a large part of them are:

- Binary Classification: In this case, the algorithm offers one of two possible values as a response $Y \in \{0, 1\}$.

- Multiclass Classification:In this case, the algorithm offers as a response a value within a set of possibilities $Y \in \{0, 1, 2, 3, 4, ...n\}$.

- Regression: In this case, the output will be of continuous value $Y \in \mathbb{R}$.
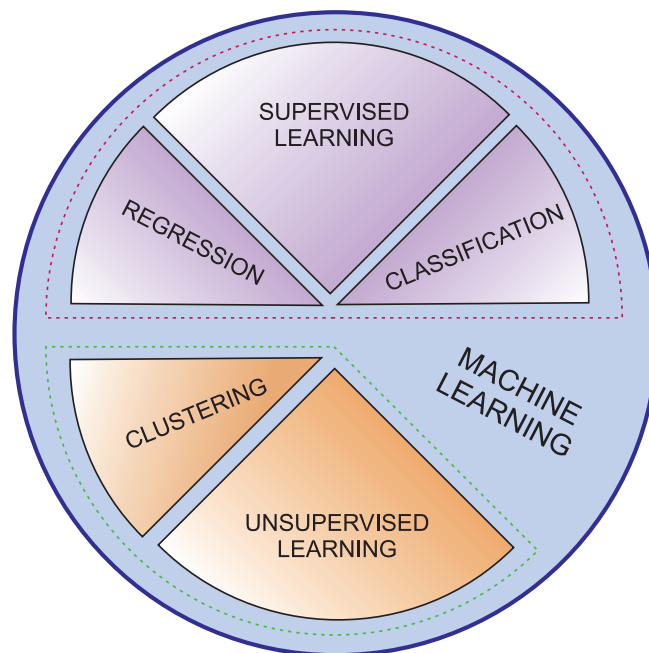
FIGURE 1.5: Machine Learning

There are crucial elements when it comes to designing a solution using machine learning, among which the following stand out: which algorithm to choose, and the selection of the data to perform the training in terms of quality and quantity[1.55]. Matlab has a lot of options for training machine learning; in particular, it has an application known as classification Lerner that allows working with the following models of machines shows in figure 1.6:

1.4.5.1 K-Nearest Neighbor (KNN)

Is a data classification algorithm very extended, introduced by Evelyn Fix and J.L. Hodges in 1951 [1.56], Is a data classification algorithm very extended, introduced by Evelyn Fix and J.L. Hodges in 1951, this methodology decide if an element belongs to a class or not, in the function of distance to the nearest to the k points of the training set.

For the classification, there are t possible categories or classes:

$$C \in \{1, 2, ...t\} \tag{1.14}$$

X is the feature vector also called predictor values, k is the number of features of the form:
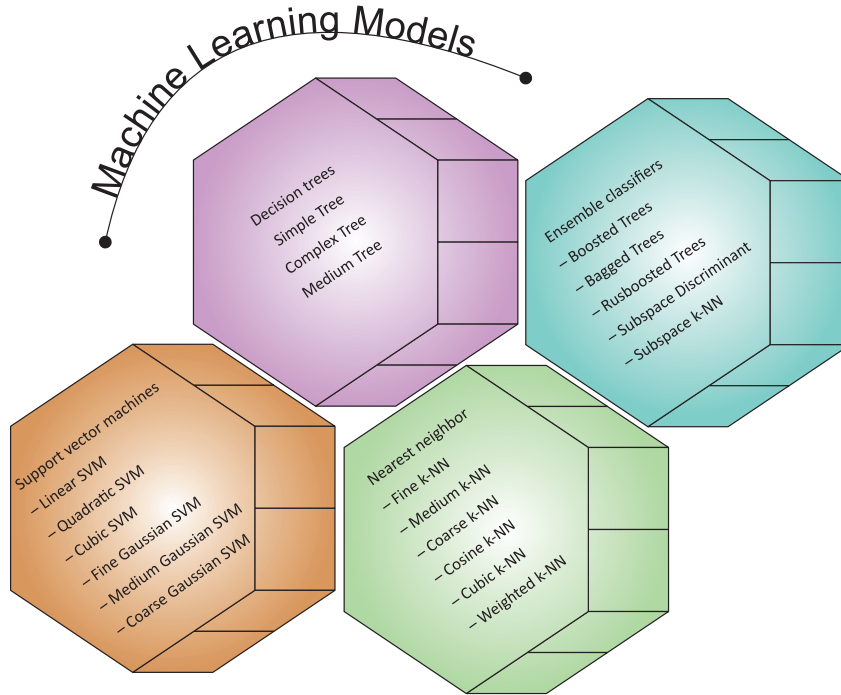
FIGURE 1.6: Machine Learning models

$$X \rightarrow \{x_1, x_2, ..., x_n\} \tag{1.15}$$

The distance function value determines the proximity or remoteness of the neighbor. There are different ways of calculating distance; the most common is Euclidean [1.57] in k-dimensional space 1.16:

$$Euclidean\_distance\left(x_i, s_j\right) = \sqrt[2]{\sum_{u=1}^{n}\left(x_{iu} - t_{ju}\right)^2} \tag{1.16}$$

In this equation t_{ju} are the features of the training set that belong to class j.

One of the tuning parameters of the algorithm is the number of neighbors k, for deficient k there may be overfitting, and for very high k, there may be underfitting because always predict the ruling class. In the case of Fine k-NN the number of neighbors is set to 1, in Medium knn is set to 10 and Coarse kNN is set to 100.

Another way of calculating the similarity between the classified training vectors and the new samples is the cosine distance for which in a multidimensional space shown in equation 1.17. In cosine kNN the number o neighbors was ten.

$$Cos\left(\Theta\right) = \frac{\sum_{u=1}^{n} x_{iu} t_{ju}}{\sqrt[2]{\sum_{u=1}^{n} x_{iu} x_{iu}}\sqrt[2]{\sum_{u=1}^{n} t_{iu} t_{iu}}} \Rightarrow \frac{X \cdot T}{\|X\| \|T\|} \tag{1.17}$$

Minkowski distance shows in equation 1.18 is a very used way to evaluate the proximity of two elements in n-dimensional space, which is a generalization of Manhattan ($\alpha = 1$), euclidean ($\alpha = 2$), and cubic ($\alpha = 3$) metric [1.58]. In cubic kNN the number o neighbors was ten.

$$Min\_dis\,(X, T) = \sqrt[\alpha]{\sum_{u=1}^{n} |x_{iu} - t_{iu}|^{\alpha}} \tag{1.18}$$

Rusboosted Trees In the case of weighted kNN introduced by Dudani in 1976 [1.59], and modified in other researchs [1.60], it presents an alternative for selecting the classification based on a weighted value w, This new parameter is a value calculated from the distances of the unknown sample to K nearest neighbors belongs to a training set of one class.

$$w_j = \begin{cases} \frac{d_k - d_j}{d_k - d_1} & \Rightarrow \quad d_k \neq d_1 \\ 1 & \Rightarrow \quad d_k = d_1 \end{cases} \tag{1.19}$$

For each neighbor associated with a class, a distance must be evaluated, then order these distances from least to greatest, then add them and classify the unknown element in the class with the highest value.

$$W_c = \sum_{j=1}^{k} w_j \Rightarrow c \in \{1, 2, ...t\} \tag{1.20}$$

In the current work for weighted kNN the number of neighbors was ten.

1.4.5.2 Decision tree machine

Decision trees are very popular classifiers for data mining; from the acquired data, they make decisions by a mechanism of divisions (also called branches) when the final decision is placed on the leaves, this is show in figure 1.7 . Its strategy is straightforward, is based on locating the measurements or data more representatives; this data is characterized for performing the largest divisions within the sample group. Iteratively is applied to a division (branches) in the function of the relevant data until the tree is built [1.61].

A criterion to found the nodes is the Gini impurity, this searching a balance in the data and fight against classification error, shown in the equation 1.21.

$$G = 1 - \sum_{x=1}^{c} \varphi \left(\frac{x}{n} \right)^2 \tag{1.21}$$

For a node n, $\varphi \left(\frac{x}{n} \right)$ is the proportion of the samples that belong to a class c.
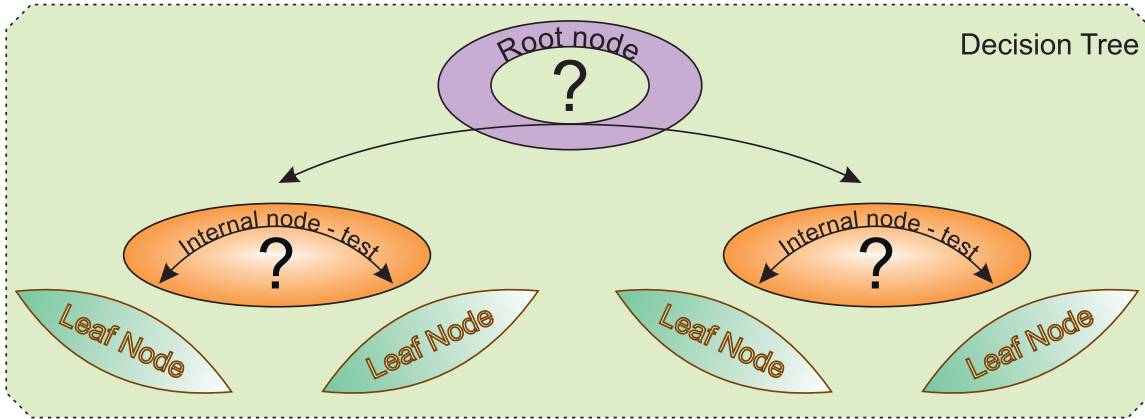
FIGURE 1.7: Desicion tree

1.4.5.3 Suport vector machine SVM

Vector support machines are a strategy introduced by Vapnik et all in the 90 decade, that initially was thought to separate problems of a binary nature; however, they have been adapted to solve multiclassification problems, including regression. Its strategy founded on finding an equidistant hyperplane that separates the entries. The description of this hyperplane with the closest examples to it through the support vectors.

Following the description by Bishop [1.62], for a binary classification problem, the separation plane is given by:

$$y(x) = w^T \phi(x) + b \tag{1.22}$$

In equation 1.22, $\phi(x)$ is the space transformation, an b the bias. The hyperplane is solving the equation 1.23 :

$$argmax(w, b) \left\{ \frac{1}{\|w\|} min \left[t_n(w^T \phi(x_n) + b) \right] \right\} \tag{1.23}$$

In this t_n correspond to targets. The solution shown in equation 1.24

$$L(a) = \sum_{n=1}^{N} a_n - \frac{1}{2} \sum_{n=1}^{N} \sum_{m=1}^{N} a_n a_m t_n t_m k(x_n, x_m) \tag{1.24}$$

where a_n is a Lagrange multipliers, and restrictions 1.25 .

$$\sum_{n=1}^{N} a_n t_n = 0 \rightarrow a_n \geq 0, n = 1, 2...., N \tag{1.25}$$

For the construction of the decision surface, which is where the samples are projected to calculate the classification hyperplane, the kernels are necessary, Matlab offers the following[1]:

For the support vector machine with gaussian kernel 1.26:

$$K(x1, x2) = x_1^T x_2 \tag{1.26}$$

$$K(x1, x2) = tanh(\beta_0 x_1^T x_2 + \beta_1)^\rho \tag{1.27}$$

For the support vector machine with gaussian kernel 1.28:

$$K(x1, x2) = exp(-\frac{\left\| x_1 - x^2 \right\|^2}{2\sigma^2}) \tag{1.28}$$

For the support vector machine with polynomial kernel 1.29:

$$K(x1, x2) = (x_1^T x_2 + 1)^\rho \tag{1.29}$$

1.4.5.4 Ensemble classifiers

The main objective of the ensemble classifiers is to improve their prediction capabilities; this makes combining the decision of various models, it is only applied to supervised learning [1.63].

The decision trees are a classification mechanism that allows constructing a predictive model where the value of splits can increase or decrease the flexibility of this algorithm, as well as the use of various trees (ensemble). A modification of decision trees machine explored in this paper is the RUS (Random Under Sampling) algorithm in RUSBoost, which is a mechanism to eliminate data distribution imbalances, the random undersampling is a technique that deletes examples randomly from the majority class to reach a balance; this tries to avoid the overfitting[1.63].

Another strategy to improve the decision trees is the Bagging, also named Bootstrap aggregating; in this case, the original data set is subdivided into various groups and training a tree with this subset after the result are aggregate to contribute the final prediction.

The boosting is another sequential technique used to improve the performance of machines; in this, the algorithm concentrate on the errors of previous training and increases the relevance of this observation. The better scenario is reached, with sequential training based on mistakes, but can produce overfitting problems.

Finally, exist the subspace learning techniques; in these, the goal is to reach a subspace of low dimension. The weighting and resampling are two strategies used for subspace definition [1.64, 1.65].

---

[1]https://www.mathworks.com/discovery/support-vector-machine.html - Date: 1/03/2020

1.4.6 Techniques to reduce and to extract information

In this work, including the use of tools that reduce information such as Principal Component Analysis (PCA) and Hierarchical Non-Linear Principal Component Analysis (h-NLPCA). These techniques seek to find specific data that define a large amount of information and simplify it out to facilitate the training of the models of machine learning. We also used the discrete wavelet transform (DWT) that makes a representation in time-frequency.

1.4.7 Discrete Wavelet Transform

Signal analysis is a vast field that allows extracting information in the domain of time and frequency in a wide variety of fields such as control, electrophysiology, instrumentation, naming a few. Some tools allow this analysis to be carried out, such as the Fourier transform that does so in the frequency domain, but more recently, a tool has appeared that does so in a scala time representation named the discrete wavelet transform (DWT). The wavelets are generated by the translation and dilation process of the wavelet mother show in equation 1.30 [1.66].

$$\Psi_{s,\delta}(x) = 2^{\frac{-s}{2}} \Psi\left(2^{-s}x - \delta\right) \tag{1.30}$$

The variable δ is dilation and the variable s the scale, and give to mother function ability to build the wavelets families.

The wavelet transform is defined by the equation 1.31.

$$\tau(s,\delta) = \int x(t)\Psi_{s,\delta}^{*}(t)dt \tag{1.31}$$

To extract the coefficients can define a filter bank structure to distinguish features through the use of low-pass filters and high-pass filters [1.67, 1.66]. This configuration allows representing the variability of a given function by means of coefficients at a specified time and scale. These coefficients are calculated by using quadrature mirror filters and are decomposed in approximation (A1,A2,. . .) and detail coefficients (D1, D2,. . .) [1.68] as it is shown in Figure 1.8.

Detail coefficients are low-scale, high-frequency components, while the approximation coefficients represent the high-scale, low-frequency components. The wavelet technique has been of great interest in recent years and has direct application for the SHM like demonstrates some research works [1.69, 1.70, 1.71, 1.72, 1.73]. For further details about DWT and its implementation, please refer to [1.74].

In the current work was used to extract some characteristics of the lamb wave signals, after reduce with h-Non Linear PCA, shown in the figure 1.9.
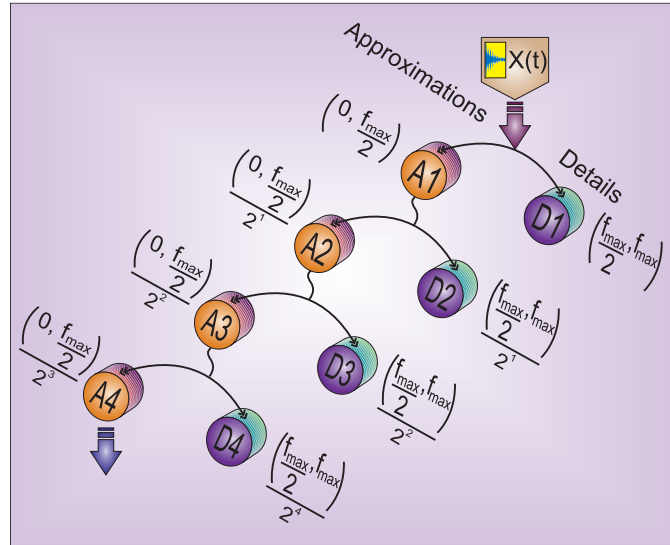
FIGURE 1.8: Wavelet decomposition
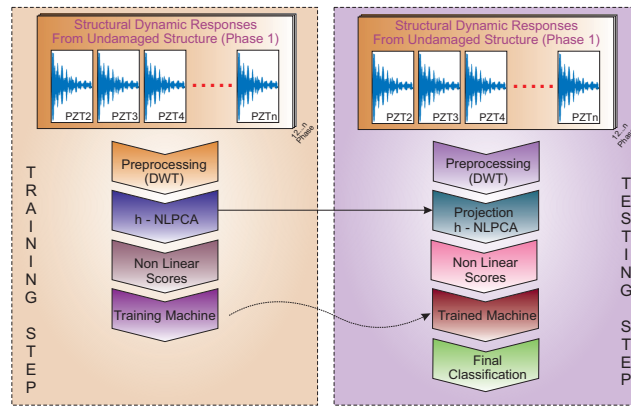
FIGURE 1.9: Wavelet into methodology

1.4.8 PCA - Principal component analysis

One of the most significant difficulties in data analysis arises when the amount of data is vast, and there is no apparent relationship between all the information or when this relationship is complicated to find. Several tools in a multivariate analysis can help with this task, such as PCA, ICA, Hierarchical nonlinear PCA, and others.

Principal component analysis was introduced by Pearson in 1901, as a tool of multivariate analysis. This method allows to find the principal components, that are a reduced version of the original dataset and include relevant information that identify the reason for the variation between the measured variables [1.75]. To find these variables, the analysis includes the transformation of the data with respect to a current coordinate space to a new space in order to re-express the original data trying to reduce the noise and possible redundancies. These redundancies are measured by means of the correlation between the variables [1.76]. .

Two methods are popular for calculating the PCA: the one based on the correlation matrix and the one based on the covariance matrix, chapter 2 shows a more detailed explanation, using the covariance matrix method.

1.4.9 Hierarchical Non-Linear Principal Component Analysis

One difficulty that the PCA has is that it looks for linear relationships between the variables, which can reduce its effectiveness with specific data; the h-NLPCA precisely looks for non-linear relationships by making more effective searches.

Nonlinear PCA searches nonlinear relationships between variables with no homogeneous ranges, This feature makes it have a better behavior with certain types of data [1.77]. The Hierarchical nonlinear PCA has this characteristic adding that consider the order in which these components [**?**].

In chapter 4 shows this method using a multi-layered perceptron (MLP) architecture with an auto-associative topology for its calculus. The auto-associative network works with the inputs and outputs to perform the identity mapping by using the square error [**?**].

1.5 Experimental setups

To fulfill the objectives and based on the results of the investigations carried out by members of the CoDAlab group, was selected a system that uses piezoelectric sensors for tests. The advantages of this sensor, such as low cost and easy installation, were decisive for the election but also were review the disadvantages, such as sophisticated data processing required. In figure 1.10 shows a block diagram of the measurement system, and in the figure 1.11 a photography, the arbitrary wave generator used was the Tiepie HS5, and the digitalization system was with Tiepie HS4.

1.5.1 Climate chamber

Finally, the research project had a Faithful climate chamber with an operating range from 0 to 80 Celsius degrees, to test the behavior of the methodologies in the face of temperature changes, this can be seen in the Figure 1.12

1.5.2 Multiplexion system

One of the first activities that were undertaken was the development of an analog signal multiplexing card that meets the objective of facilitating the acquisition of signals from piezoelectric devices installed on the object under observation, automating the process. It was designed for two tasks, in the first instance to automate the process of carrying the stimulation signal
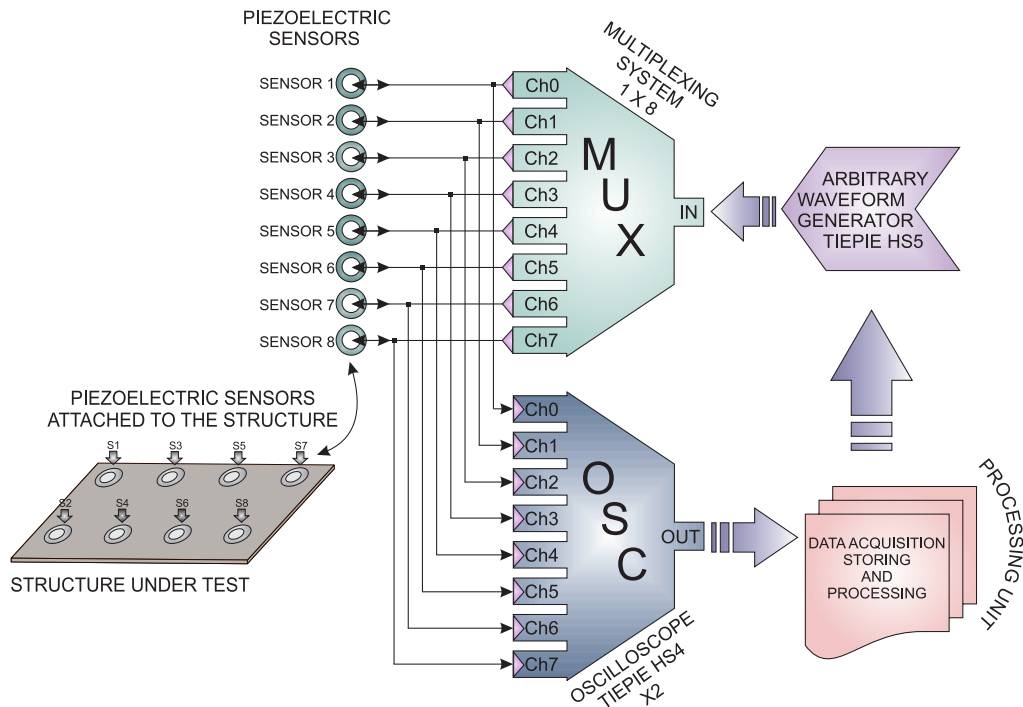
FIGURE 1.10: Measurement system scheme

FIGURE 1.11: Photo measurement system

to each of the transducers by routing the signal from an arbitrary wave generator, and on the other hand it can carry any signal from a sensor to a digitizing element, as shown in Figure .

1.5.3 Experimental specimens

,

The specimens that we consider in this work is an aluminum rectangular profile shown in figure 1.14, an aluminum rectangular plate shown in figure 1.15, a Composite plate shown in

FIGURE 1.12: Climate chamber
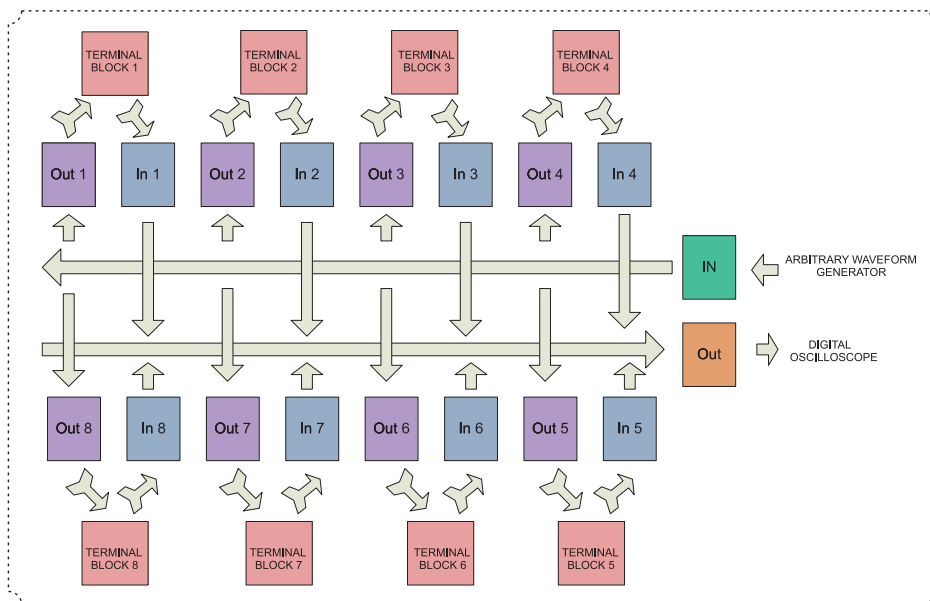
FIGURE 1.13: Multiplexor

figure 1.16,CFRP sandwich 1 composite plate shown in figure 1.17, a CFRP sandwich 2 composite plate shown in figure 1.18, and Composite drone wing shown in figure 1.19. The distribution of the piezoelectric transducers and the number was determined individually based on the experiments, minimum two and maximum eight.

(a) Specimen 1. Aluminium profile squematic

(b) Photo Specimen 1
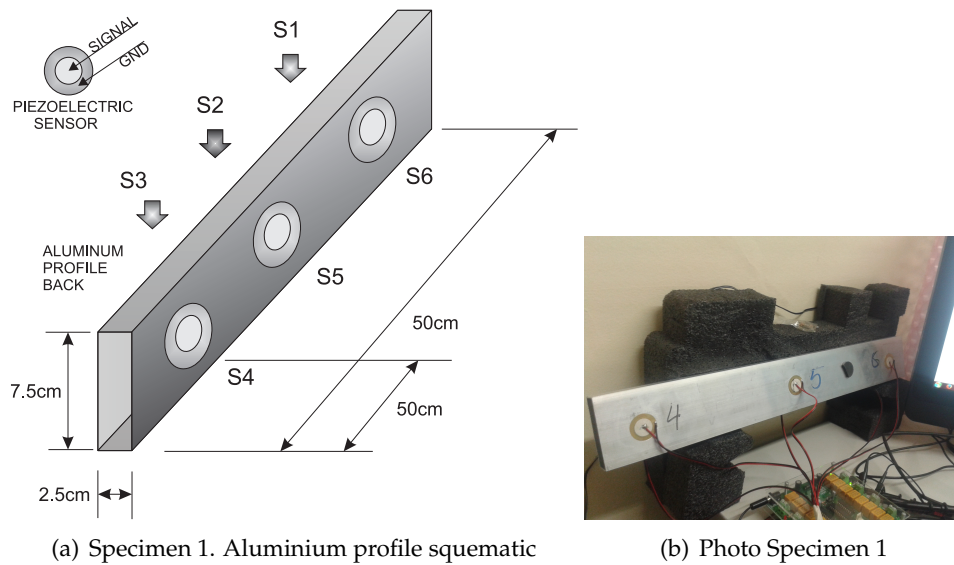
FIGURE 1.14: Specimen 1. Alumninium profile

(a) Specimen 2. Aluminium plate squematic

(b) Photo Specimen 2
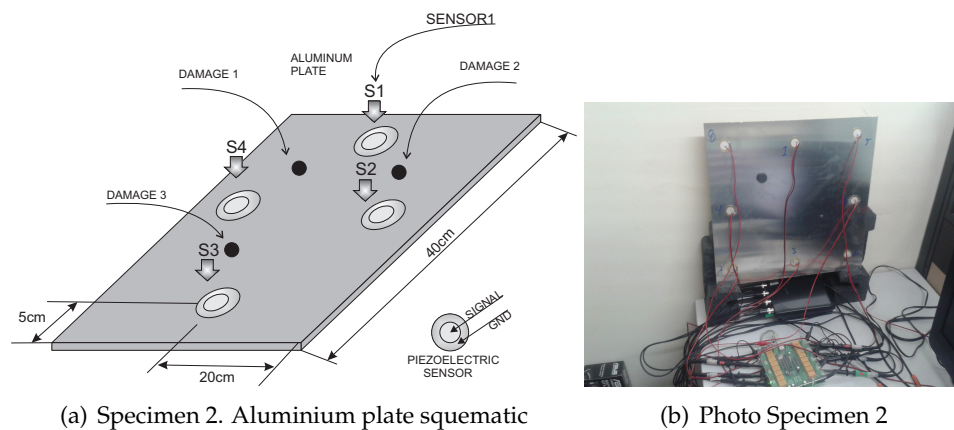
FIGURE 1.15: Specimen 2. Alumninium plate

1.6 Research Support

This work has been funded on CoDAlab research group, Department of Civil and Environmental Engineering of the Universitat Politècnica de Catalunya, through the grants Spanish Ministry of Economy and Competitiveness through the grant DPI2014-58427-C2-1-R, and by the Catalan Government (Generalitat de Catalunya) through the grant 2014 SGR 859 Spanish Ministry of Science, Innovation and Universities, the Agencia Estatal de Investigación (AEI) and the European Regional Development Fund (ERDF/FEDER) through the research projects DPI2014-58427-C2-1-R and DPI2017-82930-C2-1-R.

The Department of Electrical and Electronic Engineering of the National University of Colombia for its experience and support contributing decisively to the achievement of the objectives.

(a) Specimen 3. Composite plate squematic

(b) Photo Specimen 2
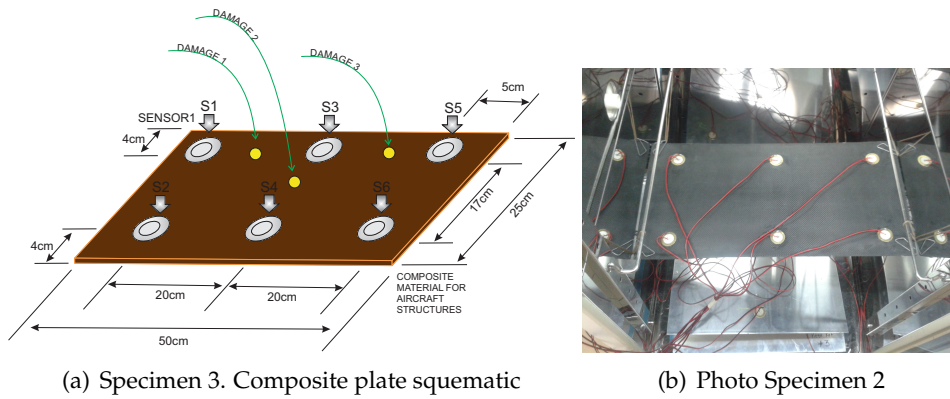
FIGURE 1.16: Specimen 3. Composite plate

(a) Specimen 4. CFRP sandwich 1 composite plate squematic

(b) Photo Specimen 2
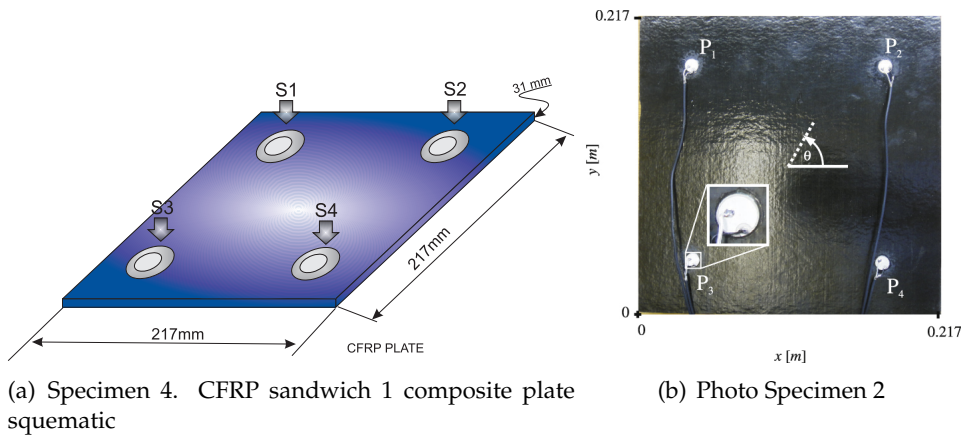
FIGURE 1.17: Specimen 4. CFRP sandwich 1 composite plate

(a) Specimen 5. CFRP sandwich 2 composite plate squematic

(b) Photo Specimen 2
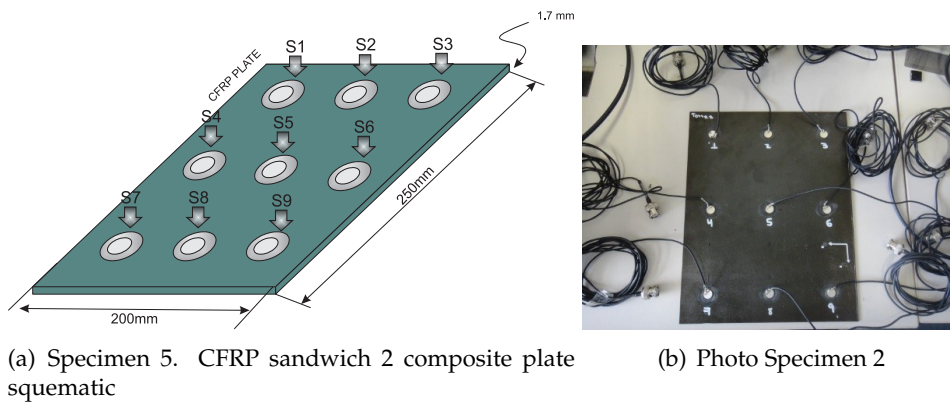
FIGURE 1.18: Specimen 5. CFRP sandwich 2 composite plate

(a) Specimen 6. Composite drone wing   (b) Photo Specimen 2

FIGURE 1.19: Specimen 6. Composite drone wing

for detection, location, and classification of damage in metal and composite material structures 1608603-017 and the research proyect, design of a structural health monitoring system using machine learning and bio-inspired computing - stages I and II - 17545020-47, 1854504, Design of a system for locating damage to metal and composite structures exposed to temperature changes stages I and II 1954505 - 2054504. ;

1.7 Concluding remarks

1.8 Organization

The current document has five chapters with the next distribution: the first chapter is the introduction, the content in this chapter are the objectives, general results, and contribution, theoretical background, research framework, research support, and concluding remark. The chapters two to four are three journal papers published in accredited journals. Chapter five are conclusions and further work. Appendix A has a complete list of publications in journals, conferences, and chapter books. Appendix B has schemes and design considerations of the multiplexor system development.

Abbreviations

The following abbreviations are used in this manuscript:
k-NN   *k*-nearest neighbors algorithm
PCA   Principal Component Analysis
PZT   Lead-zirconate-titanate
SHM   Structural Health Monitoring

Bibliography

[1.1] Charles J. Hellier, *handbook of nondestructive evaluation, 2nd edition*. McGraw-Hill Education: New York, Chicago, San Francisco, Athens, London, Madrid, Mexico City, Milan, New Delhi, Singapore, Sydney, Toronto, 2013.

[1.2] D. Balageas, "Introduction to structural health monitoring," in *Structural Health Monitoring*, ch. Introducti, pp. 13–29, 2006.

[1.3] F. Gharibnezhad, *Robust Damage Detection in Smart Structures*. PhD thesis, Universitat Politècnica de Catalunya, 2014.

[1.4] N. Mrad, "SHM implementation," in *Fly by Wireless Workshop (FBW), 2011 4th Annual Caneus*, pp. 1–4, 2011.

[1.5] J.-m. Zhao, D. Feng, D.-a. Li, and B.-f. Zhao, "Power-free Structural Health Monitoring via compressive sensing," in *Computing and Communications Conference (IPCCC), 2015 IEEE 34th International Performance*, pp. 1–8, 2015.

[1.6] D. M. Laveuve, M. Lehmann, K. Erdmann, and A. Büter, "SHM - Reliability demands on the multidisciplinary challenge of structural health monitoring," in *NDT in Progress 2009 - 5th International Workshop of NDT Experts, Proceedings*, (Prague), pp. 173–182, 2009.

[1.7] W. Staszewski, G. Tomlinson, and C. Boller, *Health monitoring of aerospace structures smart sensor technologies and signal processing*. 2004.

[1.8] A. Rytter, "Vibrational Based Inspection of Civil Engineering Structures," 1993.

[1.9] C. R. Farrar and K. Worden, "An introduction to structural health monitoring," *Philosophical Transactions of the Royal Society of London A: Mathematical, Physical and Engineering Sciences*, vol. 365, no. 1851, pp. 303–315, 2007.

[1.10] C. Winkler and U. Schwarz, "Multifunctional Wood-Adhesives for Structural Health Monitoring Purposes," in *Materials and Joints in Timber Structures*, pp. 381–394, Springer, 2014.

[1.11] V. Giurgiutiu, *Structural Health Monitoring of Aerospace Composites*. Academic Press - ELSEVIER, 2015.

[1.12] K. M. Qatu, A. Abdelgawad, and K. Yelamarthi, "Structure damage localization using a reliable wave damage detection technique," in *2016 International Conference on Electrical, Electronics, and Optimization Techniques (ICEEOT)*, pp. 1959–1962, 2016.

[1.13] J. Cheng, "Perspectives on long-term performance assessment of bridges based on structural health monitoring system," in *Electric Technology and Civil Engineering (ICETCE), 2011 International Conference on*, pp. 553–556, 2011.

[1.14] K. S. Raju, Y. Pratap, Y. Sahni, and M. Naresh Babu, "Implementation of a WSN system towards SHM of civil building structures," in *Intelligent Systems and Control (ISCO), 2015 IEEE 9th International Conference on*, pp. 1–7, 2015.

[1.15] Pagan-Ortiz, "State of the Practice and Art for Structural Health Monitoring of Bridge Substructures," no. May, p. 100, 2014.

[1.16] C. Rainieri, D. Gargaro, L. Cieri, and G. Fabbrocino, "Stand-alone NDT system for tensile force estimation in cables and tie rods," in *Environmental Energy and Structural Monitoring Systems (EESMS), 2014 IEEE Workshop on*, pp. 1–6, sep 2014.

[1.17] S. Kim, S. Pakzad, D. Culler, J. Demmel, G. Fenves, S. Glaser, and M. Turon, "Health Monitoring of Civil Infrastructures Using Wireless Sensor Networks," in *Information Processing in Sensor Networks, 2007. IPSN 2007. 6th International Symposium on*, pp. 254–263, 2007.

[1.18] C. Riziotis, L. Eineder, L. Bancallari, and G. Tussiwand, "Polymer fiber optic sensors for strain monitoring in Solid Rocket Motors' propellant," in *Lasers and Electro-Optics Europe (CLEO EUROPE/IQEC), 2013 Conference on and International Quantum Electronics Conference*, p. 1, may 2013.

[1.19] Q. Wang, Z. Su, and M. Hong, "Online Damage Monitoring for High-Speed Train Bogie Using Guided Waves: Development and Validation," *7th European Workshop on Structural Health Monitoring July 8-11, 2014. La Cité, Nantes, France*, 2014.

[1.20] A. Güemes, "SHM Technologies and Applications in Aircraft Structures," *5th International Symposium on NDT in Aerospace*, no. November, pp. 13–15, 2013.

[1.21] C. Vendittozzi, G. Sindoni, C. Paris, and P. P. del Marmo, "Application of an FBG sensors system for structural health monitoring and high performance trimming on racing yacht," in *Sensing Technology (ICST), 2011 Fifth International Conference on*, pp. 617–622, nov 2011.

[1.22] G. Ferin, Y. Muralidharan, N. Mesbah, P. Chatain, C. Bantignies, and H. L. Khanh, "aeronautical SHM applications," pp. 3–6, 2015.

[1.23] S. Casciati and R. Rossi, "Embedding SHM algorithms into a microcontroller for real-time and fully-automated civil applications," *Proc., Structural Health Monitoring 2006*, pp. 539–546, 2006.

[1.24] A. Abdelgawad and K. Yelamarthi, "Internet of things (IoT) platform for structure health monitoring," *Wireless Communications and Mobile Computing*, vol. 2017, 2017.

[1.25] S. Wirtz, A. Cunha, M. Labusch, S. Barcikowski, G. Marzun, and D. Söffker, "Development of A Low-Cost FPGA-Based Measurement System for Real-Time Processing of Acoustic Emission Data: Proof of Concept Using Control of Pulsed Laser Ablation in Liquids," *Sensors*, vol. 18, 2018.

[1.26] C. Cremona and J. Santos, "Structural health monitoring as a big-data problem," *Structural Engineering International*, vol. 28, no. 3, pp. 243–254, 2018.

[1.27] H. Malik and W. Zatar, "Software Agents to Support Structural Health Monitoring (SHM)-Informed Intelligent Transportation System (ITS) for Bridge Condition Assessment," *Procedia Computer Science*, vol. 130, pp. 675–682, 2018.

[1.28] C. R. Farrar, T. a. Duffey, S. W. Doebling, and D. a. Nix, "A Statistical Pattern Recognition Paradigm for Vibration-Based Structural Health Monitoring," p. 10, 1999.

[1.29] D. A. Tibaduiza Burgos, R. C. Gomez Vargas, C. Pedraza, D. Agis, and F. Pozo, *Damage identification in structural health monitoring: A brief review from its implementation to the use of data-driven applications*, vol. 20. 2020.

[1.30] M. Anaya, D. A. Tibaduiza, E. Forero, R. Castro, and F. Pozo, "An acousto-ultrasonics pattern recognition approach for damage detection in wind turbine structures," in *Signal Processing, Images and Computer Vision (STSIVA), 2015 20th Symposium on*, pp. 1–5, sep 2015.

[1.31] V. Giurgiutiu, A. Zagrai, and J. Bao, "Damage Identification in Aging Aircraft Structures with Piezoelectric Wafer Active Sensors," *Journal of Intelligent Material Systems and Structures*, vol. 15, no. 9-10, pp. 673–687, 2004.

[1.32] A. Perelli, C. Caione, L. De Marchi, D. Brunelli, A. Marzani, and L. Benini, "Design of an ultra-low power device for aircraft structural health monitoring," in *Design, Automation Test in Europe Conference Exhibition (DATE), 2013*, pp. 1127–1130, 2013.

[1.33] B. Babjak, S. Szilvasi, P. Volgyesi, O. Yapar, and P. K. Basu, "Analysis and efficient onset time detection of acoustic emission signals with power constrained sensor platforms," in *SENSORS, 2013 IEEE*, pp. 1–4, nov 2013.

[1.34] L. Schubert, B. Frankenstein, and G. Reppe, "Match-X Based Microsystem for Structural Health Monitoring," in *Electronics Systemintegration Technology Conference, 2006. 1st*, vol. 1, pp. 635–641, sep 2006.

[1.35] F. G. Baptista, J. V. Filho, and D. J. Inman, "Sizing PZT Transducers in Impedance-Based Structural Health Monitoring," *Sensors Journal, IEEE*, vol. 11, no. 6, pp. 1405–1414, 2011.

[1.36] Z. Su and L. Ye, *Identification of damage using Lamb waves: from fundamentals to applications*, vol. 48. Springer Science & Business Media, 2009.

[1.37] J. L. Rose, *Ultrasonic guided waves in solid media*, vol. 9781107048. Cambridge University Press, 2014.

[1.38] T. L. Jordan and N. Langley, "Piezoelectric Ceramics Characterization," *Contract*, p. 23, 2001.

[1.39] N. Kaur and B. S., "Integrated Piezoelectric energy harvesting and structural health monitoring for transportation infrastructure," in *Power Electronics Systems and Applications (PESA), 2015 6th International Conference on*, pp. 1–4, 2015.

[1.40] J. D. N. Cheeke, *Fundamentals and applications of ultrasonic waves, second edition*. Taylor & Francis Group, 2017.

[1.41] V. Giurgiutiu, a. Zagrai, and J. Jing Bao, "Piezoelectric Wafer Embedded Active Sensors for Aging Aircraft Structural Health Monitoring," *Structural Health Monitoring*, vol. 1, no. 1, pp. 41–61, 2002.

[1.42] T. G. Overly, G. Park, K. M. Farinholt, and C. R. Farrar, "Piezoelectric Active-Sensor Diagnostics and Validation Using Instantaneous Baseline Data," *Sensors Journal, IEEE*, vol. 9, pp. 1414–1421, nov 2009.

[1.43] D. Tibaduiza, M. Anaya, E. Forero, R. Castro, and F. Pozo, "A Sensor Fault Detection Methodology applied to Piezoelectric Active Systems in Structural Health Monitoring Applications," *IOP Conference Series: Materials Science and Engineering*, vol. 138, no. 1, 2016.

[1.44] R. Akerkar and P. S. Sajja, "Bio-inspired computing: Constituents and challenges," *International Journal of Bio-Inspired Computation*, vol. 1, no. 3, pp. 135–150, 2009.

[1.45] B. Xing and W.-J. Gao, *Introduction to Computational Intelligence*, pp. 3–17. Cham: Springer International Publishing, 2014.

[1.46] A. Chakraborty and A. K. Kar, "A review of bio-inspired computing methods and potential applications," *Lecture Notes in Electrical Engineering*, vol. 396, pp. 155–161, 2016.

[1.47] M. G. Arenas, A. M. Mora, G. Romero, and P. A. Castillo, "GPU computation in bioinspired algorithms: A review," *Lecture Notes in Computer Science (including subseries Lecture Notes in Artificial Intelligence and Lecture Notes in Bioinformatics)*, vol. 6691 LNCS, no. PART 1, pp. 433–440, 2011.

[1.48] J. R. H. González and V. J. M. Hernando, *Redes neuronales artificiales: fundamentos, modelos y aplicaciones*. Paradigma : fundamentos teóricos. Informática, RA-MA, 1994.

[1.49] D. Rumelhart, G. Hinton, and J. Mcclelland, "A General Framework for Parallel Distributed Processing," *Parallel Distributed Processing: Explorations in the Microstructure of Cognition*, vol. 1, 1986.

[1.50] F. Rosenblatt, "The perceptron: A probabilistic model for information storage and organization in the brain," *Psychological Review*, vol. 65, no. 6, pp. 386–408, 1958.

[1.51] D. Graupe, *Principles of Artificial Neural Networks*, vol. 7 of *Advanced Series in Circuits and Systems VOL. 7*. WORLD SCIENTIFIC, sep 2013.

[1.52] J. Russell and P. Norvig, *Artificial Intelligence: A Modern Approach*. Prentice Hall, 2010.

[1.53] I. El Naqa and M. J. Murphy, *What Is Machine Learning?*, pp. 3–11. Cham: Springer International Publishing, 2015.

[1.54] E. Alpaydin, *Introduction to Machine Learning*. Adaptive Computation and Machine Learning series, MIT Press, 2009.

[1.55] T. M. Mitchell, *Machine Learning*. McGraw-Hill international editions - computer science series, McGraw-Hill Education, 1997.

[1.56] E. Fix and J. L. Hodges, "Discriminatory Analysis, Nonparametric Discrimination: Consistency Properties," tech. rep., USAF School of Aviation Medicine, Randolph Field, Texas, 1951.

[1.57] K. Schliep, K. Hechenbichler, and A. Lizee, "kknn: Weighted k-Nearest Neighbors," *2016*, vol. 399, p. 15, 2016.

[1.58] S. Alfere and A. Y. A. Maghari, "Prediction of Student ' s Performance Using Modified KNN Classifiers," *1st International Conference on Engineering & Future Technology (ICEFT 2018)*, no. May, pp. 143–150, 2018.

[1.59] S. A. Dudani, "The Distance-Weighted k-Nearest-Neighbor Rule," *IEEE Transactions on Systems, Man, and Cybernetics*, vol. SMC-6, no. 4, pp. 325–327, 1976.

[1.60] M. Bicego and M. Loog, "Weighted K-Nearest Neighbor revisited," *Proceedings - International Conference on Pattern Recognition*, vol. 0, pp. 1642–1647, 2016.

[1.61] C. E. Brodley and M. A. Friedl, "Decision tree classification of land cover from remotely sensed data," *Remote Sensing of Environment*, vol. 61, no. 3, pp. 399–409, 1997.

[1.62] C. M. Bishop, *Pattern Recognition and Machine Learning*. Springer, 2006.

[1.63] C. Seiffert, T. M. Khoshgoftaar, J. Van Hulse, and A. Napolitano, "RUSBoost: A hybrid approach to alleviating class imbalance," *IEEE Transactions on Systems, Man, and Cybernetics Part A:Systems and Humans*, vol. 40, no. 1, pp. 185–197, 2010.

[1.64] A. S. Ashour, Y. Guo, A. R. Hawas, and G. Xu, "Ensemble of subspace discriminant classifiers for schistosomal liver fibrosis staging in mice microscopic images," *Health Information Science and Systems*, vol. 6, no. 1, 2018.

[1.65] M. Bioucas-dias, A. Plaza, and J. Li, "A NEW SUBSPACE DISCRIMINANT ANALYSIS APPROACH FOR SUPERVISED HYPERSPECTRAL IMAGE CLASSIFICATION," in *2011 IEEE International Geoscience and Remote Sensing Symposium*, pp. 3911–3914, IEEE, 2011.

[1.66] A. Graps, "An introduction to wavelets," *IEEE Computational Science and Engineering*, vol. 2, no. 2, pp. 50–61, 1995.

[1.67] M. J. Shensa, "The Discrete Wavelet Transform: Wedding the À Trous and Mallat Algorithms," *IEEE Transactions on Signal Processing*, vol. 40, no. 10, pp. 2464–2482, 1992.

[1.68] D. A. T. Burgos, "Design and Validation of a Structural Health Monitoring System for Aeronautical Structures -," *PhD thesis*, vol. 1, 2012.

[1.69] H. Z. Hosseinabadi, B. Nazari, R. Amirfattahi, H. R. Mirdamadi, and A. R. Sadri, "Wavelet network approach for structural damage identification using guided ultrasonic waves," *IEEE Transactions on Instrumentation and Measurement*, vol. 63, no. 7, pp. 1680–1692, 2014.

[1.70] X. Chen, X. Li, S. Wang, Z. Yang, B. Chen, and Z. He, "Composite damage detection based on redundant second-generation wavelet transform and fractal dimension tomography algorithm of lamb wave," *IEEE Transactions on Instrumentation and Measurement*, vol. 62, no. 5, pp. 1354–1363, 2013.

[1.71] A. Medda, E. Chicken, and V. DeBrunner, "Sigma-Sampling Wavelet Denoising for Structural Health Monitoring," in *Statistical Signal Processing, 2007. SSP '07. IEEE/SP 14th Workshop on*, pp. 119–122, 2007.

[1.72] M. V. Golub, A. N. Shpak, I. Buethe, C.-P. Fritzen, H. Jung, and J. Moll, "Continuous wavelet transform application in diagnostics of piezoelectric wafer active sensors," in *Days on Diffraction (DD), 2013*, pp. 59–64, may 2013.

[1.73] H. Jeong, "Analysis of plate wave propagation in anisotropic laminates using a wavelet transform," *Ndt & E International*, vol. 34, no. 3, pp. 185–190, 2001.

[1.74] M. A. Torres-Arredondo, I. Buethe, D. A. Tibaduiza, J. Rodellar, and C.-P. Fritzen, "Damage detection and classification in pipework using acousto-ultrasonics and non-linear

data-driven modelling," *Journal of Civil Structural Health Monitoring*, vol. 3, no. 4, pp. 297–306, 2013.

[1.75] L. E. Mujica, M. Ruiz, F. Pozo, J. Rodellar, and a. Güemes, "A structural damage detection indicator based on principal component analysis and statistical hypothesis testing," *EWSHM - 7th European Workshop on Structural Health Monitoring*, vol. 23, no. 2, p. 025014, 2014.

[1.76] M. Anaya, D. A. Tibaduiza, and F. Pozo, "A bioinspired methodology based on an artificial immune system for damage detection in structural health monitoring," *Shock and Vibration*, vol. 501, p. 648097, 2015.

[1.77] Y. Mori, M. Kuroda, and N. Makino, *Nonlinear Principal Component Analysis and Its Applications SPRINGER BRIEFS IN STATISTICS*. Springer, 2016.

Chapter 2

A Sensor Data Fusion System Based on k-Nearest Neighbor Pattern Classification for Structural Health Monitoring Applications

Publishing information

Contents

A Sensor Data Fusion System Based on k-Nearest Neighbor Pattern Classification for Structural Health Monitoring Applications

abstract

Civil and military structures are susceptible and vulnerable to damage due to the environmental and operational conditions. Therefore, the implementation of technology to provide robust solutions in damage identification (by using signals acquired directly from the structure) is a requirement to reduce operational and maintenance costs. In this sense, the use of sensors permanently attached to the structures has demonstrated a great versatility and benefit since the inspection system can be automated. This automation is carried out with signal processing tasks with the aim of a pattern recognition analysis. This work presents the detailed description of a structural health monitoring (SHM) system based on the use of a piezoelectric (PZT) active system. The SHM system includes: (i) the use of a piezoelectric sensor network to excite the structure and collect the measured dynamic response –in several actuation phases–; (ii) data organization; (iii) advanced signal processing techniques to define the feature vectors;

and, finally, (iv) nearest neighbor algorithm as a machine learning approach to classify different kind of damage. A description of the experimental setup, the experimental validation and a discussion of the results from two different structures are included and analyzed.

Keywords: piezoelectric; sensors; active system; data fusion; machine learning; damage classification

2.1 Introduction

Service life of structures is affected by several factors, such as the quality of the materials and components, environmental effects, operational conditions and quality of the building, among others. For these reasons, it is essential to inspect the structure during its service life. The revision and maintenance operation may depend on the kind of structure. However, in an automated monitoring system, some common elements are of interest, being damage detection, localization and classification some of the most important. The damage identification reliability is associated to the use of a reliable sensor network since faults in the sensors can lead to false positives in the damage detection process. Sensor fault or damage is commonly based on sensor debonding, piezoeletric fractures or bad connections –produced at the very moment of the installation of the monitoring system or during its lifetime–. To detect these kind of failures, several approaches have been developed, among them, data-driven algorithms to detect cristal cuts and debonding at different temperatures [2.1], crystal removals [2.2], the effects of cracks and debonding in the usability of the signals for structural damage detection [2.3].

When it is possible to ensure the proper performance of the sensors, damage identification tasks can be applied. On this topic, it is possible to find some strategies for damage detection, localization and classification including robust detection [2.4] that considers the variations in the environmental conditions. Or even the use of a robust regression technique to analyze data from an SHM system in order to distinguish between damage and environmental conditions [2.5], the development of a methodology to remove the environmental effects from the SHM data by using principal component analysis and Helbert-Huang transformation [2.6], or the use of adaptive kernel spectral clustering that detects damage in its initial stage [2.7].With respect to the use of machine learning approaches, several strategies have been explored. For instance, He and Wang [2.8] use *k*-NN algorithm (*k*-nearest neighbor rule) for the fault detection in semiconductors manufacturing processes. Similarly, numerical and experimental investigations to compare metrics to assess and compensate the degradation of the adhesive layer of surface-bonded piezoelectric (lead zirconate titanate, PZT) transducers for SHM are performed in [2.9]. Other techniques include support vector machines [2.10], naive Bayes classifiers, feed-forward neural networks, random forest and AdaBoost [2.11], among others. This paper is not focused on the analysis of the sensor faults or the effects of the environmental condition in the damage

identification process but on the structural damage classification by means of a data driven algorithm which considers the use of data from healthy piezoelectric sensors in a sensor network permanently attached to the structure that has to be inspected.

Previous works by the authors include the use and development of multivariate analysis techniques such as linear principal component analysis (PCA), non-linear PCA [2.12] and independent component analysis (ICA) to detect [2.13], classify and localize damage in structures [2.2]. In this paper, a smart system with data acquisition and data management is described. The system considers the use of a piezoelectric sensor network, multivariate analysis and machine learning. The proposed system presents new contributions since it introduces the use of a novelty sensor data fusion for data organization, the use of featured vectors and *k*-nearest neighbors machines which allows to detect and classify different kind of damage.

The structure of the paper is as follows: In Section 2.2, a brief description of the theoretical background required to construct the SHM system is presented. Section 2.3 describes the SHM system that is used to inspect the structures and the strategies that are applied to classify the damage. In Section 2.4, the experimental setup is introduced together with some results. Finally, in Section 5.1, some concluding remarks are discussed.

2.2 Theoretical Background

2.2.1 Piezoelectric sensors

Knowledge about changes in a system due to enviromental or operational conditions is a requirement in modern control and monitoring systems. In this sense, it is necessary to be in possession of devices that can convert analog information –temperature, pressure, sound, acceleration, acoustic emission, among others– in electric information to be used in control or acquisition systems. Different kind of sensors based on physical effects can be currently found. One of these are the piezoelectric sensors which are transducers able to sense pressure, acceleration, temperature, strain of force and acoustic emission by means of the piezoelectric effect and convert this information in an electrical charge [2.14].

Some advantages about the inspection with piezoelectric transducers includes high sensitivity to the damage, easy installation and operation since relatively long distance inspection can be covered with low attenuation and reduced price, compared with other sensors. Additionally, these kind of sensors can be used as passive or active sensors since they can work both as a sensor or as actuators. Some limitations in the use of piezoelectric transducers for inspection processes are, for instance a low output. This means that it is required to use an additional circuit to amplify the excitation/collected signals and high impedance output [2.15].

2.2.2   Principal component analysis

One of the greatest difficulties in data analysis arises when the amount of data is very large and there is no apparent relationship between all the information or when this relationship is very difficult to find. In this sense, principal component analysis was born as a very useful tool to reduce and analyze a big quantity of information. Principal component analysis was described for the first time by Pearson in 1901, as a tool of multivariate analysis and was also used by Hotelling in 1933 [2.16]. This method allows to find the principal components, that are a reduced version of the original dataset and include relevant information that identify the reason for the variation between the measured variables. To find these variables, the analysis includes the transformation of the data with respect to a current coordinate space to a new space in order to re-express the original data trying to reduce, filter or eliminate the noise and possible redundancies. These redundancies are measured by means of the correlation between the variables [2.17].

There are two mechanisms to implement the analysis of principal components: (i) the first method is based on correlations; and (ii) a second strategy that is based on the covariance. It is necessary to highlight that PCA is not invariant to scale, so the data under study must be normalized. Many methods can be used to perform this normalization as it is shown in [2.18, 2.17]. In many applications, PCA is also used as a tool to reduce the dimensionality of the data. Currently, there are several useful toolbox that implement PCA and analyze the reduced data provided by this strategy [2.19]. For the sake of completeness, we present in the following Sections a succint description of the PCA modelling that includes how the measured data is arranged in matrix form. We also present the normalization procedure (group scaling) and how the new data to inspect is projected onto the PCA model.

2.2.2.1   PCA modelling

The first step to build a PCA model is to measure, from a healthy structure, different sensors or variables during $(L-1)\Delta$ seconds –where Δ is the sampling time– and $n \in \mathbb{N}$ experimental trials. The discretized measures of the sensors can be arranged in matrix form as follows:

$$
\mathbf{X} = \begin{pmatrix}
x_{11}^1 & x_{12}^1 & \cdots & x_{1L}^1 & x_{11}^2 & \cdots & x_{1L}^2 & \cdots & x_{11}^N & \cdots & x_{1L}^N \\
\vdots & \vdots & \ddots & \vdots & \vdots & \ddots & \vdots & \ddots & \vdots & \ddots & \vdots \\
x_{i1}^1 & x_{i2}^1 & \cdots & x_{iL}^1 & x_{i1}^2 & \cdots & x_{iL}^2 & \cdots & x_{i1}^N & \cdots & x_{iL}^N \\
\vdots & \vdots & \ddots & \vdots & \vdots & \ddots & \vdots & \ddots & \vdots & \ddots & \vdots \\
x_{n1}^1 & x_{n2}^1 & \cdots & x_{nL}^1 & x_{n1}^2 & \cdots & x_{nL}^2 & \cdots & x_{n1}^N & \cdots & x_{nL}^N
\end{pmatrix} \in \mathcal{M}_{n \times (N \cdot L)}(\mathbb{R}) \quad (2.1)
$$

$$
= \left(\mathbf{X}^1 \mid \mathbf{X}^2 \mid \cdots \mid \mathbf{X}^N \right)
$$

where $\mathcal{M}_{n \times (N \cdot L)}(\mathbb{R})$ is the vector space of $n \times (N \cdot L)$ matrices over $\mathbb{R}$ and $N \in \mathbb{N}$ is the number of sensors. It is worth noting that each row vector $\mathbf{X}(i,:) \in \mathbb{R}^{N \cdot L}$, $i = 1, \ldots, n$ of matrix $\mathbf{X}$ in equation (2.1) represents the measurements from all the sensors at a given experimental trial. Similarly, each column vector $\mathbf{X}(:,j) \in \mathbb{R}^n$, $j = 1, \ldots, N \cdot L$, contains measurements from one sensor at one specific time instant in the whole set of experimental trials.

As stated before, one of the goals of PCA is to *eliminate* the redundancies in the original data. This objective is achieved through a linear transformation orthogonal matrix

$$\mathbf{P} \in \mathcal{M}_{(N \cdot L) \times (N \cdot L)}(\mathbb{R})$$

that is used to transform or project the original data matrix $\mathbf{X}$ in equation (2.1) according to the matrix product:

$$\mathbf{T} = \mathbf{X}\mathbf{P} \in \mathcal{M}_{n \times (N \cdot L)}(\mathbb{R})$$

where the resulting matrix $\mathbf{T}$ has a diagonal covariance matrix.

2.2.2.2 Normalization: Group Scaling

Since the data in matrix $\mathbf{X}$ come from several sensors and could have different magnitudes and PCA is not invariant to scale, a preprocessing stage must be applied to rescale the data. This normalization is based on the mean of all measurements of the sensor at the same time instant and the standard deviation of all measurements of the sensor. In this sense, for $k = 1, \ldots, N$ we define

$$\mu_j^k = \frac{1}{n}\sum_{i=1}^{n} x_{ij}^k, \ j = 1, \ldots, L, \tag{2.2}$$

$$\mu^k = \frac{1}{nL}\sum_{i=1}^{n}\sum_{j=1}^{L} x_{ij}^k, \tag{2.3}$$

$$\sigma^k = \sqrt{\frac{1}{nL}\sum_{i=1}^{n}\sum_{j=1}^{L}(x_{ij}^k - \mu^k)^2}, \tag{2.4}$$

where μ_j^k is the mean of the measures placed at the same column, that is, the mean of the n measures of sensor k in matrix $\mathbf{X}^k$ at time instants $(j-1)\,\Delta$ seconds; μ^k is the mean of all the elements in matrix $\mathbf{X}^k$, that is, the mean of all the measures of sensor k; and σ^k is the standard deviation of all the measures of sensor k. Then, the elements x_{ij}^k of matrix $\mathbf{X}$ are scaled to define a new matrix $\check{\mathbf{X}}$ as

$$\check{x}_{ij}^k := \frac{x_{ij}^k - \mu_j^k}{\sigma^k}, \ i = 1, \ldots, n, \ j = 1, \ldots, L, \ k = 1, \ldots, N. \tag{2.5}$$

For the sake of simplicity, the scaled matrix $\check{\mathbf{X}}$ is renamed again as $\mathbf{X}$. One of the properties of the scaled matrix $\mathbf{X}$ is that it is mean-centered [2.20]. Consequently, the covariance matrix of $\mathbf{X}$ can be defined and computed as:

$$\mathbf{C_X} = \frac{1}{n-1}\mathbf{X}^T\mathbf{X} \in \mathcal{M}_{(N \cdot L) \times (N \cdot L)}(\mathbb{R}). \tag{2.6}$$

The subspaces in PCA are defined by the eigenvectors and eigenvalues of the covariance matrix as follows:

$$\mathbf{C_X}\mathbf{P} = \mathbf{P}\Lambda \tag{2.7}$$

where the columns of $\mathbf{P} \in \mathcal{M}_{(N \cdot L) \times (N \cdot L)}(\mathbb{R})$ are the eigenvectors of $\mathbf{C_X}$ and are defined as the *principal components*. The diagonal terms of matrix $\Lambda \in \mathcal{M}_{(N \cdot L) \times (N \cdot L)}(\mathbb{R})$ are the eigenvalues λ_i, $i = 1, \ldots, N \cdot L$, of $\mathbf{C_X}$ whereas the off-diagonal terms are zero, that is,

$$\Lambda_{ii} = \lambda_i, \ i = 1, \ldots, N \cdot L \tag{2.8}$$

$$\Lambda_{ij} = 0, \ i, j = 1, \ldots, N \cdot L, \ i \neq j \tag{2.9}$$

The goal of principal component analysis is twofold. On one hand, to eliminate the redundancies of the original data. This is achieved by transforming the original data through the projection defined by matrix $\mathbf{P}$ in equation (2.7). On the other, a second goal is to reduce the dimensionality of the data set $\mathbf{X}$. This second objective is achieved by selecting only a limited number $\ell < N \cdot L$ of principal components related to the ℓ highest eigenvalues. In this manner, given the reduced matrix

$$\hat{\mathbf{P}} = (p_1|p_2|\cdots|p_\ell) \in \mathcal{M}_{N \cdot L \times \ell}(\mathbb{R}), \tag{2.10}$$

matrix $\hat{\mathbf{T}}$ is defined as

$$\hat{\mathbf{T}} = \mathbf{X}\hat{\mathbf{P}} \in \mathcal{M}_{n \times \ell}(\mathbb{R}). \tag{2.11}$$

2.2.2.3 Projection of new data onto the PCA model

The current structure to inspect is excited by the same signal as the one that excited the healthy one in Section 2.2.2.1. Therefore, when the measures are obtained from $N \in \mathbb{N}$ sensors during $(L-1)\Delta$ seconds and $\nu \in \mathbb{N}$ experimental trials, a new data matrix $\mathbf{Y}$ is constructed as in

equation (2.1):

$$\mathbf{Y} = \begin{pmatrix} y_{11}^1 & y_{12}^1 & \cdots & y_{1L}^1 & y_{11}^2 & \cdots & y_{1L}^2 & \cdots & y_{11}^N & \cdots & y_{1L}^N \\ \vdots & \vdots & \ddots & \vdots & \vdots & \ddots & \vdots & \ddots & \vdots & \ddots & \vdots \\ y_{i1}^1 & y_{i2}^1 & \cdots & y_{iL}^1 & y_{i1}^2 & \cdots & y_{iL}^2 & \cdots & y_{i1}^N & \cdots & y_{iL}^N \\ \vdots & \vdots & \ddots & \vdots & \vdots & \ddots & \vdots & \ddots & \vdots & \ddots & \vdots \\ y_{v1}^1 & y_{v2}^1 & \cdots & y_{vL}^1 & y_{v1}^2 & \cdots & y_{vL}^2 & \cdots & y_{v1}^N & \cdots & y_{vL}^N \end{pmatrix} \in \mathcal{M}_{v \times (N \cdot L)}(\mathbb{R}) \quad (2.12)$$

It is worth noting, at this point, that the natural number v (the number of rows of matrix $\mathbf{Y}$) is not necessarily equal to n (the number of rows of $\mathbf{X}$), but the number of columns of $\mathbf{Y}$ must agree with that of $\mathbf{X}$; that is, in both cases the number N of sensors and the number of time instants L must be equal.

Before the collected data arranged in matrix $\mathbf{Y}$ is projected into the new space spanned by the eigenvectors in matrix $\mathbf{P}$ in equation (2.7), the matrix has to be scaled to define a new matrix $\check{\mathbf{Y}}$ as in equation (2.5):

$$\check{y}_{ij}^k := \frac{y_{ij}^k - \mu_j^k}{\sigma^k}, \ i = 1, \ldots, v, \ j = 1, \ldots, L, \ k = 1, \ldots, N, \quad (2.13)$$

where μ_j^k and σ^k are the real numbers defined and computed in equations (2.2) and (2.4), respectively.

The projection of each row vector $r^i = \check{\mathbf{Y}}(i,:) \in \mathbb{R}^{N \cdot L}, i = 1, \ldots, v$ of matrix $\check{\mathbf{Y}}$ into the space spanned by the eigenvectors in $\hat{\mathbf{P}}$ is performed through the following vector to matrix multiplication:

$$t^i = r^i \cdot \hat{\mathbf{P}} \in \mathbb{R}^\ell. \quad (2.14)$$

For each row vector $r^i, i = 1, \ldots, v$, the first component of vector t^i is called the *first score* or *score* 1; similarly, the second component of vector t^i is called the *second score* or *score* 2, and so on.

2.2.3 Machine learning

Machine learning has revolutionized the way that complex problems has been tackled with the help of computer programs. In the incessant and relentless pursuit of best tools for data analysis, machine learning has been highlighted for its capability for providing a quite remarkable set of strategies for pattern recognition. More precisely, when a deterministic mathematical model is difficult to define and data has, at first glance, no correlation, these pattern recognition techniques are generally able to find some kind of relationship. Machine learning strategies and bio-inspired algorithms allow to avoid this difficulty through mechanisms designed to find the

answer by themselves. In SHM or related areas, it is possible to find some applications about how machine learning has been used to detect problems such as breaks, corrosion, cracks, impact damage, delamination, disunity, breaking fibers (some pertinent to metals and the others to composite materials) [2.21]. In addition, machine learning has been also used to provide information about the future behavior of a structure under extreme events such as earthquakes [2.22].

Depending on how the algorithms are implemented, machine learning can be classified in two main approaches: unsupervised and supervised learning. In the first case, the information is grouped and interpreted using uniquely the input data. However, to perform the learning task in the second case, information about the output data is required. Figure 2.1 shows this classification and includes information about the kind of tasks that can be performed – clustering, classification, regression –.
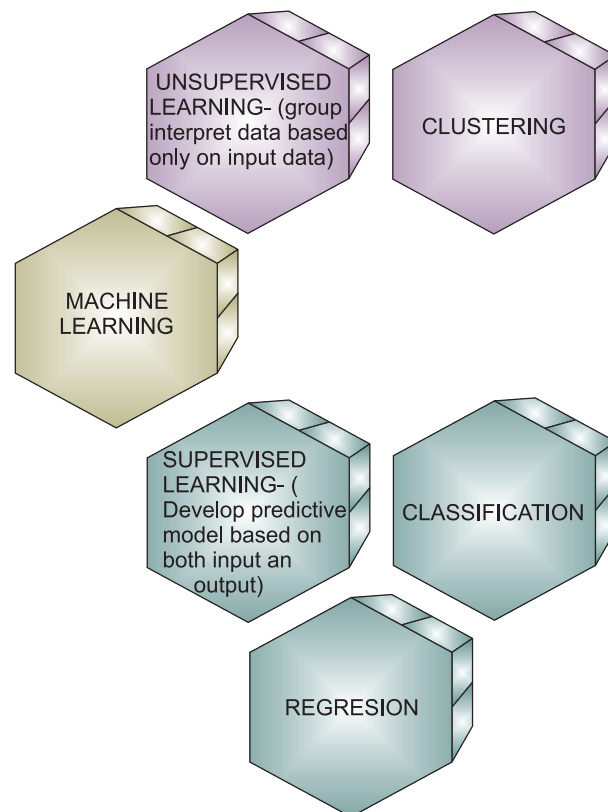
FIGURE 2.1: Classification of the Machine learning approaches according to the learning.

This paper is focused on the use of a supervised learning approach and, particularly, in the use of nearest neighbor classification.A brief description of the nearest neighbor pattern classification is introduced in the following subsection.

2.2.4 Nearest neighbor pattern classification

The nearest neighbor (NN) is a simple nonparametric and highly efficient technique [2.23] that has been used in several areas such as pattern recognition, ranking models or text categorization and classification for big data [2.24, 2.25], just to name a few. One of the most used algorithms in machine learning applications is the *k*-NN also known as *k*-nearest neighbors. *k*-NN outstands due to its simplicity and the excellent results obtained when this technique is applied to diverse problems [2.26]. This algorithm works by using an input vector with the *k* closest training samples in the feature space. To perform the classification, the algorithm identify the most common class among the *k* nearest neighbors. The algorithm requires a training to define the neighbors based on the distance from the test sample and a testing step to determine the class to which this test sample belong [2.26].

The number of neighbors can be changed to adjust the *k*-NN algorithm. In this sense, for instance, the use of one neighbor is known as fine *k*-NN and a coarse *k*-NN uses 100 neighbors. Many neighbors can be time consuming to fit. There are six different *k*-NN classifiers available in Matlab that can be used to classify data [2.27], and these classifiers are based on different distances. Some of them –fine, medium and coarse *k*-NN algorithms– make use of the Euclidean distance to determine the nearest neighbors. According to Matlab, each classifier works as follows [2.26]:

- Fine *k*-NN: A nearest neighbor classifier that makes finely-detailed distinctions between classes with the number of neighbors set to 1.

- Medium *k*-NN: A nearest neighbor classifier with fewer distinctions than a Fine *k*-NN with the number of neighbors set to 10.

- Coarse *k*-NN: A nearest neighbor between classes, with the number of neighbors set to 100.

- Cosine *k*-NN: A nearest neighbor classifier that uses the cosine distance metric. The cosine distance between two vectors u and v is defined as

$$1 - \frac{u \cdot v}{|u| \cdot |v|},$$

  that is, one minus the ratio of the inner product of u and v over the product of the norms of u and v.

- Cubic *k*-NN: A nearest neighbor classifier that uses the cubic distance metric. The cubic distance between two *n*-dimensional vectors u and v is defined as

$$\sqrt[3]{\sum_{i=1}^{n} |u_i - v_i|^3}.$$

47

- Weighted k-NN: A nearest neighbor classifier that uses distance weighting. The weighted Euclidean distance between two n-dimensional vectors u and v is defined as

$$\sqrt{\sum_{i=1}^{n} w_i(x_i - y_i)^2},$$

where $0 < w_i < 1$ and $\sum_{i=1}^{n} w_i = 1$.

k-NN has been used successfully in fault detection for gas sensor arrays [2.24], classification for big data [2.28], fault detection and classification for high voltage DC transmission lines [2.26], traffic state prediction [2.29], among others.

2.3 Structural Health Monitoring (SHM) System

2.3.1 Hardware of the SHM System

The inspection system considers the use of a sensor network which is distributed on the surface of the structure. In this work, piezoelectric sensors are used. However, the methodology that is is introduced here is suitable for several kind of vibration sensors. This is because the system considers the use of a baseline with signals from the structure in a healthy state and the analysis is performed by the comparison of the new experiments under the same conditions (guided waves) with the baseline. The piezoelectric sensor network works in several actuation phases. Each actuation phase is defined by the use of a PZT as actuator and the rest of the piezoelectrics are used as sensors. This information is collected and organized in a matrix per actuator. Therefore, the measured signals are organized from sensor 1 to sensor N for N sensors as it can be seen in Figure 2.10. To this goal, a Tie Pie arbitrary wave generator (HS5) is used and a signal –as in Figure 2.2– is applied. This signal is defined because it has a collection of signals in a reduced bandwidth that ensures that the acquired signal does not have as many components as to make it difficult to hide the damage. The specifications of the signal are: 8 volts of amplitud and a frequency of 10 kHz.
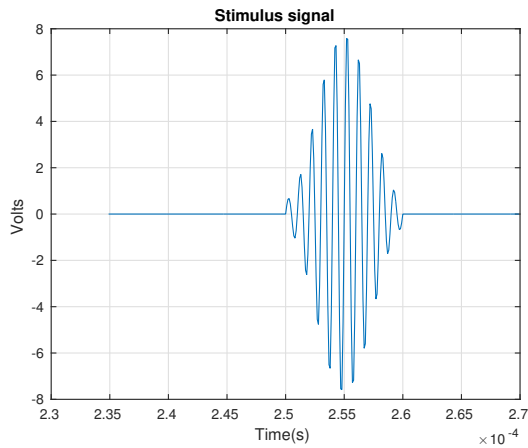
FIGURE 2.2: Excitation signal applied to the piezoelectric acting as actuator, in each actuation phase.

Figure 2.3 presents the captured and organized signals for an aluminum plate instrumented with six sensors. It shows the actuation phase 1 (PZT 1 as actuator and the rest of PZTs as sensors). These signals are captured by two oscilloscopes from Tie Pie company (HS4) from each sensor at a rate of up to 2 millions of samples per second, and each channel contributes with signals of 60000 samples. Figure 2.3 shows the result of the organization in the pre-processing step. As it can be observed, there is a continuous signal that corresponds to the concatenation of the five signals measured by the PZT acting as sensors.
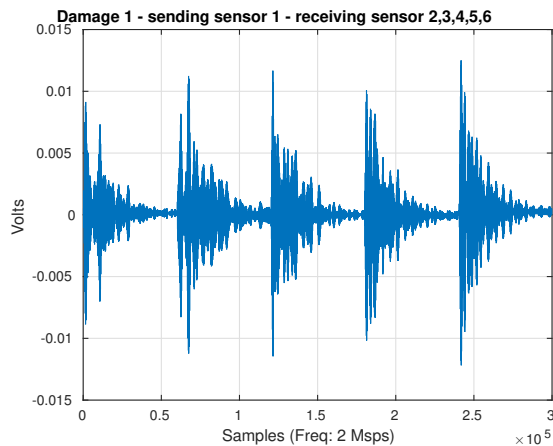
FIGURE 2.3: Received signals in the actuation phase 1 when damage 1 is performed to the structure.

Due to the fact that the system only considers the use of an arbitrary waveform generator (HS5) with one channel, a multiplexer card was developed (Figure 2.4). This system works by connecting the analog input with one of the analog outputs defined by software.

(a) Multiplexor circuit   (b) Multiplexor model
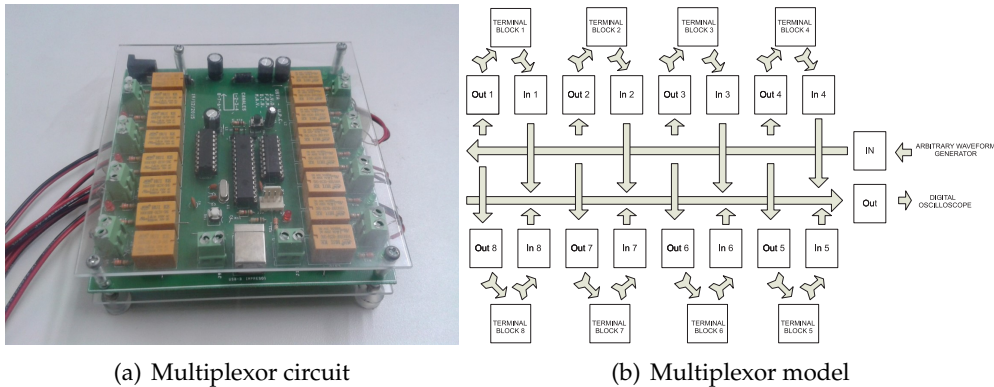
FIGURE 2.4: Multiplexor system used in the data acquisition system.

Similarly, with the multiplexer card it is possible to provide a direct way to the digitizers, which are, also in this case, from the company Tie Pie and with reference HS04. These devices are 4 channel oscilloscopes with 14 bit resolution. In this work, two devices are used to involve eight channels. However, and depending on the necessities, it is possible to add more of these devices.

Figure 2.5 shows the general schema of the hardware in the SHM system. To sum up, the system defines one PZT as actuator, the arbitrary wave generator applies a known signal (Figure 2.6), then the signal is converted into a mechanical wave (lamb waves) and transferred to the structure. This wave travels superficially all across the structure interacting with the damage and the elements presented on the surface. The sensors convert the mechanical wave into an electric signal and the digitizer collect the signals propagated thought the structure in the rest of the sensors. Depending on the kind of structure, the system may require a power amplifier to amplify the signals applied to the actuators and to ensure a good captured information.
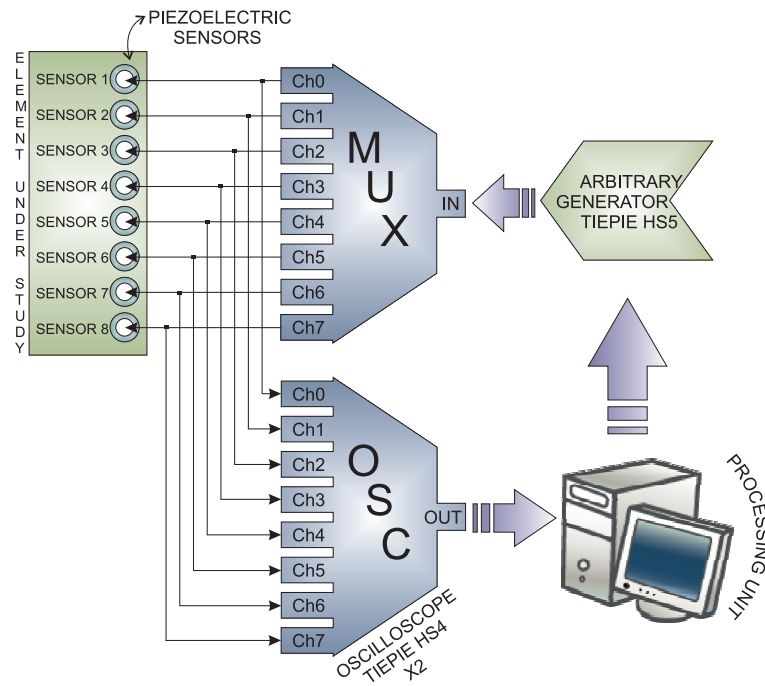
FIGURE 2.5: Representation of the structural health monitoring (SHM) system.
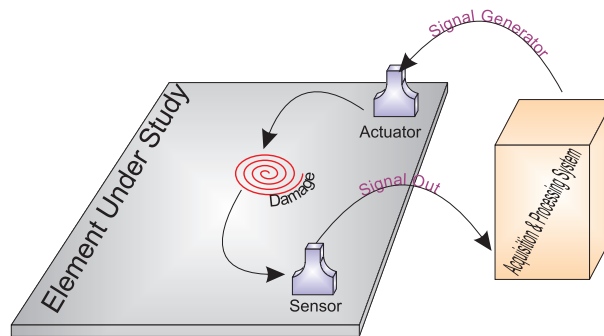
FIGURE 2.6: General scheme of the SHM system.

2.3.2 Software of the SHM System

The methodology is based on a pattern recognition perspective. In this sense, the strategy is considered to have two different steps. On one hand, in the first step, a pattern is developed with the signals from the structure in a healthy and damaged states as it is shown in Figure 2.7–. To do that, the collected signals are pre-processed and organized by each actuation phase as it was previously explained. These signals require the pre-processing in order to be comparable because the data comes from different places of the structure and are acquired with different amplitude values. In this case, group-scaling normalization is applied as detailed in Section 2.2.2.2. To define the pattern or the baseline, a feature vector is obtained by each actuation

phase. A huge number of possible features can be extracted from the signals. In particular, the use of multivariate methods such as principal component analysis has proven to be very useful to perform this task. In the classification process, and since *k*-NN is a supervised learning algorithm, different known damage and data from the healthy state are used to train the *k*-NN machines.
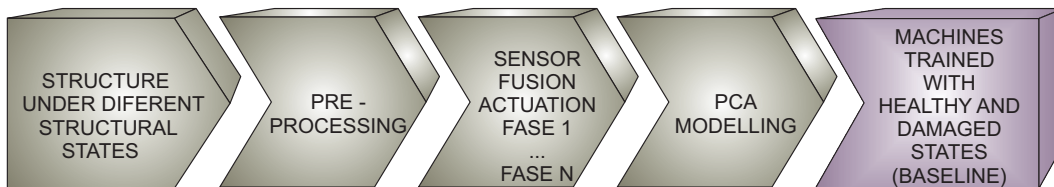
FIGURE 2.7: Training process with the data from the structure under different structural states.

On the other hand, the second step corresponds to the testing. In this phase, the trained maps are used as a pattern whereas experiments from the structure in unknown states are used to classify the current state of the structure –as it is shown in Figure 2.8–. The procedure to acquire and process the information is the same as in the development of the pattern. That is, the system digitize the information from the sensors and thereafter the data is organized and pre-processed. In order to reduce the noise and to normalize the data a Savitzky–Golay filter is applied. Subsequetly the sensor data fusion is applied to organize the information by each actuation phase. Finally, principal component analysis is applied and the resulting projections are used to define the feature vectors that will be the inputs to the machine learning approach.
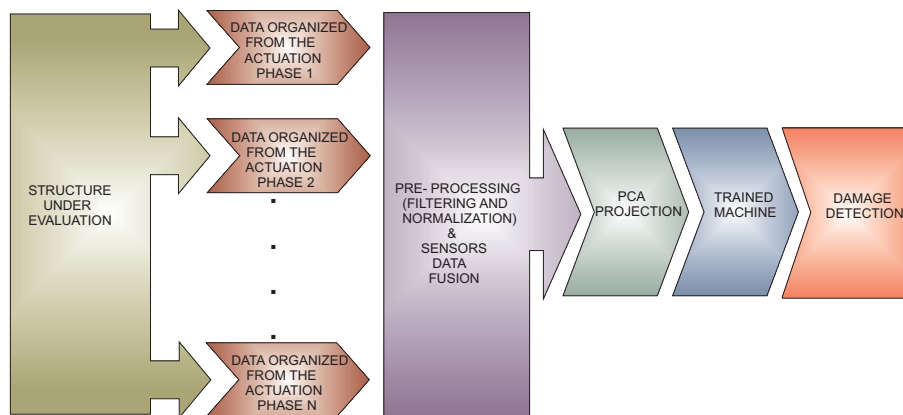
FIGURE 2.8: Testing step with data from the structure in an unknown structural state.

The sensor data fusion takes also place in two steps: In the first stage –data acquisition and organization–, a single PZT is used as an actuator and the data collected from the rest of the piezoelectric transducers installed in the structure are used and organized in a vector. With this strategy, the information on how the sensors sense the damage –by each actuation

phase– is available. In a second stage, an experiment from each actuation phase is extracted and organized in a matrix, as shown in the Figure 2.13. After that, PCA is applied to this matrix to obtain a reduced version of these data, which is organized in a vector and submitted to a machine learning algorithm. Assembling the feature vectors by each actuation phase and the use of these vectors in the machine allows to analyze the information from all the actuation phases in a single machine. This process allows a reduction in the number of variables or figures that are needed to analyze or to organize all the information.

Figure 2.9 provides a general outline of the training process and the testing step (online execution or off-line execution). The system has the capability to detect and classify damage in off-line mode. To work in this mode, the state is stored in a file an the software loads this information to apply the methodology. Otherwise, the system works in online mode when the data is acquired, analyzed and the result of the evaluation is provided in a short time.
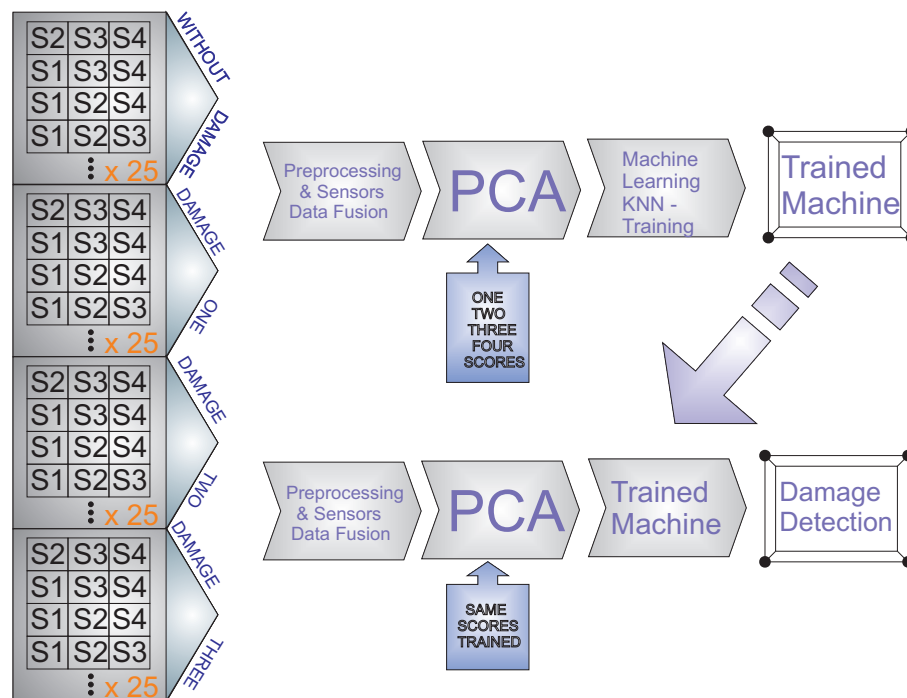
FIGURE 2.9: Data organization and Testing step for damage detection and classi-
fication.

A distinguishing feature of the work that is presented in this paper with respect to previous works [2.18, 2.30] is the way the data is organized and arranged. With the data organization as in Figure 2.10, we provide the structural health monitoring system all the sensor data fusion that includes information from all the actuation phases. More precisely, and with respect to Figure 2.10, a structure instrumented with six piezoelectric transducers is considered. As it can be observed in the left side of this figure, five structural states are considered: four different kind of damage and the healthy state. Since there are six actuation phases, these phases are

used to build 5 matrices corresponding to each structural state. Each matrix is organized as follows: the first row contains the information from the actuation phase 1; the second row include the information from the actuation phase 2; and so on for the rest of the actuation phases. In this case, 25 experiments were performed by each structural state by each actuation phase. Consequently, each matrix consist of a number of rows equal to 25 experiment $\times$ 6 actuation phases $=$ 150 rows and 5 columns. It is necessary to highlight that each column contains the collected samples from each sensor.
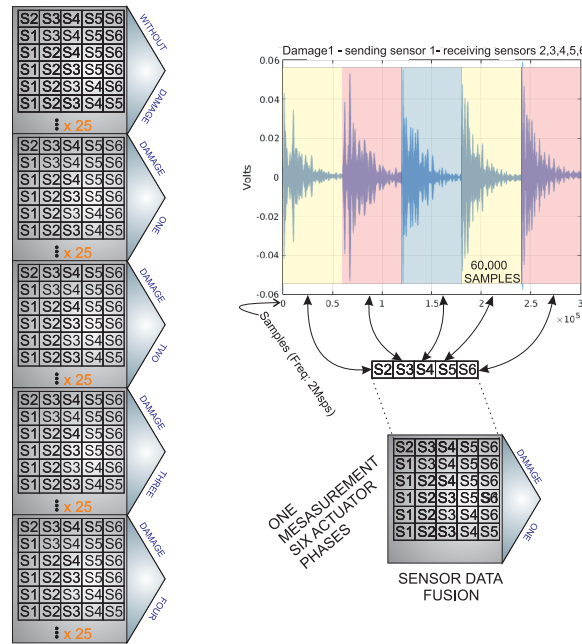
FIGURE 2.10: Data organization for sensor data fusion.

2.4 Experimental Setup and Results

In this paper, three specimens (structures) are used to demonstrate the feasibility of the structural health monitoring system introduced in Section 2.3. These three specimens are:

(i) An aluminum rectangular profile with a sensor network formed by six piezoelectric transducers bonded on both sides of the profile –see Figure 2.11–;

(ii) An aluminum plate with four piezoelectric transducers –see Figure 2.23–;

(iii) Composite plate of carbon fiber polymer with six piezoelectric transducers –see Figure 2.29–.

These structures have a different shape. Besides, both the size and number of piezoelectric transducers installed in theses structures and the number and location of the damage are different.

Damage were simulated by adding a mass to the structure in different positions and 25 experiments were performed by each case (structural state), interpreting *case* as damage one, damage two, damage three, damage four or the absence of damage.

The classification is performed considering six classifiers from Matlab Statistics and Machine Learning Toolbox:

- *Fine k-NN*

- *Medium k-NN*

- *Coarse k-NN*

- *Cosine k-NN*

- *Cubic k-NN*

- *Weighted k-NN*

We consider this selection of classifiers since these kind of machines are recommended to solve problems with data as the one used in this paper. For this reason, this toolbox is used to train the machines, so the number of *k*-nearest neighbors is defined by the different classifiers as detailed in Section 2.2.4.

2.4.1 First specimen: aluminum rectangular profile

The first specimen that we consider in this paper is an aluminum rectangular profile that is instrumented with six piezoelectric sensors. The distribution of the piezoelectric transducers and the size and geometry of the specimen are shown in Figure 2.11. This Figure also specifies the position of the fourdamage.
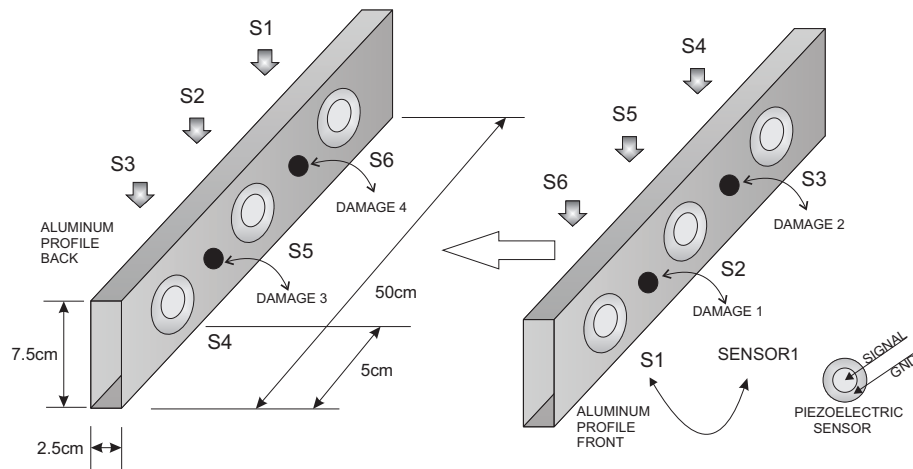
FIGURE 2.11: Aluminum rectangular profile instrumented with 6 piezoelectric sensors.

Figure 2.12 shows a composition of photographies of the experiment where the four different kind of damage can be observed. As it can also be seen from the pictures, the specimen is isolated from the noise and vibration –from different sources– that affect the laboratory. Isolation from possible external perturbations is critical since the noise and vibration could lead the structural health monitoring system to erroneous results.

Damage 1

Damage 2

Damage 3

Damage 4

FIGURE 2.12: Aluminum rectangular profile instrumented with 6 piezoelectric sensors.

The feature vector is formed by the projections or *scores* of the original data into the PCA model created as described in Section 2.2.2.1 and illustrated in Figure 2.13. The performance of the machines will be compared as a function of the number of scores that are considered. In general, the number of scores that have to be used depends on the cumulative contribution of variance that it is accounted for. More precisely, if the *i*-th score is related to the eigenvector p_i –defined in equation (2.10)– and the eigenvalue λ_i –in equation (2.8)–, the cumulative contribution rate of variance accounted for the first $\sigma \in \mathbb{N}$ scores is defined as

$$\frac{\sum_{i=1}^{\sigma} \lambda_i}{\sum_{i=1}^{\ell} \lambda_i}, \tag{2.15}$$

where $\ell \in \mathbb{N}$ is the number of principal components. In this sense, the cumulative contribution

of the first five scores is depicted in Figure 2.14. It can be seen that the first two principal components account for 50% of the variance while the first three principal components account for almost 75% and the first four account for 90%. *A priori*, better results should be obtained if we use as many principal components as possible. However, in some cases, as reported in the literature [2.31, 2.32], less principal components may lead to more accurate results.
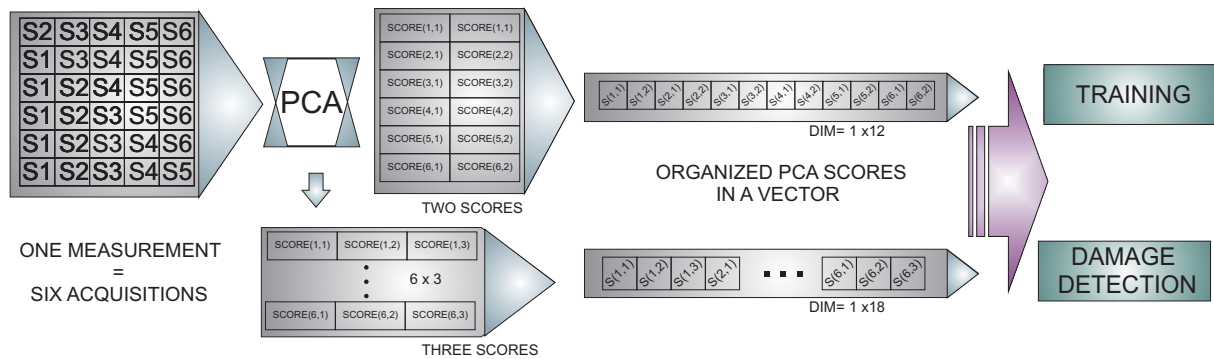
FIGURE 2.13: Feature vector organization.
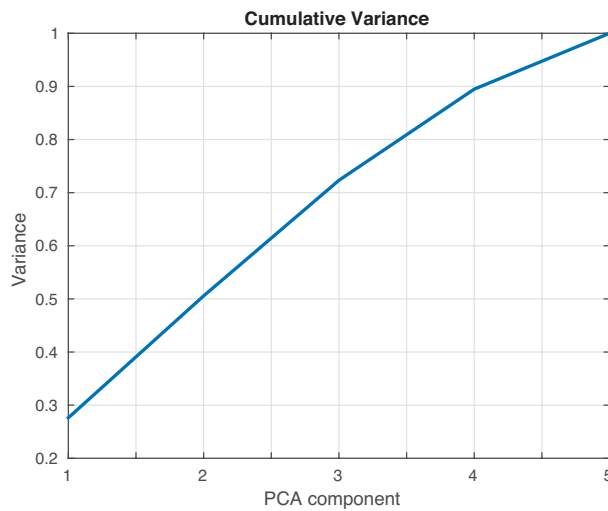
FIGURE 2.14: Cumulative contribution rate of variance accounted for the principal components.

Figures 2.15 to 2.17 show the classification results per machine or classifier where just the first score is used in the training process. These results include experiments where the damage are slightly displaced with respect to the original placement of the damage. The results with maximum accuracy in the classification are obtained when considering the weighted k-NN, the fine k-NN and the cosine k-NN classifiers. For instance, in the weighted k-NN classifier, 101 cases have been correctly classified out of 125 cases. This magnitude represents a 81% of correct decisions. It is worth noting that, in all the machines, the specimen with no damage is correctly classified in the totality of the cases. Similarly, all the machines are able to separate

the structure with no damage with respect to the structure with damage, with the exception of the coarse k-NN. In this case, the coarse k-NN fail to distinguish between the structure with damage and the structure with no damage in 14 out of 100 cases.

(a) Fine k-NN
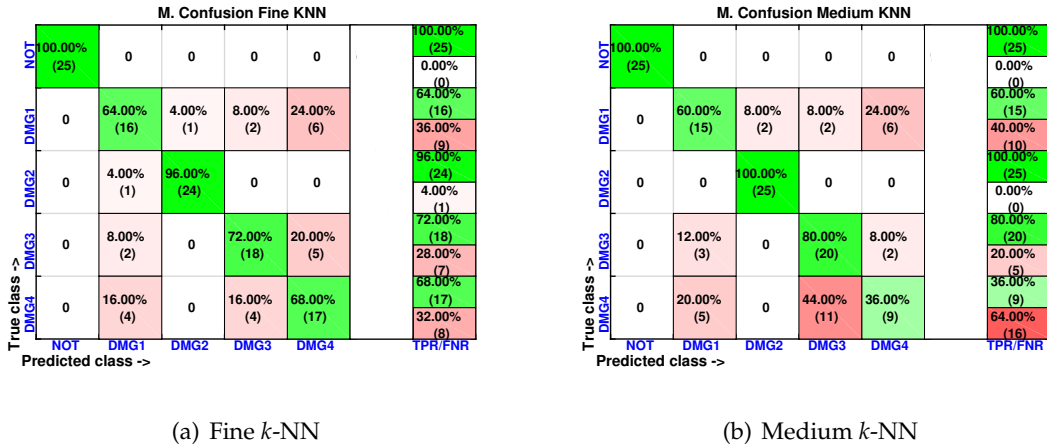
(b) Medium k-NN

FIGURE 2.15: Confusion matrix using fine k-NN and medium k-NN when the feature vector is formed by the first principal component.

(a) Coarse k-NN
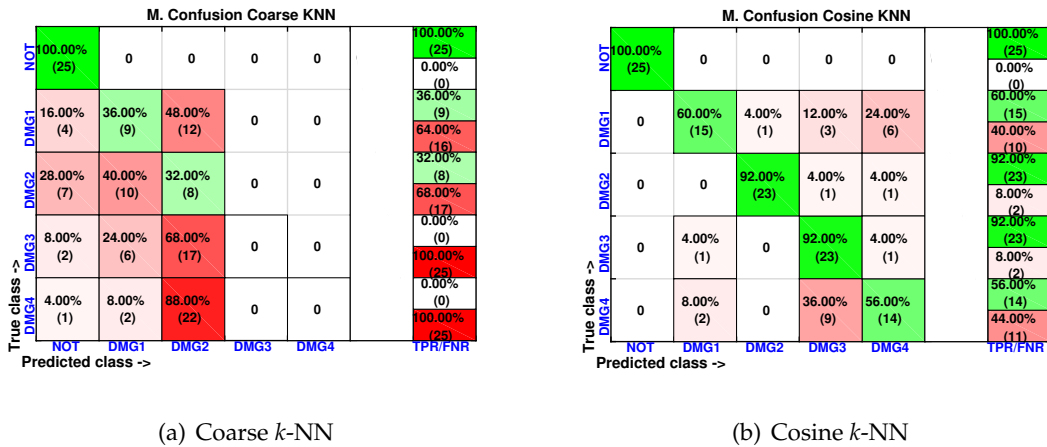
(b) Cosine k-NN

FIGURE 2.16: Confusion matrix using coarse k-NN and cosine k-NN when the feature vector is formed by the first principal component.

(a) Cubic *k*-NN
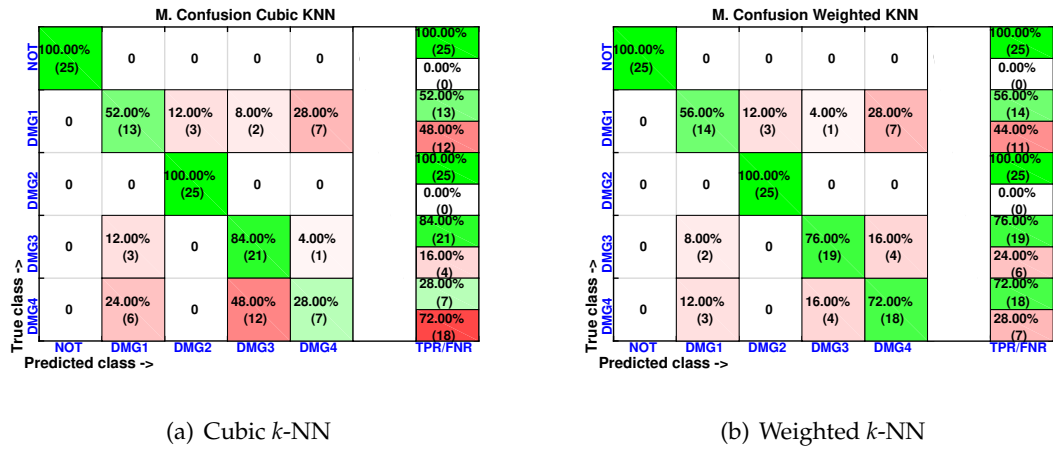
(b) Weighted *k*-NN

FIGURE 2.17: Confusion matrix using cubic *k*-NN and weighted *k*-NN when the feature vector is formed by the first principal component.

In order to analyze the effect of the inclusion of more scores in the feature vector, the confusion matrices are calculated again for two of the best classifiers (weighted *k*-NN and fine *k*-NN) and with feature vectors of one, two, three and four scores. The results for the weighted *k*-NN classifier can be found in Figures 2.18 and 2.19 whereas those corresponding to the fine *k*-NN classifier are summarized in Figures 2.20 and 2.21.

(a) Weighted *k*-NN (one score)

(b) Weighted *k*-NN (two scores)
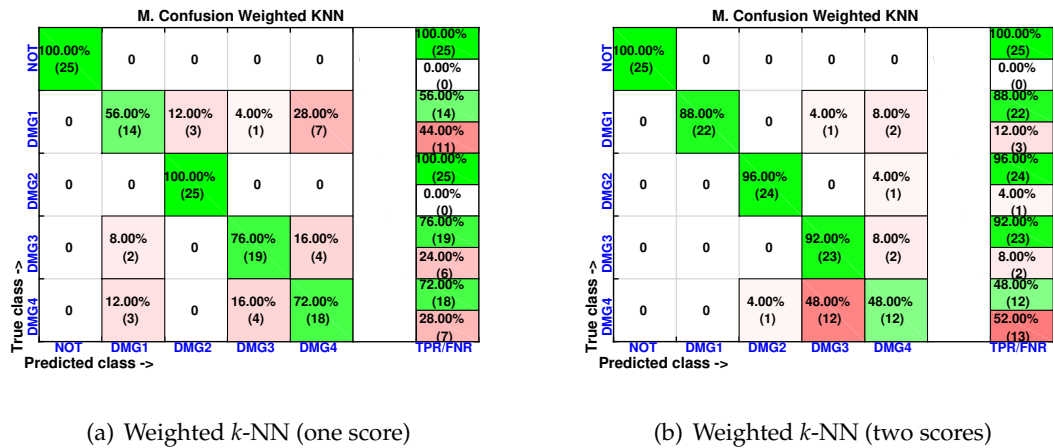
FIGURE 2.18: Confusion matrix using weighted *k*-NN when the feature vector is formed by the first principal component (left) or by the first two principal components (right).

It may seem surprising that the best results are obtained in this case when just two scores are used to define the feature vector. More precisely, in the weighted *k*-NN classifier, 106 cases have been correctly classified out of 125 cases while in the fine *k*-NN classifier, this number rises up to 112 cases. This represents, 85% and 90% of correct decisions, respectively. It is also

M. Confusion Weighted KNN

True class ↓ / Predicted class →	NOT	DMG1	DMG2	DMG3	DMG4	TPR/FNR
NOT	100.00% (25)	0	0	0	0	100.00% (25) / 0.00% (0)
DMG1	0	60.00% (15)	20.00% (5)	8.00% (2)	12.00% (3)	60.00% (15) / 40.00% (10)
DMG2	0	0	100.00% (25)	0	0	100.00% (25) / 0.00% (0)
DMG3	0	4.00% (1)	0	60.00% (15)	36.00% (9)	60.00% (15) / 40.00% (10)
DMG4	0	0	0	24.00% (6)	76.00% (19)	76.00% (19) / 24.00% (6)

(a) Weighted *k*-NN (three scores)

M. Confusion Weighted KNN

True class ↓ / Predicted class →	NOT	DMG1	DMG2	DMG3	DMG4	TPR/FNR
NOT	100.00% (25)	0	0	0	0	100.00% (25) / 0.00% (0)
DMG1	0	60.00% (15)	20.00% (5)	0	20.00% (5)	60.00% (15) / 40.00% (10)
DMG2	0	4.00% (1)	92.00% (23)	0	4.00% (1)	92.00% (23) / 8.00% (2)
DMG3	0	4.00% (1)	0	60.00% (15)	36.00% (9)	60.00% (15) / 40.00% (10)
DMG4	0	4.00% (1)	4.00% (1)	36.00% (9)	56.00% (14)	56.00% (14) / 44.00% (11)

(b) Weighted *k*-NN (four scores)

FIGURE 2.19: Confusion matrix using weighted *k*-NN when the feature vector is formed by the first three principal component (left) or by the first four principal components (right).

M. Confusion Fine KNN

True class ↓ / Predicted class →	NOT	DMG1	DMG2	DMG3	DMG4	TPR/FNR
NOT	100.00% (25)	0	0	0	0	100.00% (25) / 0.00% (0)
DMG1	0	64.00% (16)	4.00% (1)	8.00% (2)	24.00% (6)	64.00% (16) / 36.00% (9)
DMG2	0	4.00% (1)	96.00% (24)	0	0	96.00% (24) / 4.00% (1)
DMG3	0	8.00% (2)	0	72.00% (18)	20.00% (5)	72.00% (18) / 28.00% (7)
DMG4	0	16.00% (4)	0	16.00% (4)	68.00% (17)	68.00% (17) / 32.00% (8)

(a) Fine *k*-NN (one score)

M. Confusion Fine KNN

True class ↓ / Predicted class →	NOT	DMG1	DMG2	DMG3	DMG4	TPR/FNR
NOT	100.00% (25)	0	0	0	0	100.00% (25) / 0.00% (0)
DMG1	0	96.00% (24)	4.00% (1)	0	0	96.00% (24) / 4.00% (1)
DMG2	0	4.00% (1)	92.00% (23)	0	4.00% (1)	92.00% (23) / 8.00% (2)
DMG3	0	0	0	80.00% (20)	20.00% (5)	80.00% (20) / 20.00% (5)
DMG4	0	0	0	20.00% (5)	80.00% (20)	80.00% (20) / 20.00% (5)

(b) Fine *k*-NN (two scores)

FIGURE 2.20: Confusion matrix using fine *k*-NN when the feature vector is formed by the first principal component (left) or by the first two principal components (right).

worth noting that in the eight different scenarios that we have considered (two classifiers and four different sizes of the feature vector), the structure with no damage is correctly classified in the whole set of experiments. Similarly, the structure with damage is never confused with the structure with no damage. This means that the errors that appear in the classification are only due to a mistake in the identification of the damage.

The first principal component versus the second principal component are depicted in Figure 2.22. It can be observed that a clear separation exists between the structure with no damage and the structure with the different kind of damage. This is one of the reasons of the fact that
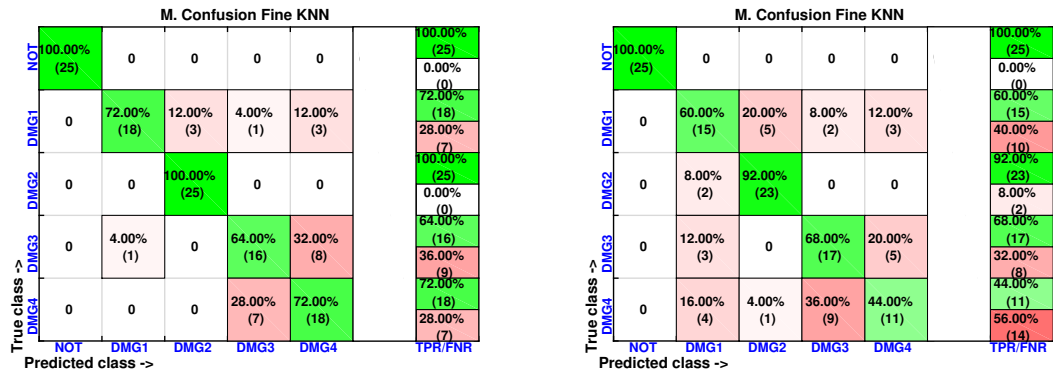
(a) Fine *k*-NN (three scores)

(b) Fine *k*-NN (four scores)

FIGURE 2.21: Confusion matrix using fine *k*-NN when the feature vector is formed by the first three principal component (left) or by the first four principal components (right).

the classifier performs quite well in terms of damage detection. However, from this figure, it is not possible to separate or classify the different damage, therefore showing the clear benefit of the use of a machine learning approach.

Finally, and back to the issue of the number of principal components that are used to define the feature vector, Mujica *et al.* [2.31] have already observed that, sometimes, the second principal component is often more effective to obtain accurate results in the damage detection or classificiation, contrarily with what it is expected. Similarly, an excessive number of principal components used to define the feature vector may lead to less good results since the SHM system may insert in the system part of the noise that we are trying to avoid.
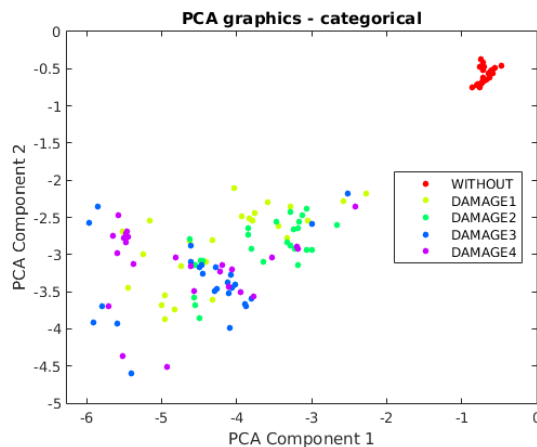
FIGURE 2.22: First principal component versus second principal component in the aluminum rectangular profile described in Section 2.4.1.

2.4.2 Second specimen: aluminium plate

The second experimental validation was performed using an aluminium plate with an area of 40 cm × 40 cm and instrumented with four piezoelectric sensors as shown in Figure 2.23. This figure also indicates the location of the three damage that are presented in the structure.
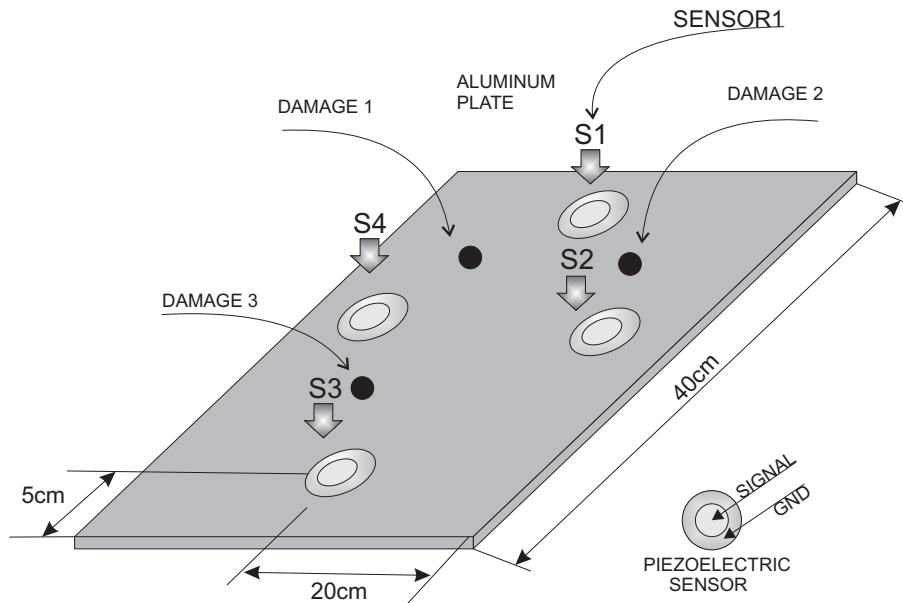
FIGURE 2.23: Aluminum plate instrumented with 4 piezoelectric sensors.

Figure 2.24 shows a composition of photographies of the experiment where the three different kind of damage and the structure with no damage can be observed. As it can be seen from the pictures, the specimen is also isolated from the noise and vibration that affect the laboratory.

As in Section 2.4.1, the cumulative contribution of the first three scores is depicted in Figure 2.25. It can be seen that the first two principal components account for 82% of the variance, so we will use in this case the first two principal component analysis to create the feature vector. Figure 2.26 show the classification result for the fine *k*-NN and the weighted *k*-NN machines. In both classifiers, 93 cases have been correctly classified out of 100 cases. Besides, as with the previous specimen, the aluminium plate with no damage is correctly classified in the totality of the cases and no confusion is made between the structure with no damage and the structure with damage.

We have also included, in Figure 2.27, the machines with the lowest accuracy in the classification. These classifiers are the coarse *k*-NN and the cosine *k*-NN. Although the percentage of correct decisions fluctuate between 72% and 100%, the cosine *k*-NN machine is still able to accurately identify the structure with no damage, and coarse *k*-NN had the worst performance.

Also in this case, the first principal component versus the second principal component are depicted in Figure 2.28. It can be observed that a clear separation exists between the aluminum

plate with no damage and the plate with the different kind of damage. However, from this figure, it is not possible to separate or classify the different damage, therefore showing the clear benefit of the approach used in this work.

Damage 1

Damage 2

Damage 3

No Damage
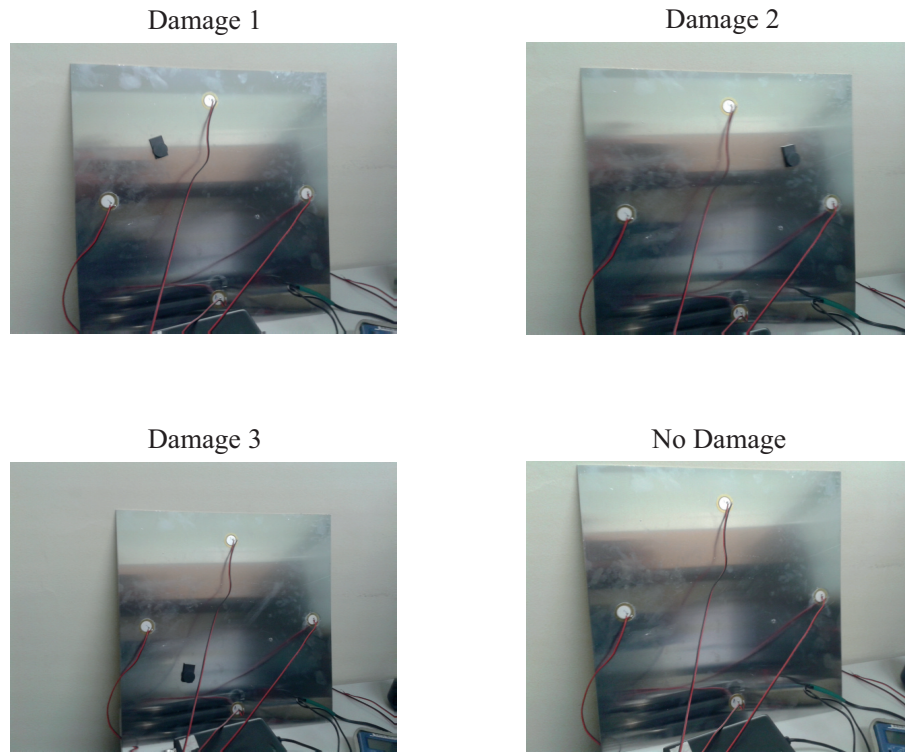
FIGURE 2.24: Experimental setup for the aluminum plate instrumented with 4 piezoelectric sensors.
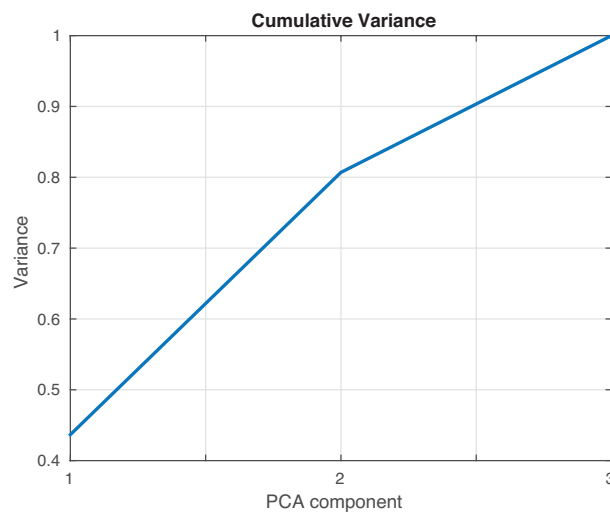
FIGURE 2.25: Cumulative contribution rate of variance accounted for the principal components from the data acquired from the aluminum plate.

(a) Fine *k*-NN (two scores)

(b) Weighted *k*-NN (two scores)
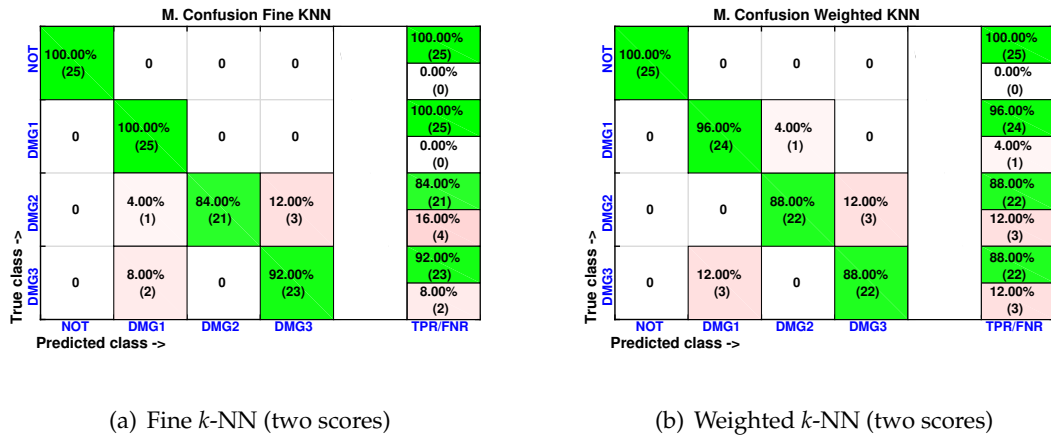
FIGURE 2.26: Confusion matrix using fine *k*-NN (left) and weighted *k*-NN (right) when the feature vector is formed by the first two principal components.

(a) Coarse *k*-NN (two scores)

(b) Cosine *k*-NN (two scores)
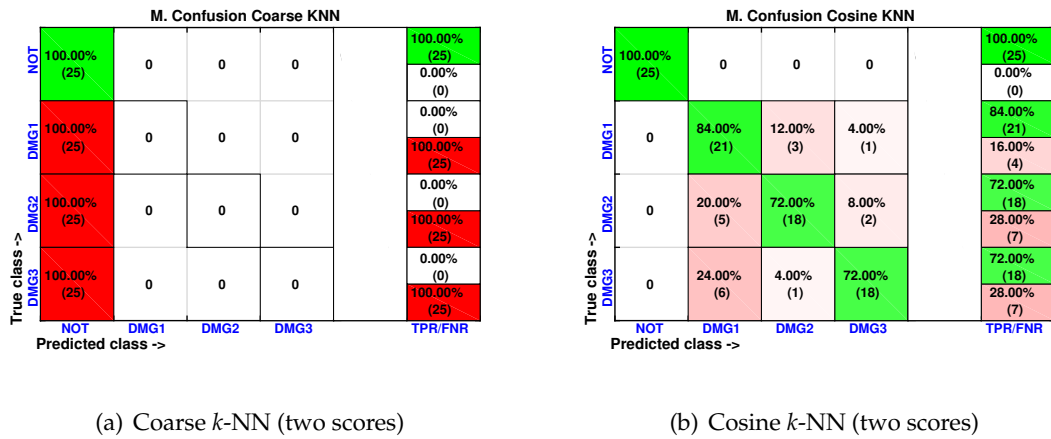
FIGURE 2.27: Confusion matrix using coarse *k*-NN (left) and cosine *k*-NN (right) when the feature vector is formed by the first two principal components.
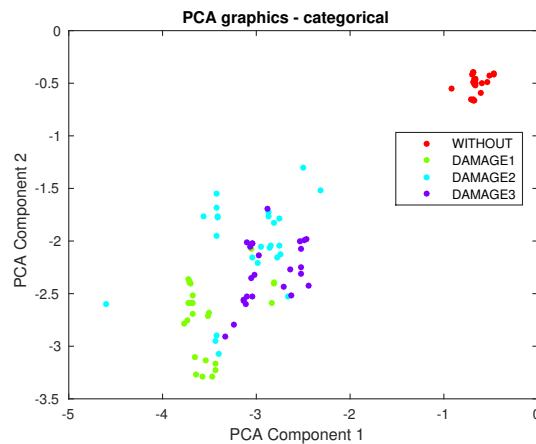
FIGURE 2.28: First principal component versus second principal component in the aluminum plate described in Section 2.4.2.

2.4.3   Third specimen: Composite plate - carbon fiber

The third specimen used for the experimental validation of the approach presented in this paper is a composite plate of carbon fiber polymer with an area of 50 cm × 25 cm, and 2 mm of thickness. The plate is instrumented with six piezoeletric transducers as shown in Figure 2.29. The Figure also illustrates the location of the three damage that are placed in the structure.

Figure 2.30 shows a composition of images of the experiment with the distribution of the sensors and the vibration isolation similar to that of the previous specimens.

As in Sections 2.4.1 and 2.4.2, the cumulative contribution of the first three scores is depicted in Figure 2.31. It can be seen that the first two principal components account for about 80% of the variance, so we will use again in this case the first two principal component analysis to create the feature vector. Figure 2.32 shows the classification result for the fine *k*-NN and the weighted *k*-NN machines. In both classifiers, 92 and 91 cases have been correctly classified out of 100 cases, respectively. These results are consistent with the results in Sections 2.4.1 and 2.4.2 since these two classifiers present the best accuracy in the classification. Besides, as with the previous specimen, the aluminium plate with no damage is correctly classified in the totality of the cases and no confusion is made between the structure with no damage and the structure with damage.

In Figure 2.33 we have also summarized the results of the coarse *k*-NN and cosine *k*-NN, that are the classifiers with the lowest accuracy in the classification approach. In particular, the coarse *k*-NN classifies all the structures with damage as undamaged and therefore making this strategy impractical to detect and classify damage.

Finally, the first principal component versus the second principal component are plotted in Figure 2.34. It can be observed that, again, a clear separation exists between the composite plate with no damage and the plate with the different kind of damage. However, it is not possible to separate or classify the different damage, therefore showing the clear benefit of the classifiers used in this work.
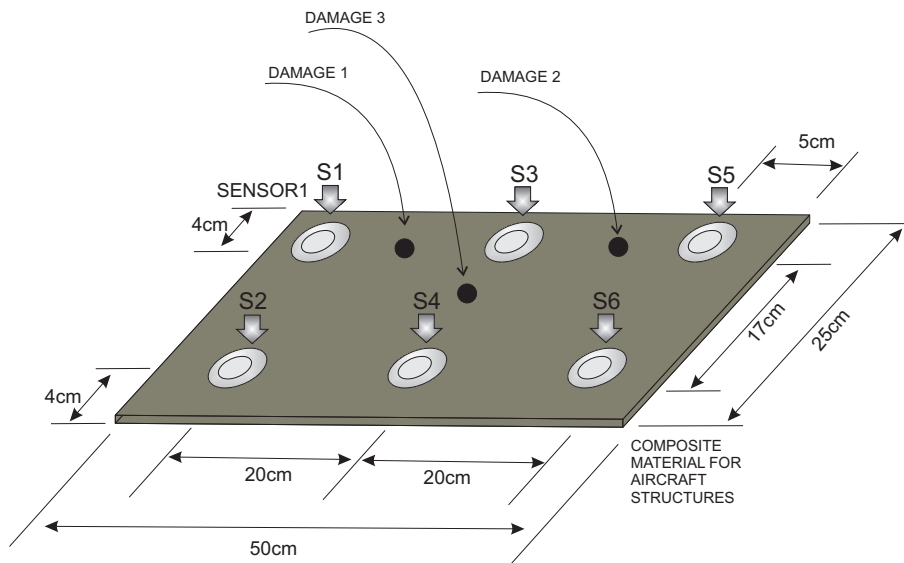
FIGURE 2.29: Composite plate instrumented with six piezoelectric sensors.
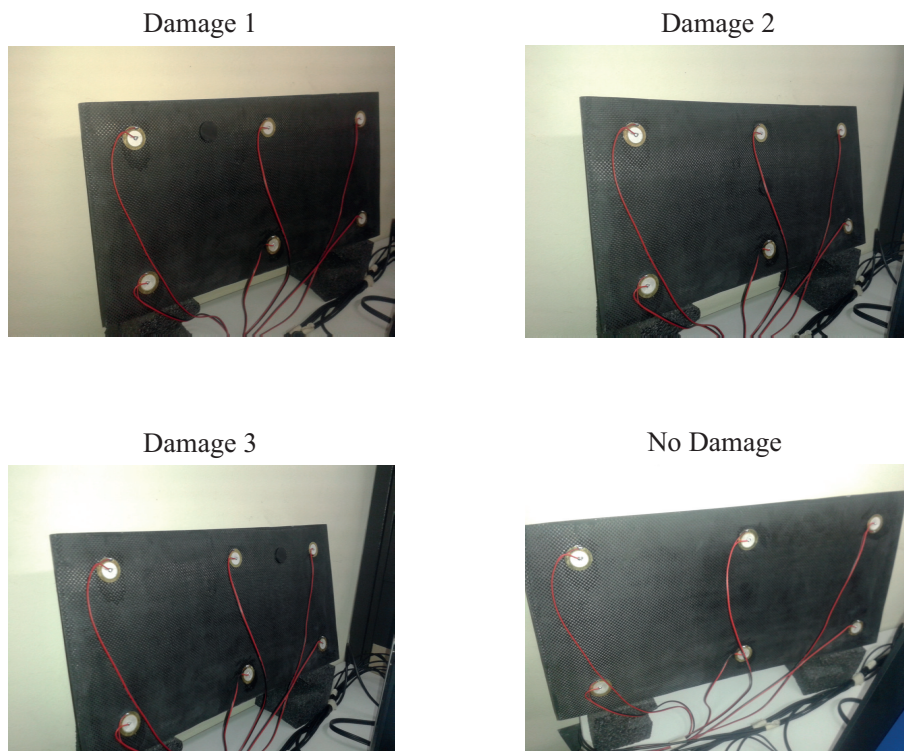
FIGURE 2.30: Experimental setup for the composite plate instrumented with 6 piezoelectric sensors.
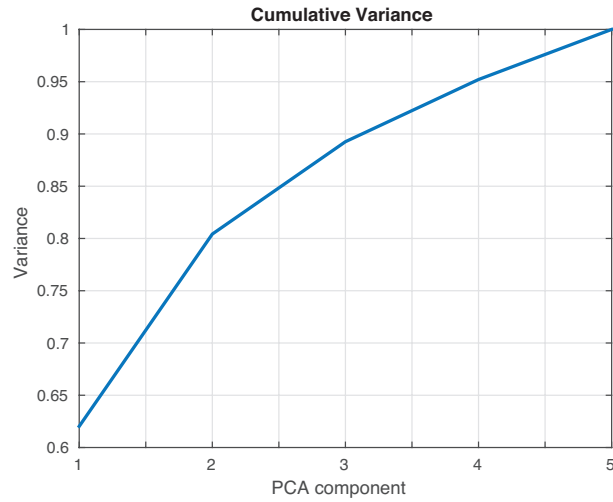
FIGURE 2.31: Cumulative contribution rate of variance accounted for the principal components from the data acquired from the composite plate.
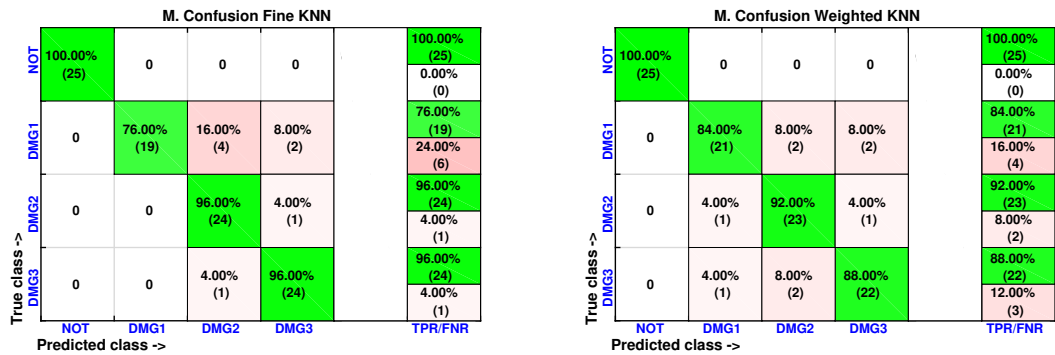
(a) Fine *k*-NN (two scores)

(b) Weighted *k*-NN (two scores)

FIGURE 2.32: Confusion matrix using fine *k*-NN (left) and weighted *k*-NN (right) when the feature vector is formed by the first two principal components.

M. Confusion Coarse KNN

True class ->	NOT	DMG1	DMG2	DMG3	TPR/FNR
NOT	100.00% (25)	0	0	0	100.00% (25) / 0.00% (0)
DMG1	100.00% (25)	0	0	0	0.00% (0) / 100.00% (25)
DMG2	100.00% (25)	0	0	0	0.00% (0) / 100.00% (25)
DMG3	100.00% (25)	0	0	0	0.00% (0) / 100.00% (25)
Predicted class ->	NOT	DMG1	DMG2	DMG3	TPR/FNR

M. Confusion Cosine KNN

True class ->	NOT	DMG1	DMG2	DMG3	TPR/FNR
NOT	100.00% (25)	0	0	0	100.00% (25) / 0.00% (0)
DMG1	0	88.00% (22)	4.00% (1)	8.00% (2)	88.00% (22) / 12.00% (3)
DMG2	0	16.00% (4)	60.00% (15)	24.00% (6)	60.00% (15) / 40.00% (10)
DMG3	0	4.00% (1)	4.00% (1)	92.00% (23)	92.00% (23) / 8.00% (2)
Predicted class ->	NOT	DMG1	DMG2	DMG3	TPR/FNR
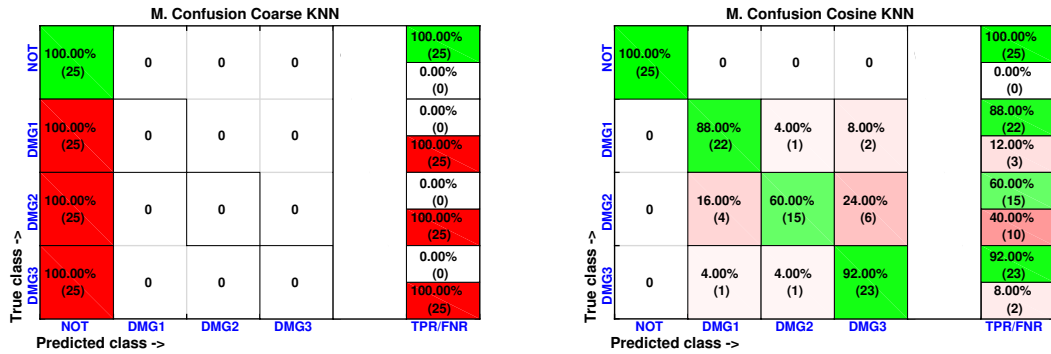
(a) Coarse *k*-NN (two scores)   (b) Cosine *k*-NN (two scores)

FIGURE 2.33: Confusion matrix using coarse *k*-NN (left) and cosine *k*-NN (right) when the feature vector is formed by the first two principal components.
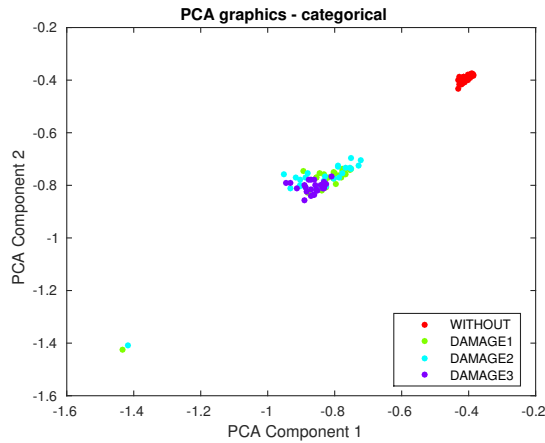
FIGURE 2.34: First principal component versus second principal component in the composite plate described in Section 2.4.3.

2.5 Concluding remarks

In this contribution a method to inspect a structure and evaluate possible damage with a piezoelectric sensor network and a machine learning approach is introduced. Results from three specimens –an aluminum rectangular profile, an aluminum plate and a composite plate– showed that just two scores were enough to detect and classify all the structural states with a very high accuracy. In addition, it is possible to conclude that the best results were obtained with fine *k*-NN and weighted *k*-NN, since the number of correct decisions fluctuate between 85% and 93%. It is worth remarking that for both the fine *k*-NN and weighted *k*-NN and for all

the three specimens, the structure with no damage is correctly classified in the totality of the cases.

Some features to highlight in the structural health monitoring system are: (i) the methodology use data-driven approaches and no physical models. This element allow to determine directly from the data the presence of a damage and to determine what kind of damage; (ii) this is a multivariable approach, in the sense that in the analysis there are measurements from all the sensors distributed along the structure; and finally, (iii) the approach is based on sensor data fusion. This element is key to obtain a final pattern by merging the results from each actuation phase. This element allows a simplified analysis in larger structures with a large number of sensors.

Another aspect in the methodology that has to be highlighted is the development of a new data organization scheme. This scheme allows the sensor data fusion to perform offering the opportunity to develop analysis of the structures in online mode since one measurement is not related with others and the methodology is able to offer immediately results as soon as they are computed. One of the possible problems with the system is the computational burden of the procedure if the calculations are to be performed in a portable equipment.

The piezoelectric active system has allowed to inspect the structures under diagnosis by applying and collecting the signals propagated through the structure and the sensor data fusion provides robustness to the system given that it allows to have information from different locations of the structure. This procedure, however, shows some difficulties if the damage is not placed in the exact same location. Further developments will deal with these issues, where it seems possible to avoid this placement problems, training the machines –to create the baseline– with the enough number of experiments.

Acknowledgments

Conflict of interests

The authors declare no conflict of interest. The founding sponsors had no role in the design of the study; in the collection, analyses, or interpretation of data; in the writing of the manuscript, and in the decision to publish the results.

Abbreviations

The following abbreviations are used in this manuscript:

k-NN	*k*-nearest neighbors algorithm
PCA	Principal Component Analysis
PZT	Lead-zirconate-titanate
SHM	Structural Health Monitoring

Bibliography

[2.1] M. Anaya, D. A. Tibaduiza, M. A. Torres-Arredondo, F. Pozo, M. Ruiz, L. E. Mujica, J. Rodellar, and C.-P. Fritzen, "Data-driven methodology to detect and classify structural changes under temperature variations," *Smart Materials and Structures*, vol. 23, no. 4, p. 45006, 2014.

[2.2] D. Tibaduiza, M. Anaya, E. Forero, R. Castro, and F. Pozo, "A Sensor Fault Detection Methodology applied to Piezoelectric Active Systems in Structural Health Monitoring Applications," *IOP Conference Series: Materials Science and Engineering*, vol. 138, no. 1, 2016.

[2.3] I. Buethe and C.-p. Fritzen, "Investigation on Sensor Fault Effects of Piezoelectric Transducers on Wave Propagation and Impedance Measurements," 2013.

[2.4] F. Gharibnezhad, *Robust Damage Detection in Smart Structures*. PhD thesis, Universitat Politècnica de Catalunya, 2014.

[2.5] N. Dervilis, K. Worden, and E. J. Cross, "On robust regression analysis as a means of exploring environmental and operational conditions for SHM data," *Journal of Sound and Vibration*, vol. 347, pp. 279–296, 2015.

[2.6] H. Zhang, J. Guo, X. Xie, R. Bie, and Y. Sun, "Environmental Effect Removal Based Structural Health Monitoring in the Internet of Things," in *2013 Seventh International Conference on Innovative Mobile and Internet Services in Ubiquitous Computing*, pp. 512–517, 2013.

[2.7] R. Langone, E. Reynders, S. Mehrkanoon, and J. A. K. Suykens, "Automated structural health monitoring based on adaptive kernel spectral clustering," *Mechanical Systems and Signal Processing*, vol. 90, pp. 64–78, 2017.

[2.8] Q. P. He and J. Wang, "Fault Detection Using the k-Nearest Neighbor Rule for Semiconductor Manufacturing Processes," *IEEE Transactions on Semiconductor Manufacturing*, vol. 20, pp. 345–354, nov 2007.

[2.9] K. R. Mulligan, N. Quaegebeur, P.-C. Ostiguy, P. Masson, and S. Létourneau, "Comparison of metrics to monitor and compensate for piezoceramic debonding in structural health monitoring," *Structural Health Monitoring*, vol. 12, no. 2, pp. 153–168, 2013.

[2.10] G. Gui, H. Pan, Z. Lin, Y. Li, and Z. Yuan, "Data-driven support vector machine with optimization techniques for structural health monitoring and damage detection," *KSCE Journal of Civil Engineering*, vol. 21, pp. 523–534, feb 2017.

[2.11] W. Nick, N. C. A, T. U. State, J. Shelton, A. Esterline, N. C. A, T. S. U. N. C. A, T. S. U. N. C. A, and T. U. State, "A Study of Supervised Machine Learning Techniques for Structural Health Monitoring," *Proceedings of the 26th Modern Artificial Intelligence and Cognitive Science Conference (MAICS 2015)*, 2015.

[2.12] M. A. Torres-Arredondo, I. Buethe, D. A. Tibaduiza, J. Rodellar, and C.-P. Fritzen, "Damage detection and classification in pipework using acousto-ultrasonics and non-linear data-driven modelling," *Journal of Civil Structural Health Monitoring*, vol. 3, no. 4, pp. 297–306, 2013.

[2.13] D. A. Tibaduiza, L. E. Mujica, M. Anaya, J. Rodellar, and A. Güemes, "Independent Component Analysis for Detecting Damages on Aircraft Wing Skeleton," *European Conference on Structural Control*, no. June, 2012.

[2.14] G. Gautschi, *Piezoelectric Sensors*, pp. 73–91. Berlin, Heidelberg: Springer Berlin Heidelberg, 2002.

[2.15] Z. Vasicek and L. Sekanina, "On area minimization of complex combinational circuits using cartesian genetic programming," in *Evolutionary Computation (CEC), 2012 IEEE Congress on*, pp. 1–8, 2012.

[2.16] I. Jolliffe, *Principal component analysis*. Wiley Online Library, 2002.

[2.17] M. Anaya, D. A. Tibaduiza, and F. Pozo, "A bioinspired methodology based on an artificial immune system for damage detection in structural health monitoring," *Shock and Vibration*, vol. 2015, 2015.

[2.18] D. A. Tibaduiza, *Design and validation of a structural health monitoring system for aeronautical structures*. PhD thesis, Universitat Politècnica de Catalunya, Barcelona, Spain, 2012.

[2.19] D. H. Jeong, C. Ziemkiewicz, B. Fisher, W. Ribarsky, and R. Chang, "ipca: An interactive system for pca-based visual analytics," in *Computer Graphics Forum*, vol. 28, pp. 767–774, Wiley Online Library, 2009.

[2.20] F. Pozo and Y. Vidal, "Wind turbine fault detection through principal component analysis and statistical hypothesis testing," *Energies*, vol. 9, no. 1, p. 3, 2015.

[2.21] C. R. Farrar and K. Worden, *Structural health monitoring: a machine learning perspective*. John Wiley & Sons, 2012.

[2.22] C. C. Ciang, J.-R. Lee, and H.-J. Bang, "Structural health monitoring for a wind tur-bine system: a review of damage detection methods," *Measurement Science and Technology*, vol. 19, no. 12, p. 122001, 2008.

[2.23] T. Cover and P. Hart, "Nearest neighbor pattern classification," *IEEE transactions on in-formation theory*, vol. 13, no. 1, pp. 21–27, 1967.

[2.24] J. Yang, Z. Sun, and Y. Chen, "Fault detection using the clustering-knn rule for gas sensor arrays," *Sensors*, vol. 16, no. 12, p. 2069, 2016.

[2.25] S. Dhanabal and S. Chandramathi, "A review of various k-nearest neighbor query pro-cessing techniques," *International Journal of Computer Applications*, vol. 31, no. 7, pp. 14–22, 2011.

[2.26] J. Johnson and A. Yadav, "Weak and electromagnetic interactions," in *Proceedings of the International Conference on ICT for Sustainable Development (ICT4SD)*, 2016.

[2.27] MathWorks, Natick, MA, USA, *Statistics and Machine Learning Toolbox for Matlab*, 2015.

[2.28] Z. Deng, X. Zhu, D. Cheng, M. Zong, and S. Zhang, "Efficient knn classification algo-rithm for big data," *Neurocomputing*, vol. 195, pp. 143–148, 2016.

[2.29] S. Oh, Y.-J. Byon, and H. Yeo, "Improvement of search strategy with k-nearest neighbors approach for traffic state prediction," *IEEE Transactions on Intelligent Transportation Systems*, vol. 17, no. 4, pp. 1146–1156, 2016.

[2.30] D. A. Tibaduiza, L. E. Mujica, and J. Rodellar, "Damage classification in structural health monitoring using principal component analysis and self-organizing maps," *Structural Control and Health Monitoring*, vol. 20, pp. 1303–1316, oct 2013.

[2.31] L. Mujica, M. Ruiz, F. Pozo, J. Rodellar, and A. Güemes, "A structural damage detection indicator based on principal component analysis and statistical hypothesis testing," *Smart materials and structures*, vol. 23, no. 2, p. 025014, 2013.

[2.32] F. Pozo, I. Arruga, L. E. Mujica, M. Ruiz, and E. Podivilova, "Detection of structural changes through principal component analysis and multivariate statistical inference," *Structural Health Monitoring*, vol. 15, no. 2, pp. 127–142, 2016.

Chapter 3

Distributed Piezoelectric Sensor System for Damage Identification in Structures Subjected to Temperature Changes

Publishing information

Contents

Distributed Piezoelectric Sensor System for Damage Identification in Structures Subjected to Temperature Changes

abstract

Structural health monitoring (SHM) is a very important area in a wide spectrum of fields and engineering applications. With a SHM system it is possible to reduce the number of non necessary inspection tasks, the associated risk and the maintenance cost in a wide range of structures during its lifetime. One of the problems in the detection and classification of damage are the constant changes in the operational and environmental conditions. Small changes on these conditions can be considered by the SHM system as damage even though the structure is healthy. Several applications for monitoring of structures has been developed and reported in the literature and some of them include temperature compensation techniques. In real applications, however, digital processing technologies have proven their value by: (i) offering a very interesting way to acquire information from the structures under test; (ii) applying methodologies to provide a robust analysis; and (iii) performing a damage identification with a practical useful accuracy. This work shows the implementation of a SHM system based on the use of piezoelectric (PZT) sensors for inspecting a structure subjected to temperature changes. The methodology includes the use of multivariate analysis, sensor data fusion and machine

learning approaches. The methodology is tested and evaluated with aluminum and composite structures that are subjected to temperature variations. Results show that damage can be detected and classified in all the cases in spite of the temperature changes

Keywords: machine learning; principal component analysis; piezoelectric sensors; temperature variations, damage classification

3.1   Introduction

The variability in the dynamic properties of a structure in service can be the result of time-varying environmental and operational conditions [3.1]. This variability is mainly one of the causes of an inaccurate damage identification process when the analysis of a structure is performed based on data-driven algorithms [3.2]. From this point of view, it is possible to affirm that the variability of environmental and operational conditions is one of the intrinsic features of the design of a structural health monitoring system [3.3].

There are many magnitudes to consider in the design of a structural health monitoring system. For instance, temperature, temperature gradients, humidity, wind or traffic [3.4]. When these factors are not considered, the results may mask or conceal the changes of the structure. Therefore, the diagnosis provided by the structural health monitoring system will not be accurate. For this reason, when designing a structural health monitoring system, it is very important to propose algorithms or methodologies that can cope with this environmental and operational conditions. The final goal is to offer an accurate damage identification process even improving the security of the structure and reducing the time and cost of its associated maintenance [3.5].

At present, it is possible to find some works in the literature that consider the effect of the environmental and operational variations. One of the most applied strategies to deal with these kind of variations is principal component analysis (PCA). One of the main advantages of PCA is their ability to reduce the dimensionality of data, which is particularly useful when this data is collected from multiple sensors. In this sense, multivariate analysis has been proven to be effective for damage detection and classification [3.6, 3.7]. In the same way, PCA is useful to perform linear analysis when it is assumed that the effect on the vibration features of the structure of the environmental conditions is linear or weakly non-linear [3.4]. PCA has also been used in combination with some other techniques or strategies. For instance, Torres-Arrendondo *et al.* [3.8] considers jointly discrete wavelet transform –for feature extraction and selection–, linear principal component analysis –for data-driven modelling– and self-organising maps – for a two-level clustering under the principle of local density– for temperature compensation in acousto-ultrasonics. Leichtle *et al.* [3.9] applies principal component analysis jointly with *k*-means clustering for discrimination of changed and unchanged buildings as a method for unsupervised change detection in dynamic urban environment. PCA has also been applied as

a way to characterize the feature vector that defines the antigens and the antibodies in an artificial immune system conceived to detect damage in structures under temperature variations [3.10]. The robust version of singular value decomposition (SVD), which is closely related to principal component analysis, has been used in [3.11] to compute the distance of an observation to the subspace spanned by the intact measurements. The distance to the subspace is therefore used to determine the presence of a damage.

Structural health monitoring strategies that do not consider principal component analysis include, for instance, the work by Deraemaeker *et al.* [3.12], where the damage detection strategy is uniquely based on vibration measurements under changing environmental conditions. More precisely, two features are considered based on the measurements: eigenproperties of the structure and peak indicators that are computed on the Fourier transform (FT) of modal filters. The effects of the changing environment are handled using factor analysis and damage is detected by means of Shewhart-*T* control charts. Similarly, Balmès *et al.* [3.13] propose a nonparametric damage detection where it is assumed that several data sets are recorded on the safe structure at different and unknown temperatures. Finally, the approach smoothes out the temperature effect using an averaging operation.

Buren *et al.* [3.14] address the damage detection problem combining three technologies to guarantee the robustness of a structural condition monitoring system subjected to environmental variability. One of these technologies is a time series algorithm that is trained with baseline data with three objectives: (a) to predict the vibration response; (b) to compare predictions to actual measurements collected on a damaged structure; and (c) to calculate a damage indicator. In this work [3.14], the robustness analysis is performed propagating the uncertainty through the time series algorithm and computing the equivalent deviation of the damage indicator.

Similarly as with PCA, time series analysis can also be combined with some other strategies, such as neural networks and statistical inference to develop damage classification strategies including ambient variations of the system. For instance, Sohn *et al.* [3.15] developed an autoregressive and autoregressive with exogenous inputs (AR-ARX) model of the structure to extract damage-sensitive features, then used a neural network for data normalization and finally applied hypothesis testing to automatically infer the damage state of the system.

Several machine learning approaches have already been reported in the literature. For instance, it is possible to find the use of auto-associative neural network (AANN), factor analysis, Mahalanobis distance, and singular value decomposition [3.16] tested in a three-story frame structure where data is collected with accelerometers. Support vector machines (SVM) have also been applied for damage detection, localization and damage assessment in a Gnat trainer aircraft [3.17] showing the advantages in the use of machine learning approaches for damage identification. Some of these works, uses novelty detectors based on outlier analysis, density estimation and an auto-associative neural network [3.18, 3.19] for these applications. Unsupervised machine learning algorithms and physic based temperature compensation was also

explored by Roy *et al.* [3.20]. More precisely, Roy *et al.* [3.20] use a neural network based sparse autoencoder algorithm to learn the compressed representation of the data from sensors in order to localize damages in a structure with the Mahalanobis squared distance.

Previous works by the authors in this field include the use and development of multivariate analysis techniques, such as linear principal component analysis (PCA), non-linear PCA [3.7] and independent component analysis (ICA) to detect [3.21], classify and localize damage in structures [3.22]. In this paper, we present a structural health monitoring system based on [3.23] that is oriented to detect and classify damage of a structure subjected to temperature variations. The system works with data collected from a piezoelectric sensor network attached permanently to the structure, and it introduces the use of a new way to organize the data, multivariate data analysis techniques and machine learning analysis. Some contributions of this system are the use of sensor data fusion which introduces a different organization of the data and feature extraction vector for including temperature during the training process. This is a multivariate approach. This means that in the analysis there are measurements from all the sensors distributed all along the structure which offers a generalized analysis from different points of view by fusing data in a only result. This procedure allows to reduce the effect of the temperature in the damage detection and classification process when machine learning approaches are applied.

The structure of the paper is as follows: In Section 3.2, a brief description of the theoretical background required to construct the SHM system is presented. This background includes principal component analysis and machine learning approaches with special focus on how the three-way matrix with the collected data is unfolded to a two-way array. Section 3.3 describes the SHM system that is used to inspect the structures and the strategies that are applied to classify the damage in structures subjected to temperatures changes. In Section 3.4, the experimental setup is introduced together with exhaustive results. Finally, in Section 3.5, some concluding remarks are discussed.

3.2 Theoretical Background

3.2.1 Principal Component Analysis

One of the greatest difficulties in data analysis arises when the amount of data is very large and there is no apparent relationship between all the information or when this relationship is very difficult to find. In this sense, principal component analysis was born as a very useful tool to reduce and analyze a big quantity of information. Principal component analysis was described for the first time by Pearson in 1901, as a tool of multivariate analysis and was also used by Hotelling in 1933 [3.24]. This method allows to find the principal components, that are a reduced version of the original dataset and include relevant information that identify the reason for the variation between the measured variables. To find these variables, the analysis

includes the transformation of the data with respect to a current coordinate space to a new space in order to re-express the original data trying to reduce, filter or eliminate the noise and possible redundancies. These redundancies are measured by means of the correlation between the variables [3.25].

There are two mechanisms to implement the analysis of principal components: (i) the first method is based on correlations; and (ii) a second strategy that is based on the covariance. It is necessary to highlight that PCA is not invariant to scale, so the data under study must be normalized. Many methods can be used to perform this normalization as it is shown in [3.26, 3.25]. In many applications, PCA is also used as a tool to reduce the dimensionality of the data. Currently, there are several useful toolbox that implement PCA and analyze the reduced data provided by this strategy [3.27]. For the sake of completeness, the following Sections present a succinct description of the PCA modelling that includes how the measured data is arranged in matrix form. We also present the normalization procedure (group scaling) and how the new data to inspect is projected onto the PCA model.

3.2.1.1 PCA modelling

As stated in Section 3.2.1, one of the considerable difficulties in data analysis emerges when the quantity of data is very large. In a general case, typical data from a batch process may consist of N variables measured at L time instants for n batches or experimental trials. This data can be easily arranged in a three-way matrix $\mathbf{Z} \in \mathcal{M}_{n \times N \times L}(\mathbb{R})$ as represented in Figure 3.1 (top, left). However, to apply multivariate statistical techniques, such as principal component analysis (PCA), this three-way matrix $\mathbf{Z}$ must be unfolded to a two-way array. Westerhuis *et al.* [3.28] discussed profoundly how to unfold this three-way matrix and what were the effects of data normalization on the multivariate statistical techniques. One of the possibilities that are presented in [3.28] is depicted in Figure 3.1 (right), where the three-way matrix $\mathbf{Z} \in \mathcal{M}_{n \times N \times L}(\mathbb{R})$ is unfolded to a two-way matrix with $n \cdot L$ rows and N columns. This way, each of the N columns in the unfolded matrix still represent the N variables that are measured in the process.

However, in our application, we propose a quite different approach to unfold the original three-way matrix $\mathbf{Z}$. As it can be observed in Figure 3.1 (bottom, left), the three-way matrix $\mathbf{Z} \in \mathcal{M}_{n \times N \times L}(\mathbb{R})$ is unfolded to a two-way matrix with n rows and $N \cdot L$ columns. This way, the columns of the unfolded matrix no longer represent the variables but the measures of the variables at the different time instants. More precisely, the submatrix defined by taking the n rows and the first L columns represent the discretized measures of the first variable for the n batches or experimental trials; similarly, the submatrix defined by taking the n rows and columns $L+1$ to $2L$ represent the discretized measures of the second variable for the n batches or experimental trials. In general, then, the submatrix defined by taking the n rows

and columns $(l - 1) \cdot L + 1$ to $l \cdot L$ represent the discretized measures of the $l-$th variable for the n batches or experimental trials.
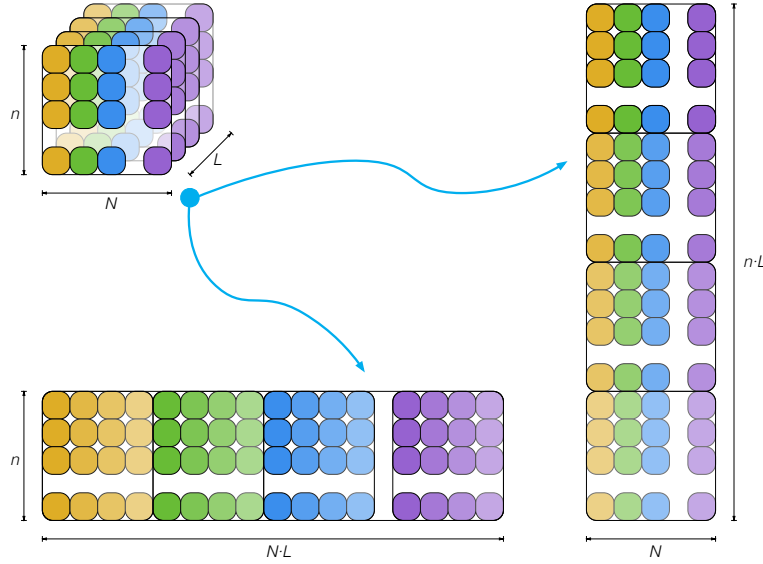
FIGURE 3.1: The three-way matrix $\mathbf{Z}$ can be unfolded to a two-way array in several ways.

The first step to build a PCA model is to measure, from a healthy structure, different sensors or variables during $(L - 1)\Delta$ seconds –where Δ is the sampling time– and $n \in \mathbb{N}$ experimental trials. The discretized measures of the sensors can be unfolded and arranged in matrix form as follows:

$$
\mathbf{X} = \begin{pmatrix}
x_{11}^1 & x_{12}^1 & \cdots & x_{1L}^1 & x_{11}^2 & \cdots & x_{1L}^2 & \cdots & x_{11}^N & \cdots & x_{1L}^N \\
\vdots & \vdots & \ddots & \vdots & \vdots & \ddots & \vdots & \ddots & \vdots & \ddots & \vdots \\
x_{i1}^1 & x_{i2}^1 & \cdots & x_{iL}^1 & x_{i1}^2 & \cdots & x_{iL}^2 & \cdots & x_{i1}^N & \cdots & x_{iL}^N \\
\vdots & \vdots & \ddots & \vdots & \vdots & \ddots & \vdots & \ddots & \vdots & \ddots & \vdots \\
x_{n1}^1 & x_{n2}^1 & \cdots & x_{nL}^1 & x_{n1}^2 & \cdots & x_{nL}^2 & \cdots & x_{n1}^N & \cdots & x_{nL}^N
\end{pmatrix} \in \mathcal{M}_{n \times (N \cdot L)}(\mathbb{R}) \qquad (3.1)
$$
$$
= \left(\ \mathbf{X}^1 \ \middle| \ \mathbf{X}^2 \ \middle| \ \cdots \ \middle| \ \mathbf{X}^N \ \right)
$$

where $\mathcal{M}_{n \times (N \cdot L)}(\mathbb{R})$ is the vector space of $n \times (N \cdot L)$ matrices over $\mathbb{R}$ and $N \in \mathbb{N}$ is the number of sensors. It is worth noting that each row vector $\mathbf{X}(i,:) \in \mathbb{R}^{N \cdot L}$, $i = 1, \ldots, n$ of matrix $\mathbf{X}$ in Equation (3.1) represents the measurements from all the sensors at a given experimental trial. Similarly, each column vector $\mathbf{X}(:,j) \in \mathbb{R}^n$, $j = 1, \ldots, N \cdot L$, contains measurements from one sensor at one specific time instant in the whole set of experimental trials.

As stated before, one of the goals of PCA is to *eliminate* the redundancies in the original data. This objective is achieved through a linear transformation orthogonal matrix

$$\mathbf{P} \in \mathcal{M}_{(N \cdot L) \times (N \cdot L)}(\mathbb{R})$$

that is used to transform or project the original data matrix $\mathbf{X}$ in Equation (3.1) according to the matrix product:

$$\mathbf{T} = \mathbf{X}\mathbf{P} \in \mathcal{M}_{n \times (N \cdot L)}(\mathbb{R})$$

where the resulting matrix $\mathbf{T}$ has a diagonal covariance matrix.

3.2.1.2 Normalization: Group Scaling

Since the data in matrix $\mathbf{X}$ come from several sensors and could have different magnitudes and PCA is not invariant to scale, a preprocessing stage must be applied to rescale the data. This normalization is based on the mean of all measurements of the sensor at the same time instant and the standard deviation of all measurements of the sensor. In this sense, for $k = 1, \ldots, N$ we define

$$\mu_j^k = \frac{1}{n} \sum_{i=1}^{n} x_{ij}^k, \; j = 1, \ldots, L, \tag{3.2}$$

$$\mu^k = \frac{1}{nL} \sum_{i=1}^{n} \sum_{j=1}^{L} x_{ij}^k, \tag{3.3}$$

$$\sigma^k = \sqrt{\frac{1}{nL} \sum_{i=1}^{n} \sum_{j=1}^{L} (x_{ij}^k - \mu^k)^2}, \tag{3.4}$$

where μ_j^k is the mean of the measures placed at the same column, that is, the mean of the n measures of sensor k in matrix $\mathbf{X}^k$ at time instants $(j-1)\,\Delta$ seconds; μ^k is the mean of all the elements in matrix $\mathbf{X}^k$, that is, the mean of all the measures of sensor k; and σ^k is the standard deviation of all the measures of sensor k. Then, the elements x_{ij}^k of matrix $\mathbf{X}$ are scaled to define a new matrix $\check{\mathbf{X}}$ as

$$\check{x}_{ij}^k := \frac{x_{ij}^k - \mu_j^k}{\sigma^k}, \; i = 1, \ldots, n, \; j = 1, \ldots, L, \; k = 1, \ldots, N. \tag{3.5}$$

For the sake of simplicity, the scaled matrix $\check{\mathbf{X}}$ is renamed again as $\mathbf{X}$. One of the properties of the scaled matrix $\mathbf{X}$ is that it is mean-centered [3.29]. Consequently, the covariance matrix of

X can be defined and computed as:

$$\mathbf{C_X} = \frac{1}{n-1}\mathbf{X}^T\mathbf{X} \in \mathcal{M}_{(N\cdot L)\times(N\cdot L)}(\mathbb{R}). \tag{3.6}$$

The subspaces in PCA are defined by the eigenvectors and eigenvalues of the covariance matrix as follows:

$$\mathbf{C_X}\mathbf{P} = \mathbf{P}\Lambda \tag{3.7}$$

where the columns of $\mathbf{P} \in \mathcal{M}_{(N\cdot L)\times(N\cdot L)}(\mathbb{R})$ are the eigenvectors of $\mathbf{C_X}$ and are defined as the *principal components*. The diagonal terms of matrix $\Lambda \in \mathcal{M}_{(N\cdot L)\times(N\cdot L)}(\mathbb{R})$ are the eigenvalues λ_i, $i = 1, \ldots, N \cdot L$, of $\mathbf{C_X}$ whereas the off-diagonal terms are zero, that is,

$$\Lambda_{ii} = \lambda_i, \ i = 1, \ldots, N \cdot L \tag{3.8}$$

$$\Lambda_{ij} = 0, \ i, j = 1, \ldots, N \cdot L, \ i \neq j \tag{3.9}$$

The goal of principal component analysis is twofold. On one hand, to eliminate the redundancies of the original data. This is achieved by transforming the original data through the projection defined by matrix **P** in Equation (3.7). On the other, a second goal is to reduce the dimensionality of the data set **X**. This second objective is achieved by selecting only a limited number $\ell < N \cdot L$ of principal components related to the ℓ highest eigenvalues. In this manner, given the reduced matrix

$$\hat{\mathbf{P}} = (p_1|p_2|\cdots|p_\ell) \in \mathcal{M}_{N\cdot L\times\ell}(\mathbb{R}), \tag{3.10}$$

matrix $\hat{\mathbf{T}}$ is defined as

$$\hat{\mathbf{T}} = \mathbf{X}\hat{\mathbf{P}} \in \mathcal{M}_{n\times\ell}(\mathbb{R}). \tag{3.11}$$

3.2.1.3 Projection of new data onto the PCA model

The current structure to inspect is excited by the same signal as the one that excited the healthy one in Section 3.2.1.1. Therefore, when the measures are obtained from $N \in \mathbb{N}$ sensors during $(L-1)\Delta$ seconds and $\nu \in \mathbb{N}$ experimental trials, a new data matrix **Y** is constructed as in Equation (3.1):

$$\mathbf{Y} = \begin{pmatrix} y_{11}^1 & y_{12}^1 & \cdots & y_{1L}^1 & y_{11}^2 & \cdots & y_{1L}^2 & \cdots & y_{11}^N & \cdots & y_{1L}^N \\ \vdots & \vdots & \ddots & \vdots & \vdots & \ddots & \vdots & \ddots & \vdots & \ddots & \vdots \\ y_{i1}^1 & y_{i2}^1 & \cdots & y_{iL}^1 & y_{i1}^2 & \cdots & y_{iL}^2 & \cdots & y_{i1}^N & \cdots & y_{iL}^N \\ \vdots & \vdots & \ddots & \vdots & \vdots & \ddots & \vdots & \ddots & \vdots & \ddots & \vdots \\ y_{\nu 1}^1 & y_{\nu 2}^1 & \cdots & y_{\nu L}^1 & y_{\nu 1}^2 & \cdots & y_{\nu L}^2 & \cdots & y_{\nu 1}^N & \cdots & y_{\nu L}^N \end{pmatrix} \in \mathcal{M}_{\nu\times(N\cdot L)}(\mathbb{R}) \tag{3.12}$$

It is worth noting, at this point, that the natural number ν (the number of rows of matrix $\mathbf{Y}$) is not necessarily equal to n (the number of rows of $\mathbf{X}$), but the number of columns of $\mathbf{Y}$ must agree with that of $\mathbf{X}$; that is, in both cases the number N of sensors and the number of time instants L must be equal.

Before the collected data arranged in matrix $\mathbf{Y}$ is projected into the new space spanned by the eigenvectors in matrix $\mathbf{P}$ in Equation (3.7), the matrix has to be scaled to define a new matrix $\check{\mathbf{Y}}$ as in Equation (3.5):

$$\check{y}_{ij}^k := \frac{y_{ij}^k - \mu_j^k}{\sigma^k}, \ i = 1, \ldots, \nu, \ j = 1, \ldots, L, \ k = 1, \ldots, N, \tag{3.13}$$

where μ_j^k and σ^k are the real numbers defined and computed in Equations (3.2) and (3.4), respectively.

The projection of each row vector $r^i = \check{\mathbf{Y}}(i,:) \in \mathbb{R}^{N \cdot L}, i = 1, \ldots, \nu$ of matrix $\check{\mathbf{Y}}$ into the space spanned by the eigenvectors in $\hat{\mathbf{P}}$ is performed through the following vector to matrix multiplication:

$$t^i = r^i \cdot \hat{\mathbf{P}} \in \mathbb{R}^\ell. \tag{3.14}$$

For each row vector $r^i, i = 1, \ldots, \nu$, the first component of vector t^i is called the *first score* or *score* 1; similarly, the second component of vector t^i is called the *second score* or *score* 2, and so on.

3.2.2 Machine learning

Machine learning has revolutionized the way that complex problems has been tackled with the help of computer programs. In the incessant and relentless pursuit of best tools for data analysis, machine learning has been highlighted for its capability for providing a quite remarkable set of strategies for pattern recognition. More precisely, when a deterministic mathematical model is difficult to define and data has, at first glance, no correlation, these pattern recognition techniques are generally able to find some kind of relationship. Machine learning strategies and bio-inspired algorithms allow to avoid this difficulty through mechanisms designed to find the answer by themselves. In SHM or related areas, it is possible to find some applications about how machine learning has been used to detect problems such as breaks, corrosion, cracks, impact damage, delamination, disunity, breaking fibers (some pertinent to metals and the others to composite materials) [3.30]. In addition, machine learning has been also used to provide information about the future behavior of a structure under extreme events such as earthquakes [3.31].

Depending on how the algorithms are implemented, machine learning can be classified in two main approaches: unsupervised and supervised learning. In the first case, the information

is grouped and interpreted using uniquely the input data. However, to perform the learning task in the second case, information about the output data is required. Figure 3.2 shows this classification and includes information about the kind of tasks that can be performed – clustering, classification, regression–.
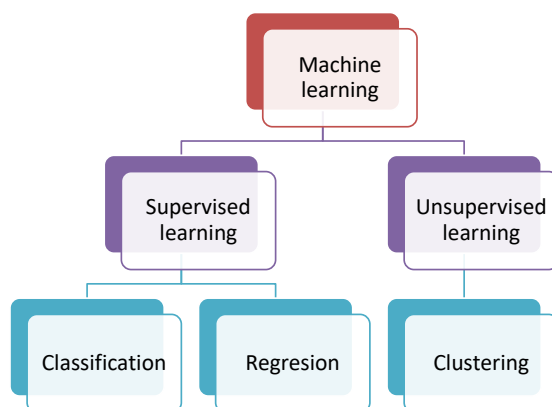
FIGURE 3.2: Classification of the machine learning approaches according to the learning.

This paper is focused on the use of supervised learning approaches and, particularly, in the use of nearest neighbor classification, decision trees and support vector machines (SVM). A brief description of the nearest neighbor pattern classification, decision tress and support vector machines is introduced in the following subsections.

3.2.2.1 Nearest neighbor pattern classification

The nearest neighbor (NN) is a simple nonparametric and highly efficient technique [3.32] that has been used in several areas such as pattern recognition, ranking models or text categorization and classification for big data [3.33, 3.34], just to name a few. One of the most used algorithms in machine learning applications is the k-NN also known as k-nearest neighbors. k-NN outstands due to its simplicity and the excellent results obtained when this technique is applied to diverse problems [3.35]. This algorithm works by using an input vector with the k closest training samples in the feature space. To perform the classification, the algorithm identify the most common class among the k nearest neighbors. The algorithm requires a training to define the neighbors based on the distance from the test sample and a testing step to determine the class to which this test sample belong [3.35].

The number of neighbors can be changed to adjust the k-NN algorithm. In this sense, for instance, the use of one neighbor is known as fine k-NN and a coarse k-NN uses 100 neighbors. Many neighbors can be time consuming to fit. There are six different k-NN classifiers available in Matlab that can be used to classify data [3.36], and these classifiers are based on

different distances. Some of them –fine, medium and coarse k-NN algorithms– make use of the Euclidean distance to determine the nearest neighbors. According to Matlab, each classifier works as follows [3.35]:

- Fine k-NN: A nearest neighbor classifier that makes finely-detailed distinctions between classes with the number of neighbors set to 1.

- Medium k-NN: A nearest neighbor classifier with fewer distinctions than a Fine k-NN with the number of neighbors set to 10.

- Coarse k-NN: A nearest neighbor between classes, with the number of neighbors set to 100.

- Cosine k-NN: A nearest neighbor classifier that uses the cosine distance metric. The cosine distance between two vectors u and v is defined as

$$1 - \frac{u \cdot v}{|u| \cdot |v|},$$

that is, one minus the ratio of the inner product of u and v over the product of the norms of u and v.

- Cubic k-NN: A nearest neighbor classifier that uses the cubic distance metric. The cubic distance between two n-dimensional vectors u and v is defined as

$$\sqrt[3]{\sum_{i=1}^{n} |u_i - v_i|^3}.$$

- Weighted k-NN: A nearest neighbor classifier that uses distance weighting. The weighted Euclidean distance between two n-dimensional vectors u and v is defined as

$$\sqrt{\sum_{i=1}^{n} w_i(x_i - y_i)^2},$$

where $0 < w_i < 1$ and $\sum_{i=1}^{n} w_i = 1$.

k-NN has been used successfully in fault detection for gas sensor arrays [3.33], classification for big data [3.37], fault detection and classification for high voltage DC transmission lines [3.35], traffic state prediction [3.38], among others.

3.2.2.2 Decision Trees

These machine learning methods are non-parametric computationally intensive method [3.39] that can be applied to regression and classification problems and can work with data sets with

a large amount of cases and variables [3.40]. In general, these methods work by segmenting the predictor space into a number of simple regions.

Some of the advantages and disadvantages of these methods are:

- Compared with other machine learning methods, trees are simple and easy to understand.

- Decision trees use different methods and can be combined to obtain a single prediction.

- The combination of different trees usually produces better results.

- Because of its simplicity, more elaborated methods can produce better results in classification and regression tasks.

Different techniques have been proposed, among them, bagging or bootstrap and boosting stand out. In the first, many bootstrap samples are obtained from the data, some prediction method is applied to each bootstrap sample, and then the results are combined. In the regression case, the combination of the results is performed by averaging, while simple voting is used for classification [3.39]. Bagging is a committee-based approach that uses a prediction method and weighted average of results to obtain an overall prediction.

3.2.2.3 Support Vector Machines

Support vector machines (SVM) are supervised methods commonly used for regression and classification tasks [3.41]. In the case of classification, SVM creates a maximum-margin hyperplane that separates all data points from different classes. The support vectors corresponds to the data points that are closest to the separating hyperplane.

3.3 Damage classification methodology

In an automated structural health monitoring system, the monitoring system should decide autonomously whether the host structure is damaged or not [3.7]. With this purpose in mind, this work proposes a damage classification methodology for structures that are subjected to temperatures changes. This strategy is described in the following sections.

3.3.1 Data acquisition system

The methodology uses data from a structure instrumented with a piezoelectric transducer network. Figure 3.3 shows the scheme of the data acquisition system where it can be observed that the sensors are attached to the structure. Each piezoelectric transducer (PZT) can operate as an actuator or as a sensor in several actuation phases. Each actuation phase defines a particular piezoelectric as an actuator and therefore this PZT excites the structure with a given excitation

signal. The rest of the PZT act as a sensors in such a way that the measured and discretized signals are organized as described in Section 3.2.1.1, ready to be used in the classification algorithms. The number of actuation phases correspond to the number of piezoelectric transducers installed in the structure.
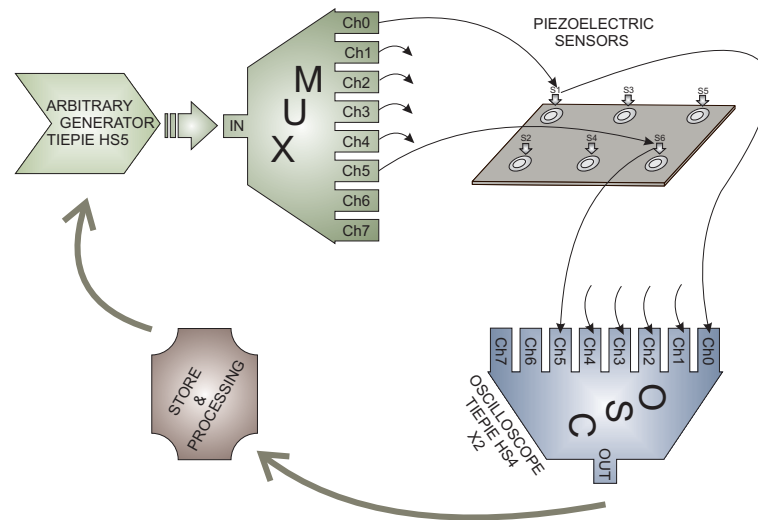
FIGURE 3.3: Representation of the structural health monitoring (SHM) system.

The use of piezoelectric transducers is justified by the fact that this kind of sensors are able to produce Lamb waves through the excitation of an actuator with an arbitrary waveform as it is represented in Figure 3.4. At the same time, the propagated wave –with information about the state of the structure at different locations– is collected by the rest of sensors, since piezoelectric transducers can sense the propagated lamb waves and the information can be captured by a digitizer card. The proposed SHM system is able to work with an arbitrary wave generator, a digitizer card, a personal computer (PC) and a multiplexor card to select the actuator/sensors in each actuation phase.
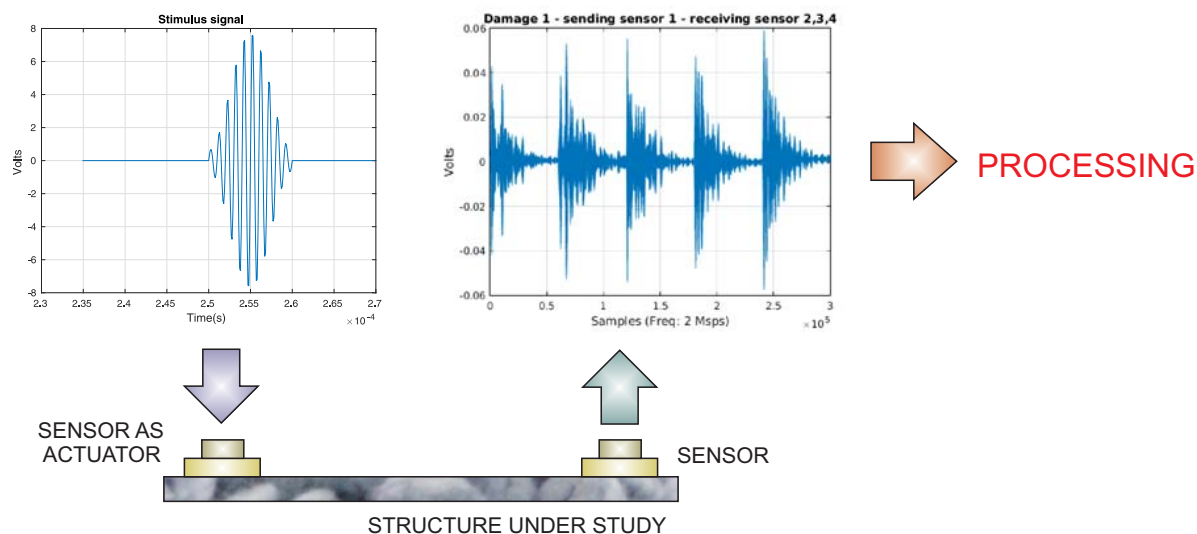
FIGURE 3.4: Signal excitation.

Figure 3.5 can be used as an schematic representation of the way data are collected and organized also shows the way as data are collected and organized for each actuation phase. That is, in the actuation phase 1, sensor 1 is used as an actuator and the measured data from sensors $2, 3, \ldots, N$ is captured and organized. In the example represented in Figure 3.5, 4 piezoelectric transducers are used. The procedure, however, is identical in the case of a different number of piezoelectric transducers.

To include the effect of the temperature in the proposed methodology, data from each temperature has to be considered. In this specific case, the system requires data from all the structural states (without damage, damage 1, damage 2 and damage 3, for instance) to consider in the classification under a wide range of temperatures $(T_1, \ldots, T_M)$. Each temperature defines a submatrix where the rows represents the different structural states and columns the different actuation phases. Figure 3.5 represents an example with four structural states (no damage, damage 1, damage 2, and damage 3) and four actuation phases and M temperatures.
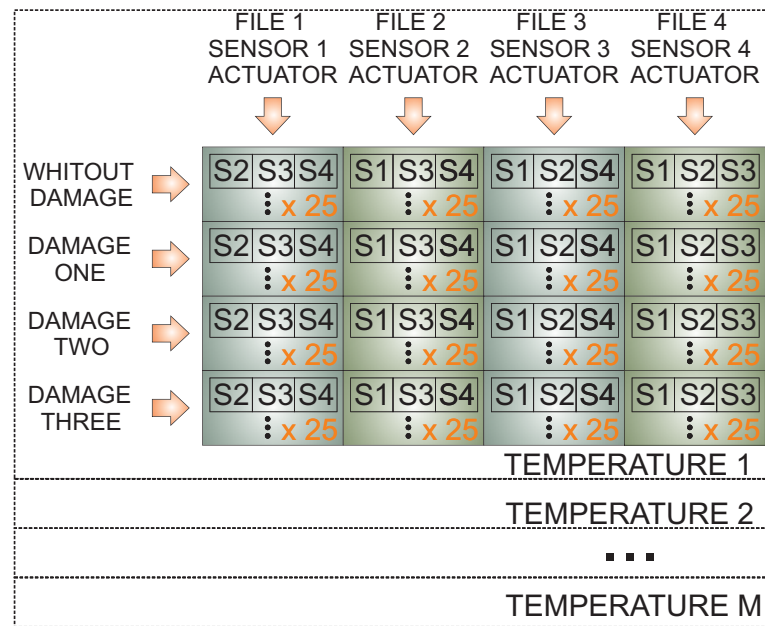
FIGURE 3.5: Data organization per each temperature

After the organization of the data for each actuation phase, the methodology considers two general steps or phases: (a) training; and (b) testing. During the training step, data from the healthy or pristine structure subjected to different temperatures are used to train the machines. Figure 3.6 includes a representation of the steps that are needed between the data acquisition and the machine training. These steps include a data normalization as in Section 3.2.1.2 [3.42, 3.43] and principal component analysis (PCA). In this case, we consider the projection onto the first two principal components (scores) as the input to train the machine. The trained machine is then considered as the pattern.
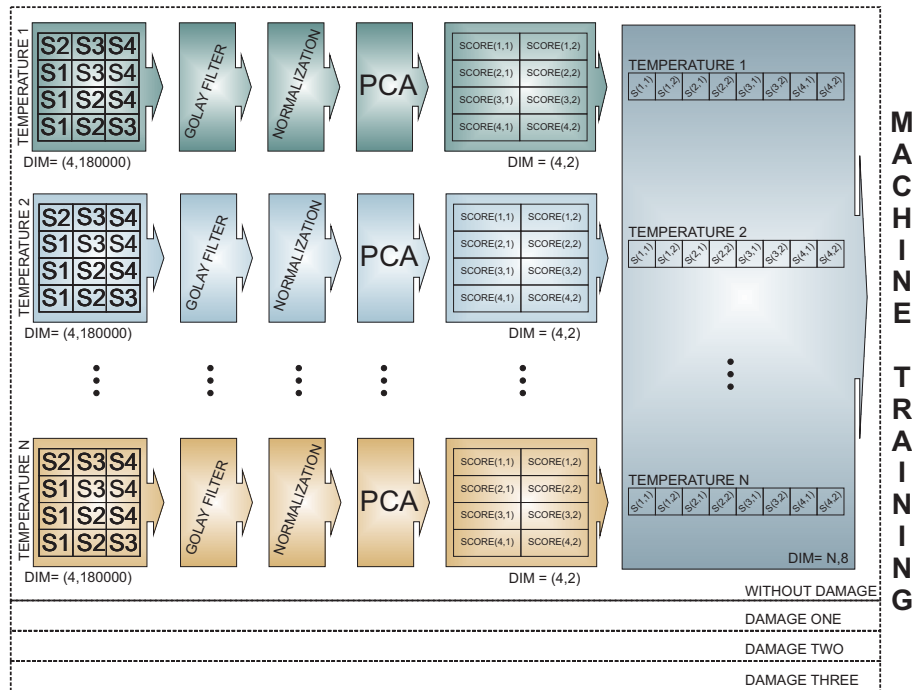
FIGURE 3.6: Methodology and training machines

The testing step considers the use of new data coming from the structure to be diagnosed in an unknown state. These collected data are pre-processed in an identical manner as the data collected from the pristine structure. This means that these data is normalized, and then the normalized data are projected onto the first two principal component of the PCA model. Finally, the pattern defined by the trained machine will be able to predict the current state of the structure, as depicted in Figure 3.7.
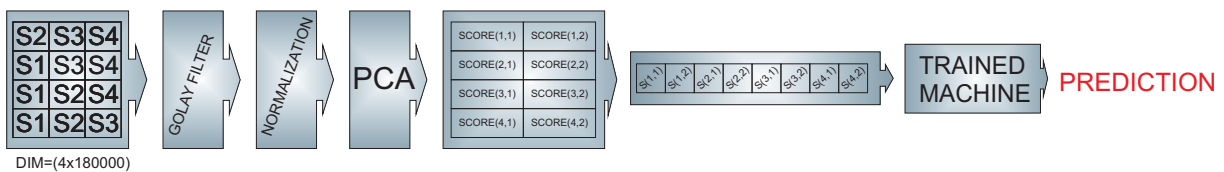
FIGURE 3.7: Metodologhy for prediction

3.4   Experimental Setup and Results

In this paper, two specimens (structures) are used to explore and demonstrate the feasibility of the structural health monitoring system –for damage identification in structures subjected to temperatures changes– introduced in Section 3.3. These two specimens are:

(i) an aluminum plate with four piezoelectric transducers; and

(ii) a composite plate of carbon fiber polymer with six piezoelectric transducers.

These two specimens differ in the kind of material, size and number of sensors used. In both cases, the same data acquisition sub-system is used as it is represented in Figure 3.3.

3.4.1 First Specimen: Aluminum Plate

The first specimen that we consider in this paper is an aluminum plate with an area of 40 cm $\times$ 40 cm that is instrumented with four piezoelectric sensors. The distribution of the piezoelectric transducers and the size and geometry of the specimen are shown in Figure 3.8. This figure also indicates the location of the three damages that are presented in the structure.
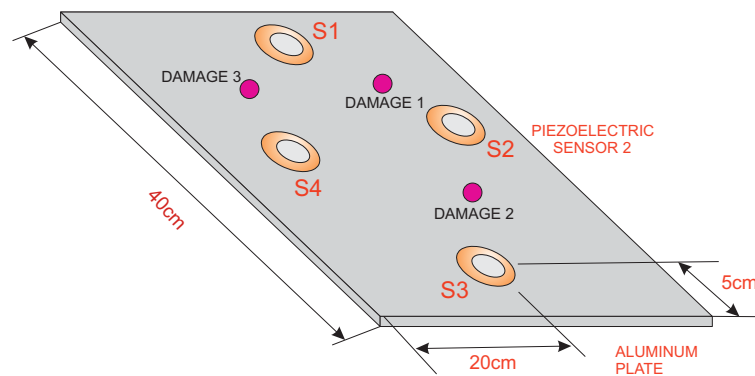
FIGURE 3.8: Aluminum plate instrumented with four piezoelectric sensors.

To test the structure under different environmental conditions and, more precisely, under different temperatures temperatures, an incubator or climatic chamber (Faithful, model HWS-250BX) is used to apply these variations. A picture of the aluminum plate inside the chamber can be found in Figure 3.9.
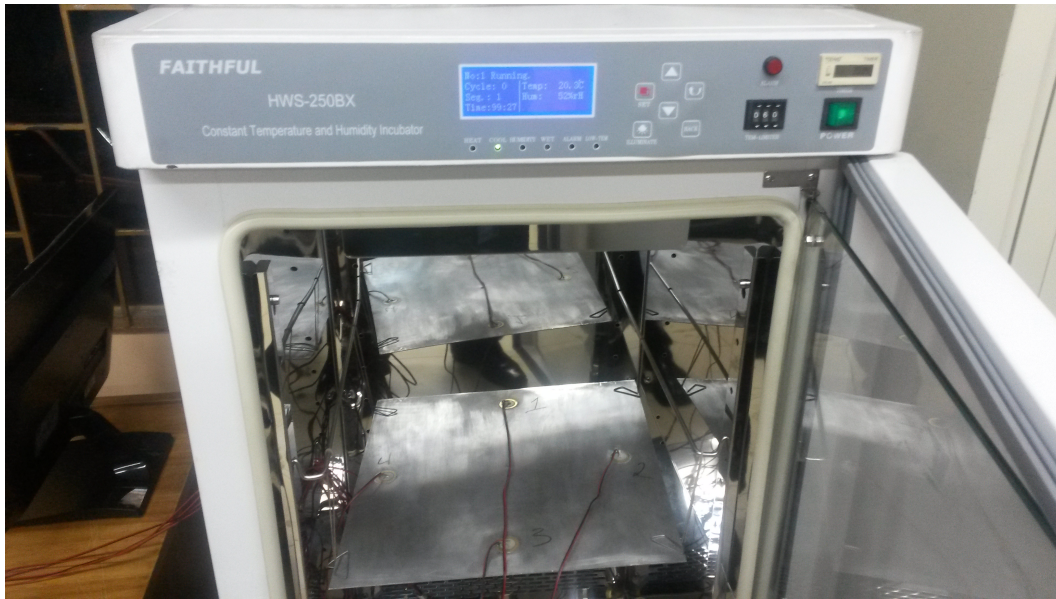
FIGURE 3.9: Aluminum plate inside the climate chamber (Faithful HWS-250BX).

The experimental setup includes testing with five different temperatures:

- $T_1 = 10°$;

- $T_2 = 20°$;

- $T_3 = 30°$;

- $T_4 = 40°$; and

- $T_5 = 45°$.

For each one of these five temperatures, data from each structural state are captured. In this case, we have considered four different structural states:

- no damage (healthy or pristine structure);

- damage 1;

- damage 2; and

- damage 3.

The location of the three damages that are presented in the structure can be found in Figure 3.8. Figure 3.10 shows the experimental setup for the four different structural states. As it can be observed, the damage is simulated in the structure –in a non-destructive way– as an added mass. The added mass is a magnet which is attached in both sides of the structure to ensure the position because aluminum is non-magnetic, the main of this kind of damage is to change

the properties of the structure and produce changes in the propagated wave.
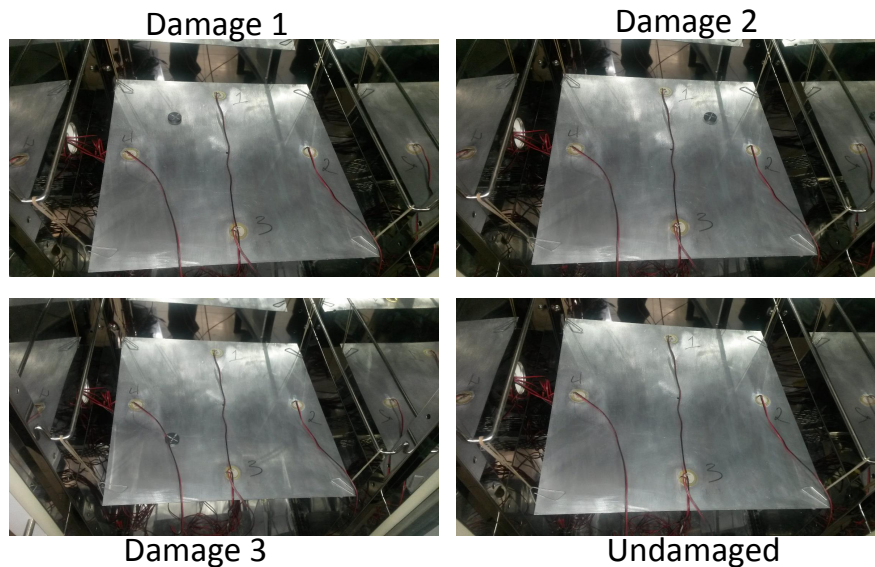
FIGURE 3.10: The plate in the climate chamber

It is well known that temperature changes affect the overall behavior of the lamb waves. More precisely, these changes affect how the lamb waves propagates, the velocity of the wave over the surface [3.44] and even the adhesive used to fix the sensors [3.45]. A very detailed study on the temperature effects in ultrasonic Lamb waves can be found in the work by Lanza di Scalea and Salamone [3.46]. One of the main conclusions of this work is that the temperature has an imperceptible effect on the wavelength tuning points and a pronounced effect on the response amplitude. In this sense, the goal of the proposed methodology is to include these variations in the structural health monitoring system to avoid false alarms and missing faults in the identification process.

The effect of the temperature changes can be perfectly illustrated in Figure 3.11, where the time-history signal that is received by sensor 2 when the first sensor is used as an actuator is depicted, for three different temperatures. From this figure it is possible to observe that changes in the temperature implies changes in the waveforms. More precisely, variations in the phase and amplitude can be easily detected, but some other and more complex changes can also be present [3.47]. Figures 3.12 and 3.13 show the signals received by sensors 3 and 4, respectively, when the first piezoelectric transducer is used as an actuator. Inspecting both figures, as in Figure 3.11, there is a clear effect of the temperature with respect to the phase and amplitude of the measured signals. It is worth keeping in mind that the distance between sensors 1–2 and sensors 1–4 is equal, while the distance between sensors 1–3 is relatively larger.
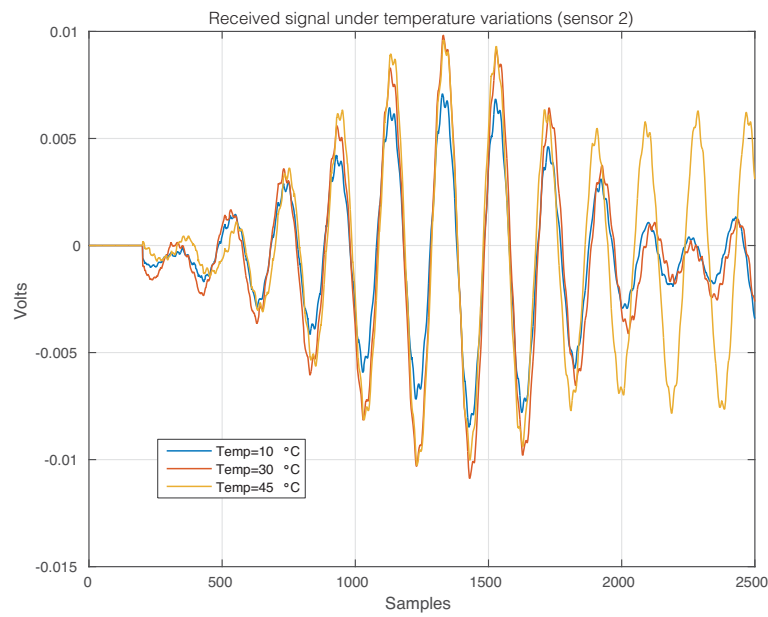
FIGURE 3.11: Signal that is received by sensor 2 when the first sensor is used as an actuator.
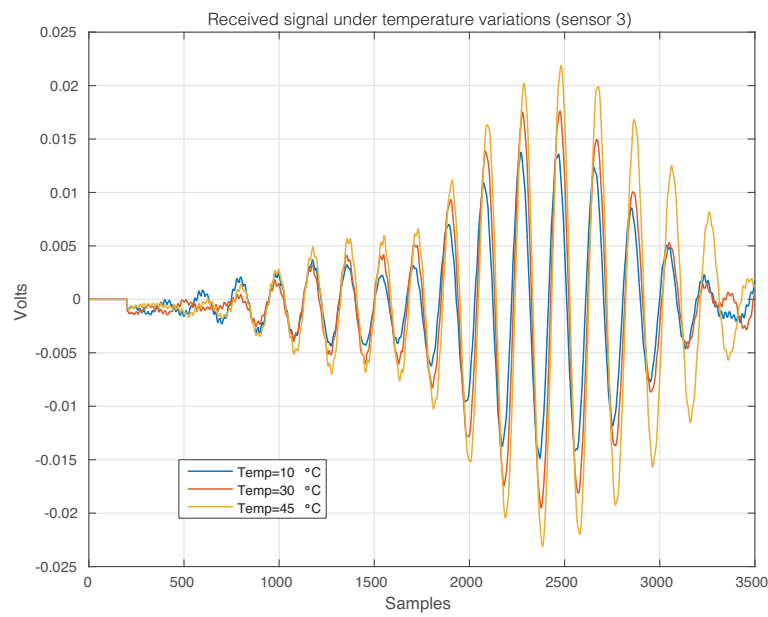
FIGURE 3.12: Signal that is received by sensor 3 when the first sensor is used as an actuator.
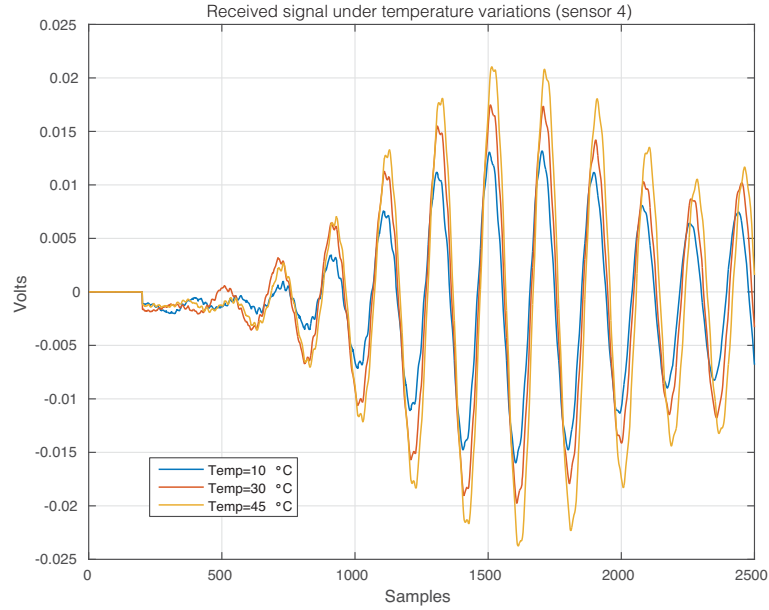
FIGURE 3.13: Signal that is received by sensor 4 when the first sensor is used as an actuator.

The feature vector that is used to train and to test the machines is formed by the projections or scores of the original data into the PCA model created as described in Section 3.2.1.1. In general, the number of scores that have to be considered depends on the cumulative contribution of variance that it is accounted for. More precisely, it the i-th score is related to the eigenvector p_i, defined in Equation (3.10), and the eigenvalue λ_i, in Equation (3.8), the cumulative contribution rate of variance accounting for the first $\sigma \in \mathbb{N}$ scores is defined as:

$$\frac{\sum_{i=1}^{\sigma} \lambda_i}{\sum_{i=1}^{\ell} \lambda_i},$$

where $\ell \in \mathbb{N}$ is the number of principal components. In this sense, the cumulative contribution of the first three scores is depicted in Figure 3.14. In this experimental setup we will use the first two principal components that account for more than 80% of the variance. A priori, better results should be obtained if we use as many principal components as possible. However, in some cases, as reported in [3.48, 3.49], less principal components may lead to more accurate results.
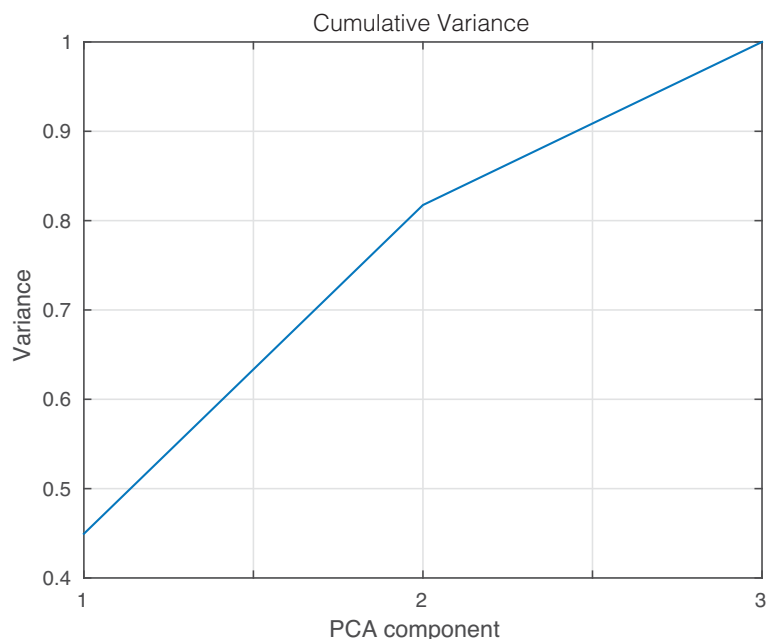
FIGURE 3.14: Cumulative contribution rate of variance for the principal components.

In a standard application of the principal component analysis strategy in the field of structural health monitoring, the scores allow a visual grouping or separation [3.50]. In some other cases, as in [3.51], two classical indices can be used for damage detection, such as the Q index (also known as square prediction error, SPE) and the Hotelling's T^2 index. In this case, however, it can be noticed in Figure 3.15 –where the projection onto the two first principal components of samples coming from the pristine structure and the structure with damage, subjected to temperatures changes are plotted– that a visual grouping, clustering or separation cannot be performed. To solve this problem, several strategies have been applied in the literature. Some of these procedures are related to univariate or multivariate statistical hypothesis testing [3.29, 3.48, 3.49]. In this work, an exhaustive number of machine learning approaches are used. This way, some orientations can be presented on the most convenient schemes.
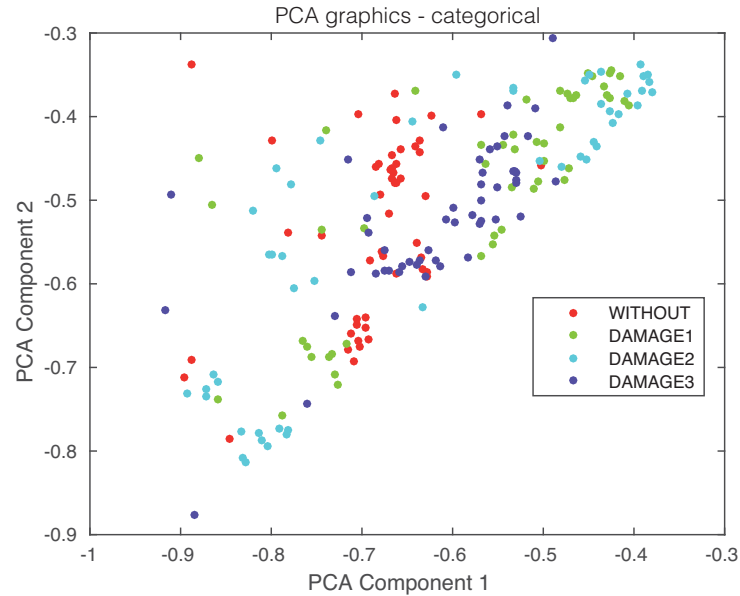
FIGURE 3.15: First principal component versus second principal component in the aluminum plate described in Section 3.4.1.

Table 3.1 shows the results of the damage identification obtained with the 20 different machine learning strategies. To this goal, the Classification Learner of Matlab was used. The columns in Table 3.1 correspond to the percentage of correct decisions for the healthy structure and the structure with damage 1, 2 and 3. The detailed results can be found in Figures 3.16 and 3.17, where the machines with the best and worst performance have been considered, respectively. More precisely, in the subspace k-NN classifier, 162 cases have been correctly classified out of 200 cases, while in the fine k-NN classifier, this number rises up to 163 cases. Similarly, with respect to the weighted k-NN and the fine Gaussian SVM classifiers, 154 and 157 cases have been correctly classified. This represents 77%-82% of correct decisions. It is worth noting that in these four cases that we have considered, the structure with no damage is correctly classified in more than 90% of cases. Similarly, the structure with damage is confused with the structure with no damage in just a few cases. For instance, in the fine Gaussian SVM classifier, 8 cases of the structure with damage are identified as healthy, which represents 5.3% out of 150 cases. As stated before, Figure 3.17 shows the confusion matrix for the machines with the poorest performance. These are: rusboosted trees, boosted trees, coarse k-NN and coarse Gaussian SVM. For instance, in both rusboosted trees and boosted trees, no one of the samples coming from the structure with damage 1 is correctly classified. However, in these two cases, 49 and 48 cases of the structure with no damage have been correctly classified, out of 50 cases, which represents 98% and 96%, respectively.

TABLE 3.1: Percentage of correct decisions for the healthy structure and the structure with damage 1, 2 and 3, for the twenty different machine learning strategies (aluminum plate).

MACHINE NAME	NOT/NOT	DMG1/DMG1	DMG2/DMG2	DMG3/DMG3
Medium Tree	66%	76%	70%	56%
Simple Tree	64%	60%	30%	58%
Complex Tree	72%	76%	58%	56%
Linear SMV	70%	60%	26%	60%
Quadratic SVM	78%	70%	56%	70%
Cubic SVM	86%	68%	66%	72%
Fine Gaussian SVM	90%	80%	66%	78%
Medium Gaussian SVM	76%	80%	56%	74%
Coarse Gaussian SVM	94%	64%	14%	38%
Fine *k*-NN	94%	78%	74%	80%
Medium *k*-NN	80%	62%	64%	74%
Coarse *k*-NN	94%	42%	2%	24%
Cosine *k*-NN	84%	58%	78%	72%
Cubic *k*-NN	80%	64%	62%	76%
Weighted *k*-NN	94%	66%	68%	80%
Boosted Trees	96%	0%	42%	42%
Bagged Trees	84%	70%	66%	78%
Subspace Discriminant	56%	44%	32%	46%
Subspace *k*-NN	94%	78%	72%	80%
Rusboosted Trees	98%	0%	42%	0%

(a) Subspace *k*-NN

(b) Weighted *k*-NN

(c) Fine *k*-NN
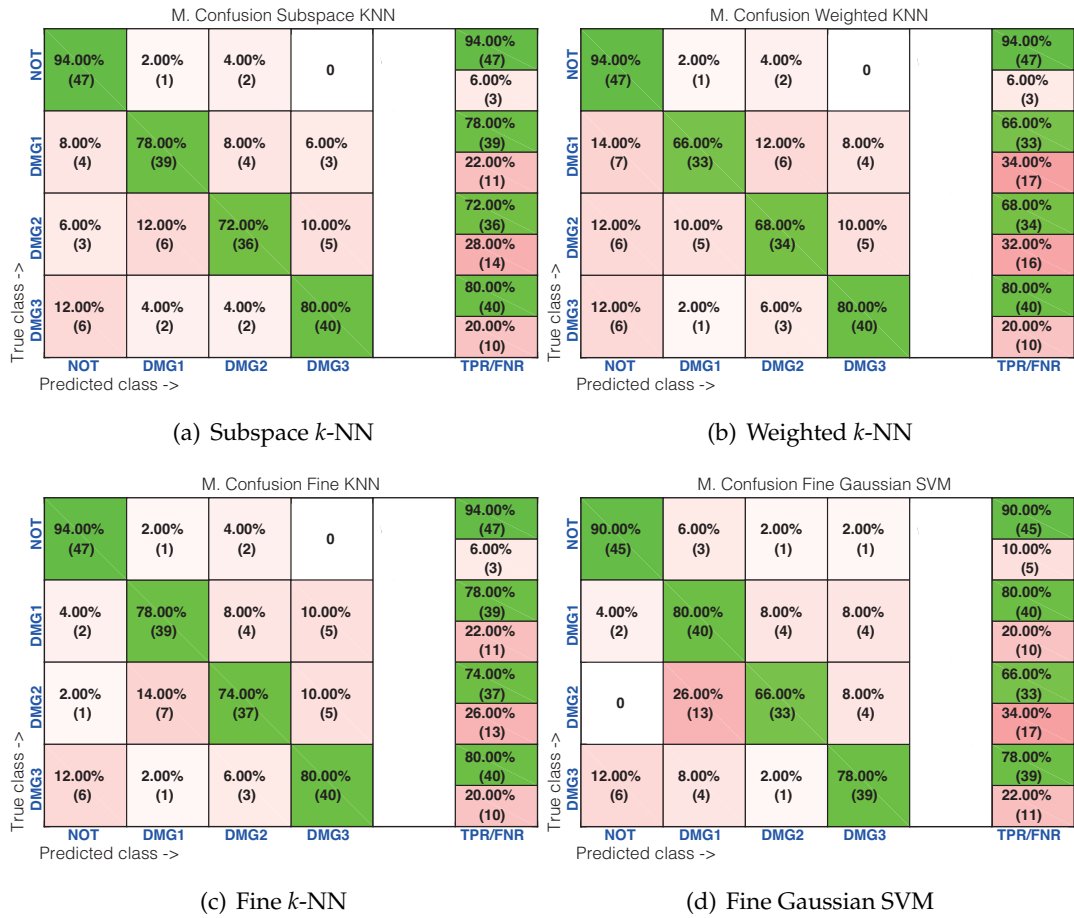
(d) Fine Gaussian SVM

FIGURE 3.16: Confusion matrix using (a) subspace *k*-NN; (b) weighted *k*-NN; (c) fine *k*-NN; and (d) fine Gaussian SVM.

(a) Rusboosted trees

(b) Boosted trees

(c) Coarse *k*-NN

(d) Coarse Gaussian SVM

FIGURE 3.17: Confusion matrix using (a) rusboosted trees; (b) boosted trees; (c) coarse *k*-NN; and (d) coarse Gaussian SVM.

3.4.2   Second Specimen: Carbon Fiber Plate

The second specimen used for the experimental validation of the approach presented in this paper is a composite plate of carbon fiber polymer with an area of 50 cm × 25 cm, and a 2 mm thickness. The plate is instrumented with piezoelectric transducers. Figure 3.18 shows the dimensions and distribution of the six piezoelectric transducers attached to the structure as well as the location of the three damages that are presented in the structure.
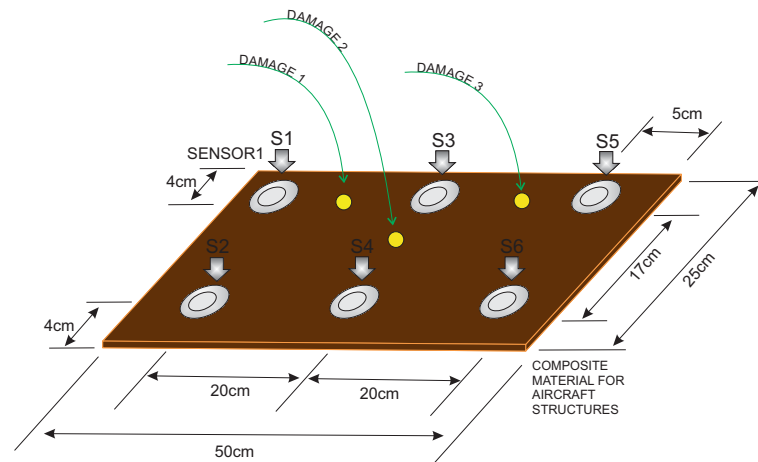
FIGURE 3.18: Experimental setup for the composite plate

As in the previous experimental setup, to test the structure under different environmental conditions and, more precisely, under different temperatures temperatures, an incubator or climatic chamber (Faithful, model HWS-250BX) is used to apply these variations. A picture of the composite plate inside the chamber can be found in Figure 3.19.

The experimental setup includes testing with six different temperatures:

- $T_1 = 0°$;

- $T_2 = 10°$;

- $T_3 = 20°$;

- $T_4 = 30°$;

- $T_5 = 40°$; and

- $T_6 = 45°$.

For each one of these six temperatures, data from each structural state are captured. In this case, we have considered four different structural states:

- no damage (healthy or pristine structure);

- damage 1;

- damage 2; and

- damage 3.

Damage 1

Damage 2

Damage 3

No Damage
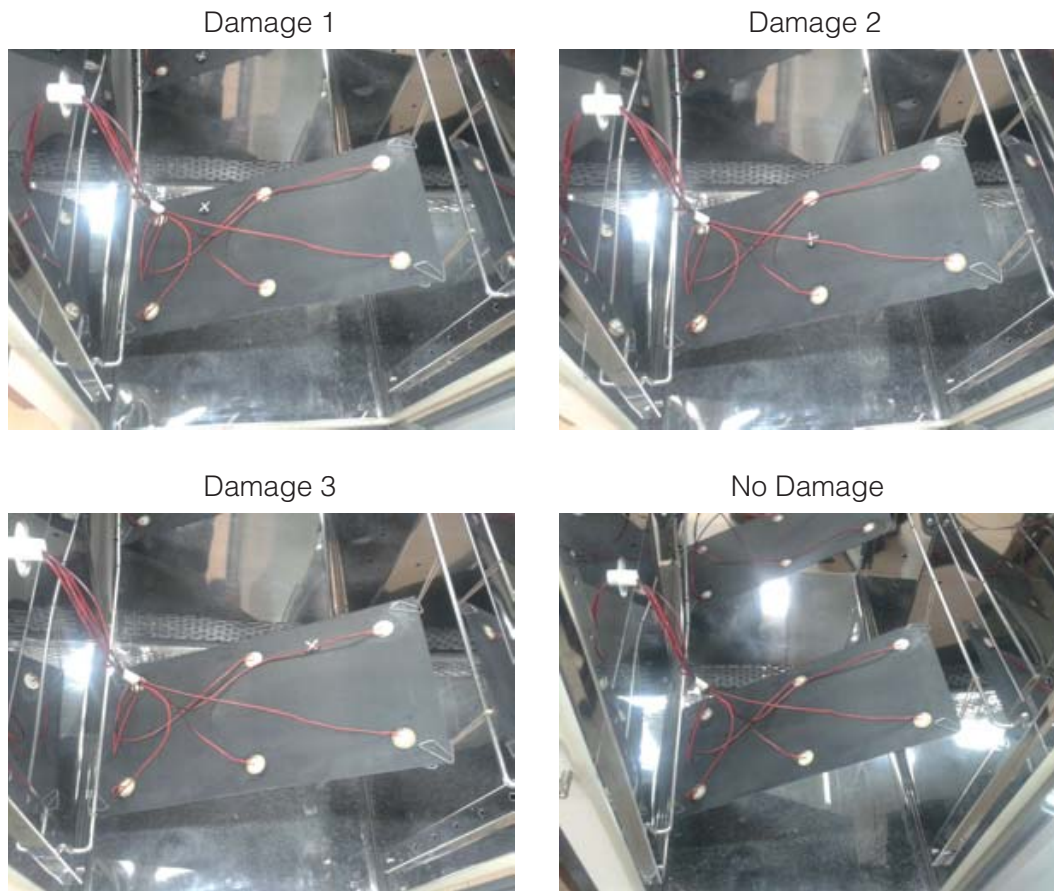
FIGURE 3.19: Composite plate in the climatic chamber

The effect of the temperature changes in the composite plate can be perfectly illustrated in Figure 3.20, where the time-history signal that is received by sensor 2 when the first sensor is used as an actuator is depicted, for the six different temperatures. As in the previous experimental setup, from this figure it is possible to observe that changes in the temperature implies changes in the waveforms. More precisely, variations in the phase and amplitude can be easily detected.
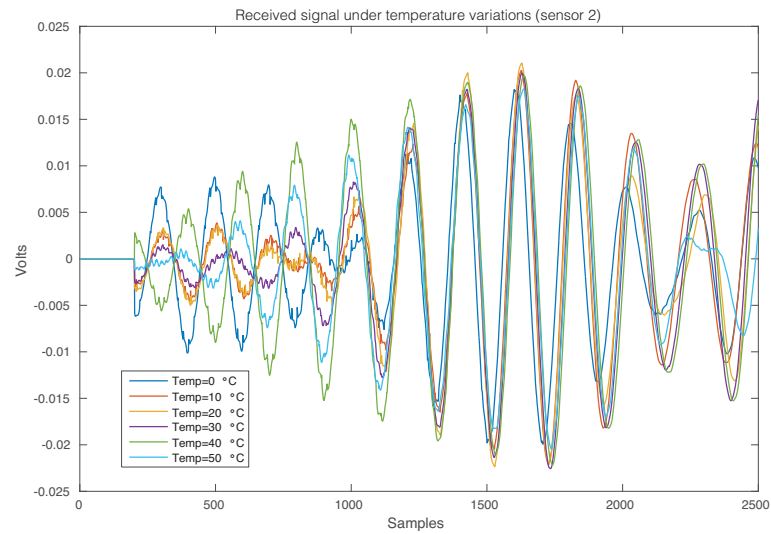
FIGURE 3.20: Signal that is received by sensor 2 when the first sensor is used as
an actuator.

Finally, the first principal component versus the second principal component are plotted in
Figure 3.21. It can be observed that, again, that a visual grouping, clustering or separation can-
not be performed. In this experimental setup we will use the first three principal components
that account for more than 80% of the variance, as can be seen in Figure 3.22.
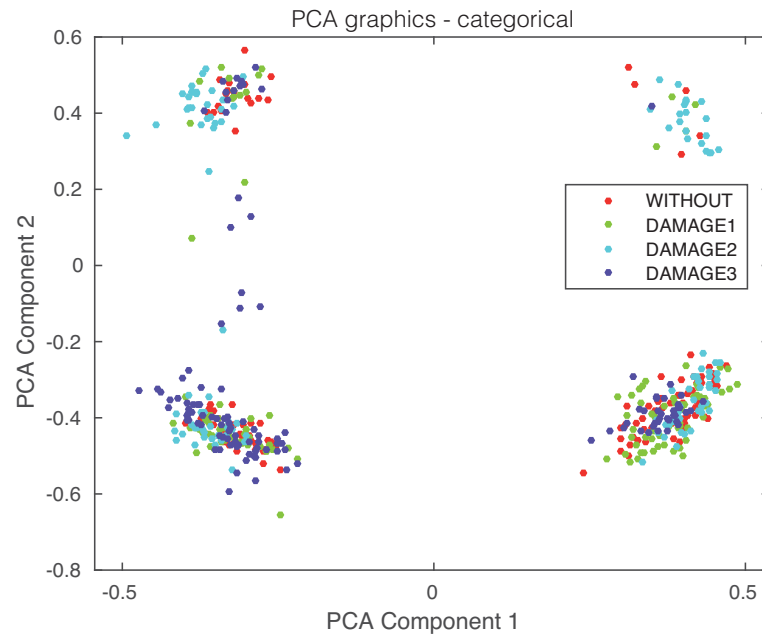
FIGURE 3.21: First principal component versus second principal component in
the carbon fiber plate described in Section 3.4.2.
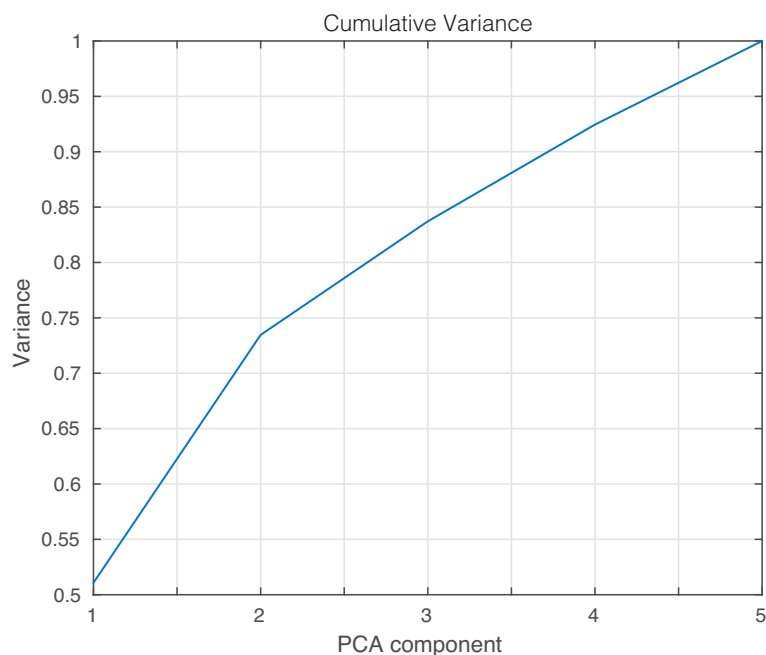
FIGURE 3.22: Cumulative variance for scores of PCA

Table 3.2 shows the results of the damage identification in the composite plate obtained with the 20 different machine learning strategies. The columns in Table 3.2 correspond to the percentage of correct decisions for the healthy structure and the structure with damage 1, 2 and 3. The detailed results can be found in Figures 3.23 and 3.24, where the machines with the best and worst performance have been considered, respectively. More precisely, in the subspace *k*-NN classifier, 378 cases have been correctly classified out of 480 cases, while in the bagged trees classifier, this number rises up to 382 cases. Similarly, with respect to the weighted *k*-NN and the cubic SVM classifiers, 336 and 368 cases have been correctly classified. This represents 70%-80% of correct decisions. It is worth noting that in these four cases that we have considered, the structure where damage 2 is present is correctly classified in more than 83% of cases. Similarly, the structure with damage is confused with the structure with no damage in just a few cases. For instance, in the bagged trees classifier, 22 cases of the structure with damage are identified as healthy, which represents 6.1% out of 360 cases. As stated before, Figure 3.17 shows the confusion matrix for the machines with the poorest performance. These are: rusboosted trees, boosted trees, coarse *k*-NN and coarse Gaussian SVM. For instance, in rusboosted trees, no one of the samples coming from the healthy structure is correctly classified. However, in this case, 75 cases of the structure with damage 2 have been correctly classified, out of 120 cases, which represents 75%.

TABLE 3.2: Percentage of correct decisions for the healthy structure and the structure with damage 1, 2 and 3, for the twenty different machine learning strategies (composite plate).

MACHINE NAME	NOT/NOT	DMG1/DMG1	DMG2/DMG2	DMG3/DMG3
Medium Tree	55.00%	63.33%	60.83%	52.50%
Simple Tree	40.00%	60.00%	63.33%	42.50%
Complex Tree	57.50%	64.17%	75.83%	65.83%
Linear SVM	41.67%	59.17%	45.00%	47.50%
Quadratic SVM	65.83%	73.33%	85.00%	75.50%
Cubic SVM	70.83%	75.00%	86.67%	74.17%
Fine Gaussian SVM	59.17%	64.17%	83.33%	78.33%
Medium Gaussian SVM	55.83%	60.00%	82.50%	63.33%
Coarse Gaussian SVM	52.50%	10.83%	33.33%	56.67%
Fine *k*-NN	63.33%	61.67%	80.00%	70.00%
Medium *k*-NN	65.00%	46.67%	75.00%	63.33%
Coarse *k*-NN	52.50%	37.50%	60.83%	35.83%
Cosine *k*-NN	65.00%	43.33%	79.17%	60.83%
Cubic *k*-NN	59.17%	47.50%	72.50%	60.00%
Weighted *k*-NN	61.67%	58.33%	83.33%	74.17%
Boosted Trees	16.67%	62.50%	60.83%	71.67%
Bagged Trees	71.67%	72.50%	90.00%	84.17%
Subspace Discriminant	33.33%	45.83%	45.00%	55.83%
Subspace *k*-NN	70.83%	72.50%	89.17%	82.50%
Rusboosted Trees	0.00%	62.50%	0.00%	93.33%

(a) Subspace *k*-NN

(b) Weighted *k*-NN

(c) Bagged Trees

(d) Cubic SVM
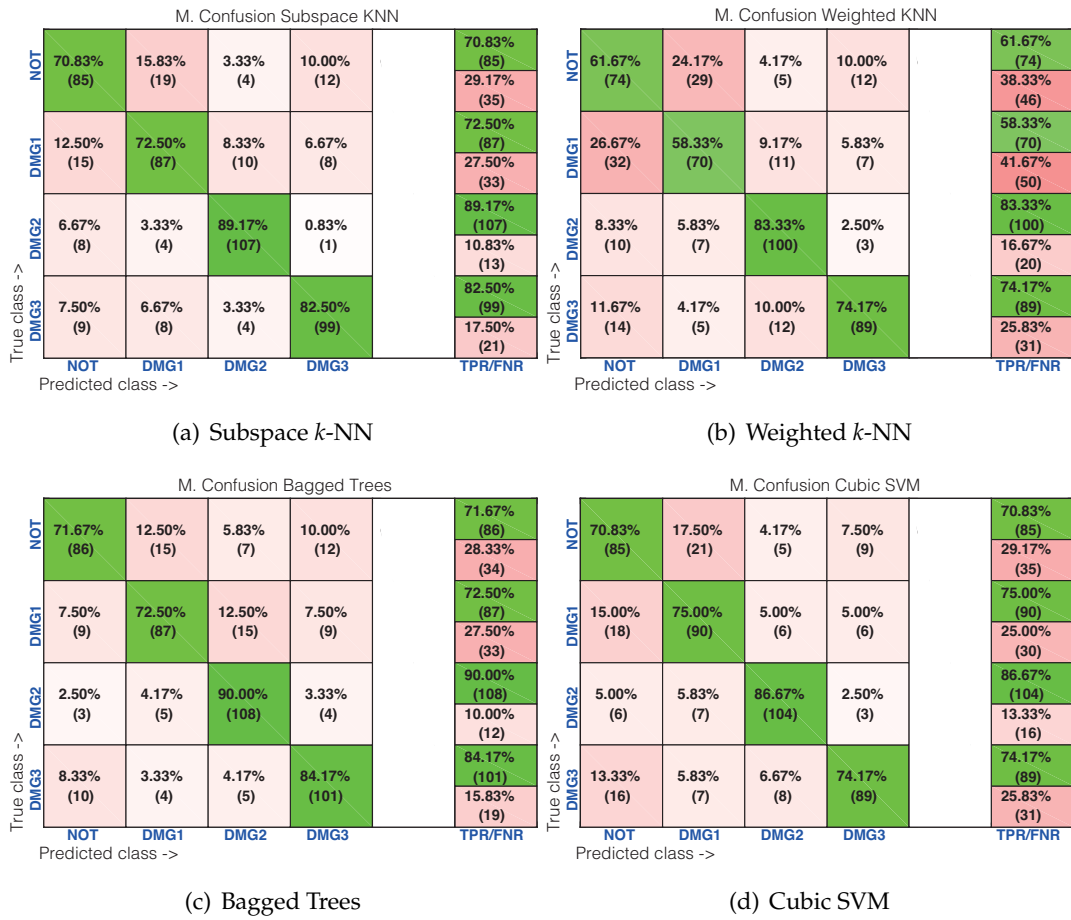
FIGURE 3.23: Confusion matrix machines with good behavior

(a) Rusboosted trees

(b) Boosted trees

(c) Coarse *k*-NN

(d) Coarse Gaussian SVM

FIGURE 3.24: Confusion matrix machines with bad behavior

3.5 Concluding Remarks

In this contribution, a structural health monitoring methodology has been developed for damage detection and classification of structures that are subjected to changes in the environmental conditions. The experimental results that have been presented in this work demonstrates that changes in the temperature affects basic damage detection strategies based on principal component analysis, this is because pattern recognition approaches in SHM applications use data from a structure under a established conditions to define a pattern and small changes in the data from the structure as the obtained by the variation of temperature produce differences with the pattern and false positive damage detection procedures even is a healthy structure. In this sense, to overcome the distortion caused by these changing environmental conditions, a more complex SHM strategy has been presented, based on: (i) ultrasonic signals through a piezoelectric sensor network; (ii) principal component analysis; and (iii) pattern recognition

based on machine learning approaches which considers data from different structural states under different temperatures.

According to the experimental results on both an aluminum plate and a composite plate of carbon fiber polymer, subspace *k*-NN and weighted *k*-NN have presented the most accurate results. Besides, for the aluminum plate, fine *k*-NN and fine Gausssian *k*-NN classifiers showed a very good behavior. For the composite plate, bagged trees and cubic SVM were also quite accurate.

Among the classifiers, the ones with the poorest accuracy were rusboosted trees, boosted trees, coarse *k*-NN and coarse Gaussian SVM. The advantages of the developed methodology include: (i) a data-driven analysis that allows the knowledge of the current state of the structure directly from the collected data and without the use of a complex mathematical model; (ii) the reduction of false positives, since data from different temperatures are considered during the training and sensor data fusion to provide a single a more reliable result. One of the disadvantages of the methodology is the big quantity of data required to cover all the structural states with respect to all the temperatures. Besides, a new damage can be detected as such, but it cannot be properly classified since there is no information about this particular damage within the pattern.

Since the methodology allows to detect and classify a damage with data collected from the structure, damage localization can be explored by understanding that a huge quantity of data of a damage in different positions of the structure can be used not only for classification but also for localization if the position of the damage is defined from the beginning in the training process. A variation of this methodology is being explored in other work where machine learning approaches are used for regression.

Acknowledgments

Conflict of interests

The authors declare no conflict of interest.

Conflicts of Interest: The authors declare no conflict of interest.

Bibliography

[3.1] H. Sohn, "Effects of environmental and operational variability on structural health monitoring," *Philosophical Transactions of the Royal Society of London A: Mathematical, Physical and Engineering Sciences*, vol. 365, no. 1851, pp. 539–560, 2007.

[3.2] M. Anaya, D. Tibaduiza, M. Torres, F. Pozo, M. Ruiz, L. Mujica, J. Rodellar, and C. Fritzen, "Data-driven methodology to detect and classify structural changes under temperature variations," *Smart Materials and Structures*, vol. 23, pp. 1–15, 2014.

[3.3] D. Chakraborty, N. Kovvali, J. J. Zhang, A. Papandreou-Suppappola, and A. Chattopadhyay, "Adaptive learning for damage classification in structural health monitoring," in *Signals, Systems and Computers, 2009 Conference Record of the Forty-Third Asilomar Conference on*, pp. 1678–1682, nov 2009.

[3.4] A.-M. Yan, G. Kerschen, P. De Boe, and J.-C. Golinval, "Structural damage diagnosis under varying environmental conditions - part i: a linear analysis," *Mechanical Systems and Signal Processing*, vol. 19, no. 4, pp. 847–864, 2005.

[3.5] F. G. Baptista, D. E. Budoya, V. A. D. de Almeida, and J. A. C. Ulson, "An experimental study on the effect of temperature on piezoelectric sensors for impedance-based structural health monitoring.," *Sensors (Basel, Switzerland)*, vol. 14, no. 1, pp. 1208–1227, 2013.

[3.6] M. Anaya, D. A. Tibaduiza, and F. Pozo, "Detection and classification of structural changes using artificial immune systems and fuzzy clustering," *International Journal of Bio-Inspired Computation*, vol. 9, no. 1, pp. 35–52, 2017.

[3.7] M. A. Torres-Arredondo, I. Buethe, D. A. Tibaduiza, J. Rodellar, and C.-P. Fritzen, "Damage detection and classification in pipework using acousto-ultrasonics and non-linear data-driven modelling," *Journal of Civil Structural Health Monitoring*, vol. 3, no. 4, pp. 297–306, 2013.

[3.8] M.-A. Torres-Arredondo, J. Sierra-Pérez, and G. Cabanes, "An optimal baseline selection methodology for data-driven damage detection and temperature compensation in acousto-ultrasonics," *Smart Materials and Structures*, vol. 25, no. 5, p. 055034, 2016.

[3.9] T. Leichtle, C. Geiß, M. Wurm, T. Lakes, and H. Taubenböck, "Unsupervised change detection in vhr remote sensing imagery–an object-based clustering approach in a dynamic

urban environment," *International Journal of Applied Earth Observation and Geoinformation*, vol. 54, pp. 15–27, 2017.

[3.10] M. Anaya, D. Tibaduiza, and F. Pozo, "Artificial immune system (ais) for damage detection under variable temperature conditions," in *European Workshop on Structural Health Monitoring*, 2016.

[3.11] S. Vanlanduit, E. Parloo, B. Cauberghe, P. Guillaume, and P. Verboven, "A robust singular value decomposition for damage detection under changing operating conditions and structural uncertainties," *Journal of Sound and Vibration*, vol. 284, no. 3 - 5, pp. 1033 – 1050, 2005.

[3.12] A. Deraemaeker, E. Reynders, G. D. Roeck, and J. Kullaa, "Vibration-based structural health monitoring using output-only measurements under changing environment," *Mechanical Systems and Signal Processing*, vol. 22, no. 1, pp. 34 – 56, 2008.

[3.13] É. Balmès, M. Basseville, F. Bourquin, L. Mevel, H. Nasser, and F. Treyssede, "Merging sensor data from multiple temperature scenarios for vibration monitoring of civil structures," *Structural health monitoring*, vol. 7, no. 2, pp. 129–142, 2008.

[3.14] K. V. Buren, J. Reilly, K. Neal, H. Edwards, and F. Hemez, "Guaranteeing robustness of structural condition monitoring to environmental variability," *Journal of Sound and Vibration*, vol. 386, pp. 134 – 148, 2017.

[3.15] H. Sohn, K. Worden, and C. R. Farrar, "Statistical damage classification under changing environmental and operational conditions," *Journal of Intelligent Material Systems and Structures*, vol. 13, no. 9, pp. 561–574, 2002.

[3.16] E. Figueiredo, G. Park, C. R. Farrar, K. Worden, and J. Figueiras, "Machine learning algorithms for damage detection under operational and environmental variability," *Structural Health Monitoring*, vol. 10, no. 6, pp. 559–572, 2011.

[3.17] K. Worden and G. Manson, "The application of machine learning to structural health monitoring," *Philosophical Transactions of the Royal Society of London A: Mathematical, Physical and Engineering Sciences*, vol. 365, no. 1851, pp. 515–537, 2007.

[3.18] K. Worden, G. Manson, and D. Allman, "Experimental validation of a structural health monitoring methodology: Part i. novelty detection on a laboratory structure," *Journal of Sound and Vibration*, vol. 259, no. 2, pp. 323–343, 2003.

[3.19] G. Manson, K. Worden, and D. Allman, "Experimental validation of a structural health monitoring methodology: Part ii. novelty detection on a gnat aircraft," *Journal of Sound and Vibration*, vol. 259, no. 2, pp. 345–363, 2003.

[3.20] S. Roy, F. Chang, P. P. S.J. Lee, and V. Janapati, *Safety, Reliability, Risk and Life-Cycle Performance of Structures and Infrastructures*, ch. A novel machine-learning approach for structural state identification using ultrasonic guided waves, pp. 321–328. CRC Press, 2013.

[3.21] D. Tibaduiza, L. Mujica, M. Anaya, J. Rodellar, and A. Güemes, "Independent component analysis for detecting damages on aircraft wing skeleton," in *Proceedings of the 5th European conference on structural control*, 2012.

[3.22] D. Tibaduiza, M. Anaya, E. Forero, R. Castro, and F. Pozo, "A sensor fault detection methodology applied to piezoelectric active systems in structural health monitoring applications," in *IOP Conference Series: Materials Science and Engineering*, vol. 138, p. 012016, IOP Publishing, 2016.

[3.23] J. Vitola, F. Pozo, D. A. Tibaduiza, and M. Anaya, "A sensor data fusion system based on k-nearest neighbor pattern classification for structural health monitoring applications," *Sensors*, 2017.

[3.24] I. Jolliffe, *Principal component analysis*. Wiley Online Library, 2002.

[3.25] M. Anaya, D. A. Tibaduiza, and F. Pozo, "A bioinspired methodology based on an artificial immune system for damage detection in structural health monitoring," *Shock and Vibration*, vol. 2015, 2015.

[3.26] D. A. Tibaduiza, *Design and validation of a structural health monitoring system for aeronautical structures*. PhD thesis, Universitat Politècnica de Catalunya, Barcelona, Spain, 2012.

[3.27] D. H. Jeong, C. Ziemkiewicz, B. Fisher, W. Ribarsky, and R. Chang, "ipca: An interactive system for pca-based visual analytics," in *Computer Graphics Forum*, vol. 28, pp. 767–774, Wiley Online Library, 2009.

[3.28] J. A. Westerhuis, T. Kourti, and J. F. MacGregor, "Comparing alternative approaches for multivariate statistical analysis of batch process data," *Journal of Chemometrics*, vol. 13, no. 3-4, pp. 397–413, 1999.

[3.29] F. Pozo and Y. Vidal, "Wind turbine fault detection through principal component analysis and statistical hypothesis testing," *Energies*, vol. 9, no. 1, p. 3, 2015.

[3.30] C. R. Farrar and K. Worden, *Structural health monitoring: a machine learning perspective*. John Wiley & Sons, 2012.

[3.31] C. C. Ciang, J.-R. Lee, and H.-J. Bang, "Structural health monitoring for a wind turbine system: a review of damage detection methods," *Measurement Science and Technology*, vol. 19, no. 12, p. 122001, 2008.

[3.32] T. Cover and P. Hart, "Nearest neighbor pattern classification," *IEEE transactions on information theory*, vol. 13, no. 1, pp. 21–27, 1967.

[3.33] J. Yang, Z. Sun, and Y. Chen, "Fault detection using the clustering-knn rule for gas sensor arrays," *Sensors*, vol. 16, no. 12, p. 2069, 2016.

[3.34] S. Dhanabal and S. Chandramathi, "A review of various k-nearest neighbor query processing techniques," *International Journal of Computer Applications*, vol. 31, no. 7, pp. 14–22, 2011.

[3.35] J. Johnson and A. Yadav, "Weak and electromagnetic interactions," in *Proceedings of the International Conference on ICT for Sustainable Development (ICT4SD)*, 2016.

[3.36] MathWorks, Natick, MA, USA, *Statistics and Machine Learning Toolbox for Matlab*, 2015.

[3.37] Z. Deng, X. Zhu, D. Cheng, M. Zong, and S. Zhang, "Efficient knn classification algorithm for big data," *Neurocomputing*, vol. 195, pp. 143–148, 2016.

[3.38] S. Oh, Y.-J. Byon, and H. Yeo, "Improvement of search strategy with k-nearest neighbors approach for traffic state prediction," *IEEE Transactions on Intelligent Transportation Systems*, vol. 17, no. 4, pp. 1146–1156, 2016.

[3.39] C. Sutton, *Handbook of Statistics*, ch. Classification and regression trees, bagging, and boosting, pp. 11–26. Elsevier, 2005.

[3.40] J. Quinlan, "Induction of decision trees," *Machine Learning*, vol. 1, no. 1, pp. 81–106, 1986.

[3.41] A. Shmilovici, *Support Vector Machines*, pp. 257–276. Boston, MA: Springer US, 2005.

[3.42] D. A. Tibaduiza, L. E. Mujica, and J. Rodellar, "Comparison of several methods for damage localization using indices and contributions based on pca," *Journal of Physics: Conference Series*, vol. 305, no. 1, p. 012013, 2011.

[3.43] M.-A. Torres-Arredondo, D.-A. Tibaduiza, M. McGugan, H. Toftegaard, K.-K. Borum, L. E. Mujica, J. Rodellar, and C.-P. Fritzen, "Multivariate data-driven modelling and pattern recognition for damage detection and identification for acoustic emission and acousto-ultrasonics," *Smart Materials and Structures*, vol. 22, no. 10, p. 105023, 2013.

[3.44] L. Yu and C. A. Leckey, "Lamb wave–based quantitative crack detection using a focusing array algorithm," *Journal of Intelligent Material Systems and Structures*, vol. 24, no. 9, pp. 1138–1152, 2013.

[3.45] R. M. F. Neto, V. Steffen, D. A. Rade, and C. A. Gallo, "System for Structural Health Monitoring based on piezoelectric sensors/actuators," in *Power Electronics Conference (COBEP), 2011 Brazilian*, pp. 365–371, sep 2011.

[3.46] F. Lanza di Scalea and S. Salamone, "Temperature effects in ultrasonic lamb wave structural health monitoring systems," *The Journal of the Acoustical Society of America*, vol. 124, no. 1, pp. 161–174, 2008.

[3.47] S. Ha, K. Lonkar, A. Mittal, and F. K. Chang, "Adhesive Layer Effects on PZT-induced Lamb Waves at Elevated Temperatures," *Structural Health Monitoring*, vol. 9, no. 3, pp. 247–256, 2010.

[3.48] L. Mujica, M. Ruiz, F. Pozo, J. Rodellar, and A. Güemes, "A structural damage detection indicator based on principal component analysis and statistical hypothesis testing," *Smart materials and structures*, vol. 23, no. 2, p. 025014, 2013.

[3.49] F. Pozo, I. Arruga, L. E. Mujica, M. Ruiz, and E. Podivilova, "Detection of structural changes through principal component analysis and multivariate statistical inference," *Structural Health Monitoring*, vol. 15, no. 2, pp. 127–142, 2016.

[3.50] L. Mujica, J. Rodellar, A. Fernandez, and A. Guemes, "Q-statistic and t2-statistic pca-based measures for damage assessment in structures," *Structural Health Monitoring*, p. 1475921710388972, 2010.

[3.51] P. F. Odgaard, B. Lin, and S. B. Jorgensen, "Observer and data-driven-model-based fault detection in power plant coal mills," *IEEE Transactions on Energy Conversion*, vol. 23, no. 2, pp. 659–668, 2008.

Chapter 4

A damage classification approach for structural health monitoring using machine learning

Publishing information

Disclaimer: This chapter is a true copy of the original paper published in the journal where the only changes are performed to fit the page setup.

Contents

A damage classification approach for structural health monitoring using machine learning

abstract

Inspection strategies with guided wave-based approaches give to structural health monitoring applications (SHM) several advantages, among them, the possibility of the use of real data from the structure which enables continuous monitoring and online damage identification. These kinds of inspection strategies are based on the fact that these waves can propagate over relatively long distances and are able to interact sensitively with and uniquely with different types of defects. The principal goal for SHM is oriented to the development of efficient methodologies to process these data and provide results associated with the different levels of the damage identification process. As a contribution, this work presents a damage detection and classification methodology which includes the use of data collected from a structure under different structural states by means of a piezoelectric sensor network taking advantage of the use of guided waves, hierarchical non-linear principal component analysis (h-NLPCA), and machine learning. The methodology is evaluated and tested in two structures: (i) a carbon fibre reinforced polymer (CFRP) sandwich structure with some damages on the multi-layered composite sandwich structure; and (ii) a CFRP composite plate. Damages in the structures were intentionally produced to simulate different damage mechanisms, that is, delamination and cracking of the skin.

Keywords: wavelet, machine learning, principal component analysis, piezoelectric sensors, damage classification.

4.1   Introduction

Data-driven algorithms have demonstrated their utility in structural health monitoring (SHM) applications. In fact, the use of this kind of approaches is a useful tool for real-time condition monitoring (CM). However, one of the challenges in the use of data-driven algorithms is associated with the size and quantity of information which is often obtained from sensor networks or multiple sensors. This information represents a great deal of data to process and analyse. In this sense, it is necessary to develop better methodologies which allow avoiding false alarms in the damage identification process. An SHM system typically includes five steps in its design, these are (i) sensor network design; (ii) data acquisition; (iii) feature extraction, (iv) diagnosis and (v) prognosis. The first four stages normally involve methods for data-sensor fusion, multivariate statistical modelling and pattern recognition algorithms. For the later, a physics-based model is almost inevitable so that reliable predictions can be performed. It is evident that structural health monitoring systems have been advancing worldwide as shown by the amount of relevant available scientific papers and recent practical applications [4.1, 4.2, 4.3]. Among the solutions in the application of data driven algorithms for SHM, there are many applications in bridges [4.4, 4.5, 4.6], aeronautics [4.7, 4.8] , aerospace [4.9, 4.10], wind turbines [4.11, 4.12, 4.13], among others.

As a contribution to the development of new ways to process and evaluate the condition of a structure using data from sensors, a methodology for damage classification and detection is presented in this chapter. This work is also motivated by the need to further develop, integrate and evaluate damage identification algorithms [4.7, 4.14, 4.15]. The proposed methodology is based on an acousto-ultrasonic approach in which ultrasonic waves are generated in a piezo-electric transducer sensor network in several actuation phases. The captured signals are pre-processed by means of the discrete wavelet transform (DWT) for feature extraction and then integrated into a non-linear multivariate model where some non-linear components are generated in order to form feature vectors for all the actuation phases and to train a machine by means of the machine learning point of view. Afterward, measurements with the sensor network are captured from the structure in an unknown state and the interaction with the training machine allows defining the current structural state according to the states defined in the training step. To validate the proposed methodology, experiments are carried out in a composite sandwich structure in which increasing damage is intentionally introduced and a composite plate with simulated damages.

The remaining part of this paper is organized as follows. For completeness, the article first presents a brief summary of the basic theoretical background for the different evaluated signal

processing algorithms. Afterward, the methodology is introduced in Section 3. Section 4 is devoted to the experimental validation, where the experimental setup and results are included. Finally, conclusions are given in Section 5.

4.2 Theoretical Background

This section introduces some brief concepts about some well-known methods that are used in the developed methodology. Authors suggest reviewing the references in each subsection if more information about each method is required.

4.2.1 Discrete Wavelet Transform

The discrete wavelet transform (DWT) is a very useful tool, used in an increasingly broad horizon, image processing, health care, energy distribution, SHM, and others. That can be defined as a filter bank structure to distinguish features through the use of low-pass filters and high-pass filters [4.16, 4.17]. This configuration allows representing the variability of a given function by means of coefficients at a specified time and scale. These coefficients are calculated by using quadrature mirror filters and are decomposed in approximation (A1, A2,...) and detail coefficients (D1, D2,...) [4.7] as it is shown in Figure 4.1.
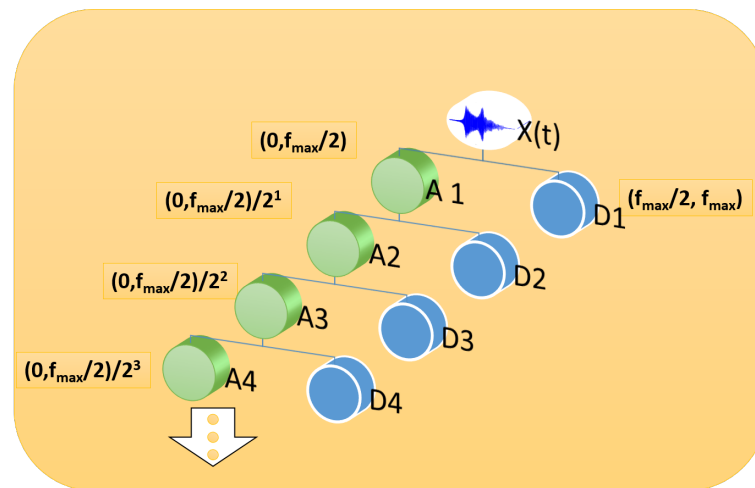
FIGURE 4.1: Discrete wavelet transform decomposition.

Detail coefficients are low-scale, high-frequency components, while the approximation coefficients represent the high-scale, low-frequency components. The wavelet technique has been of great interest in recent years and has direct application for the SHM like demonstrates some research works [4.18, 4.19, 4.20, 4.21, 4.22]. For further details about DWT and its implementation, please refer to [4.23].

4.2.2 Hierarchical Non-Linear Principal Component Analysis

The hierarchical non-linear principal component analysis is also known as h-NLPCA and is also defined as a non-linear generalization of traditional PCA [4.24]. This is a method based on a multi-layered perceptron (MLP) architecture with an auto-associative topology. The auto-associative network works with the inputs and outputs to perform the identity mapping by using the square error [4.24]. This architecture, shown in Figure 4.2, includes a bottleneck layer which allows to compress data and reduce the dimension of the original data. Note that the nodes in the mapping and de-mapping layers must have nonlinear transfer functions; nonlinear transfer functions are not necessary for the bottleneck layer [4.25]. With the purpose of guaranteeing that the calculated nonlinear components have the same hierarchical order as the linear components in standard principal component analysis (PCA), and in contrast to standard NLPCA, the reconstruction error is controlled by searching a k dimensional subspace of minimum mean square error (MSE) under the constraint that the (k-1) dimensional subspace is also of minimal MSE [4.26]. This process is repeated for any k-dimensional subspace where all subspaces must be of minimal MSE. h-NLPCA describes the data with greater accuracy and/or by fewer factors than PCA, provided that there are sufficient data to support the formulation of more complex mapping functions [4.27, 4.28].
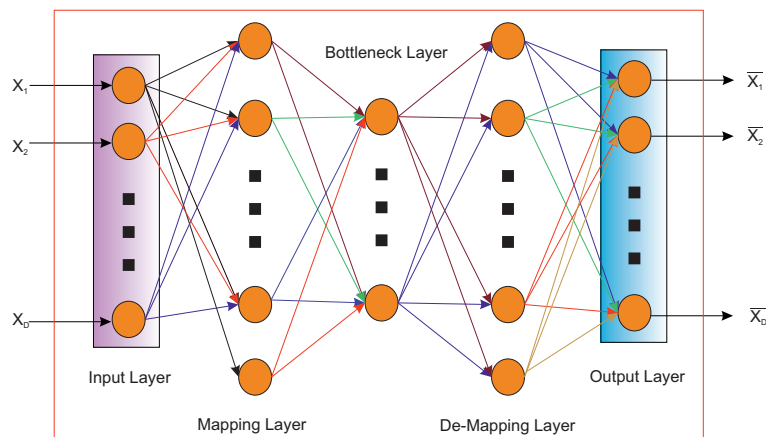
FIGURE 4.2: Network architecture for h-NLPCA.

4.2.3 Machine learning

In the recent years, the machine learning (ML) has been the focus of many researchers in the area of structural health monitoring (SHM) by its effectiveness and continuous development [4.29, 4.30, 4.31, 4.32]. Machine learning is a set of algorithms that can extract -in an automatic way- the hidden patterns in a large group of data [4.33, 4.34]. There are two different approaches according to ML according to the training process:

(i) Supervised, where the machine gets the inputs and the expected outputs. The machine is trained to find the complex patterns and relationships between them and obtain generalized responses based on this training with right answers [4.35, 4.36]. (ii) Unsupervised, where the machine is trained to find the similarities in the data and provide a clustering organization to indicate its proximity [4.37, 4.38].

In this work, a supervised training is explored, in this sense, some of the supervised machines used in the methodology are subsequently explained. On one hand, k nearest neighbours (kNN) is a machine learning algorithm that has a very simple strategy. More precisely, the elements are classified by the distance to others and the frequency with which this proximity is presented. It is important not to take the risk of overfitting. In this case, the trained machine will only apply for the current group of data. Therefore, to ensure that this does not occur, it is important to keep a moderate number of characteristics and training examples.

On the other hand, decision trees are a predictive model used in, for instance, data mining and statistics. This mechanism maps the observations in a structure that allows to reveal conclusions about these observations. This structure also allows to extrapolate these conclusions and predict new behaviours with new observations. To extract the desired structure that describes the information, an analysis of the data and the critical values that builds a better division of them is performed. This division is performed after locating the choice nodes and the change nodes in the decision structure with the aim of obtaining a better decision branches, and a best behaviour in the prediction.

In order to facilitate that the machine reaches the goal, it is very common to simplify the input data through some techniques [4.2, 4.39]. In this work, only the supervised type is explored and results are presented by the use of the confusion matrices. These types of matrices are a very useful tool to classify data considering the following classes: true positives, false negatives, false positives and true negatives.

4.3 Damage classification methodology

In the current work piezoelectric transducers were used because these devices are cheap, easy to install, lightweight, and with several other good characteristics [4.40, 4.41]. Figure 4.3 shows a representation of the methodology applied. This can be divided into two parts: training and testing, where in both cases the strategy use data from the structure collected by a piezoelectric sensor network in several actuation phases. This network is built with several piezoelectric transducers which are attached to the structure under test in a permanent way and distributed over its surface as in Figure 9 and Figure 13. Because these transducers can work as actuators or as sensors, each actuation phase is defined by a PZT working as an actuator and using the rest of PZTs as sensors, this procedure is repeated for each PZT in the sensor network [4.42]. This means that an excitation signal is applied to a piezoelectric sensor and propagated signals

through the structure are collected by the rest of sensors, organized and pre-processed. This process is repeated for each sensor in the structure [4.43, 4.44]. Each signal captured by the acquisition system is pre-processed by the Discrete Wavelet Transform at a defined decomposition level and as result, a reduced signal is obtained and organized by each actuation phase as in [4.43]. These steps are the same for training and testing steps. Once, data is pre-processed and organized, during the training step, h-NLPCA is applied to the data by each actuation phase and a determined number of non-linear components are obtained and used for training the machines. As result, a machine with the information of the structural states is trained and is available for testing step. Data coming from the structure or specimen to be classified is projected into the non-linear components to obtain the so-called scores. Some of measurements per each damage state (including undamage state) are used to training the machines and the others to test the behaviour of the prediction, variations of this setup can change the machines performance, in particular, the first three scores (S1, S2, S3) by each actuation phase are used to define the feature vector for training the machines as it is shown in Figure 4.4. This Figure is an example when only four sensors are used as in the case of the specimen 1.
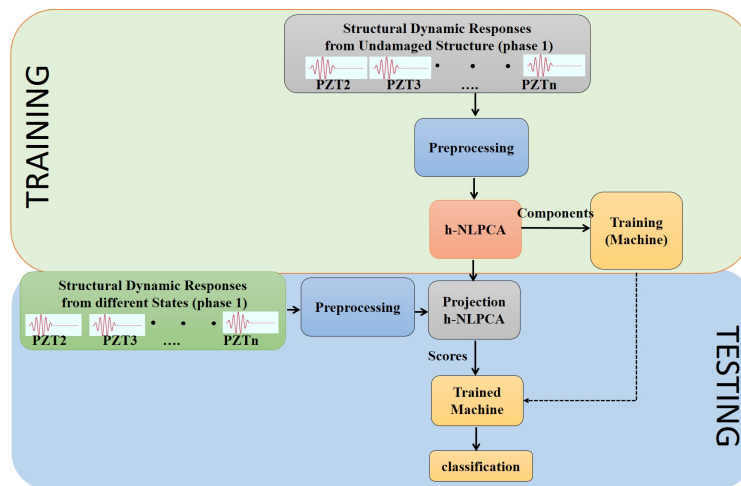
FIGURE 4.3: Damage classification methodology.

Testing is performed by using data from the structure in an unknown structural state and projecting the information to the non-linear components, as results of this projection appear the scores which are used as input to the trained machine to predict the kind of structural state. This procedure allows to detect and classify the structural state.
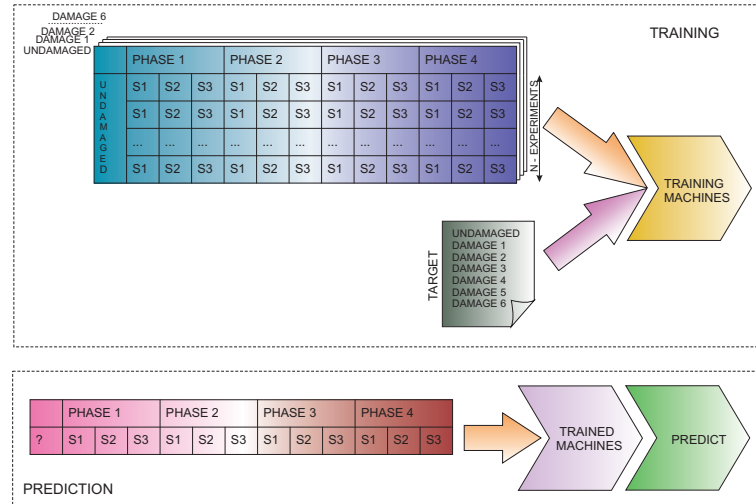
FIGURE 4.4: Methodology - machine learning.

4.4 Experimental Validation

To validate the methodology, data from two structures are considered. A carbon fiber-reinforced plastic (CFRP) sandwich structure with some damages on the multi-layered composite sandwich structure and a CFRP plate were used. In the upcoming sections there is a detailed description of the measurement procedure, the structures and the results obtained from the use of the developed methodology.

TABLE 4.1: Damage description.

Damage Number	Description
1	Delamination: started symmetrically from the right side of the sample at its middle position along the y-axis. Its width along the is is 16mm and its depth along the x-axis is 10 mm.
2	Extended the previous damage to a width of 33 mm and depth of 42mm.
3	A crack of 25 mm length initiated at the middle position along the vertical y-axis and in the parallel direction to the x-axis.
4	Extended the previous crack to a length of 30 mm.
5	Extended the previous crack to a length of 45 mm.
6	Extended the previous crack to a length of 70 mm.

4.4.1   Measurement procedure

As it has been previously introduced in the last section, the interaction with the structure is performed by the signals applied and collected to the piezoelectric sensor network. In the cases of the structures evaluated in this paper, piezoelectric sensors PIC-151 were used. The inspection is performed in four phases for the specimen 1 and nine phases for the specimen 2 due to the number of piezoelectric sensors installed in each structure. During the first actuation phase (phase I), the first piezoelectric was stimulated with a Hamming windowed cosine signal, 12 volts of the peak value and a frequency determined for each structure, and the information of the interaction of the propagated waves with the structure is collected in different places of the structure by the rest of the sensors. Figure 4.5 describes an example of this actuation phase. The second actuation phase (phase II) implies the use of the second piezoelectric as an actuator and the rest used as sensors, and so on. This process ends when all piezoelectric transducers have been used as an actuator. All this information is stored for the subsequent process in several matrices and files, one per each actuation phase.
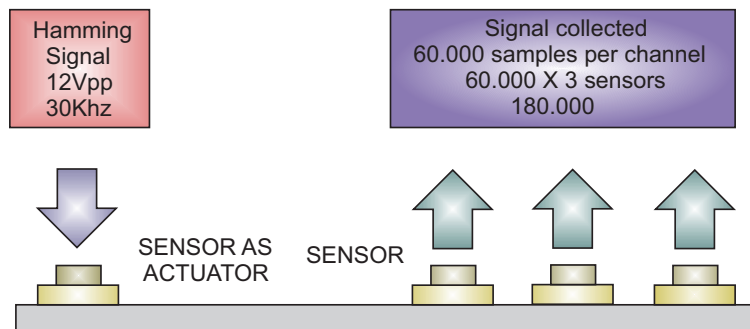
FIGURE 4.5: Structure exploration

Experiments consider different structural states (healthy and structure with damage in different positions) as it will be explained in the following subsections. Number of samples of each sensor is 60.000. This means that the number of columns in this matrix is (n-1) sensors x 60.000 samples. Figure 4.6 shows this organization, the corresponding pre-processing and the procedure to extract the h-NLPCA scores, the training were made with a vector of twelve elements (three scores from each actuation phase) in the case of specimen 1 (4 sensors – 4 actuation phases); these data were extracted of the calculated scores from each phase. One hundred and fifty (150) experiments were made for each damage state; one hundred (100) of these were used for the training, and fifty (50) for prediction and its behaviour test. Another setup was selected to demonstrate variation in the training and its impact over the behaviour of prediction. With respect to the normalization, group scaling was used in each matrix from each actuation phase [4.45].
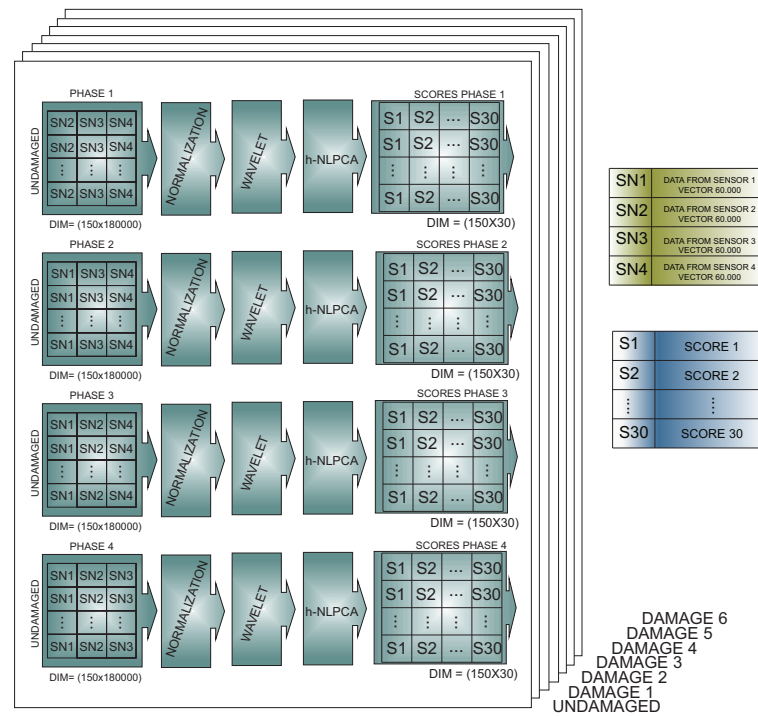
FIGURE 4.6: Data organization - h-NLPCA scores, before build the training vector

As it has been explained in the methodology, the obtained h-NLPCA scores are used to build the training vectors of the machines with three scores per phase. Figure 4.7 shows the assembled training vector.
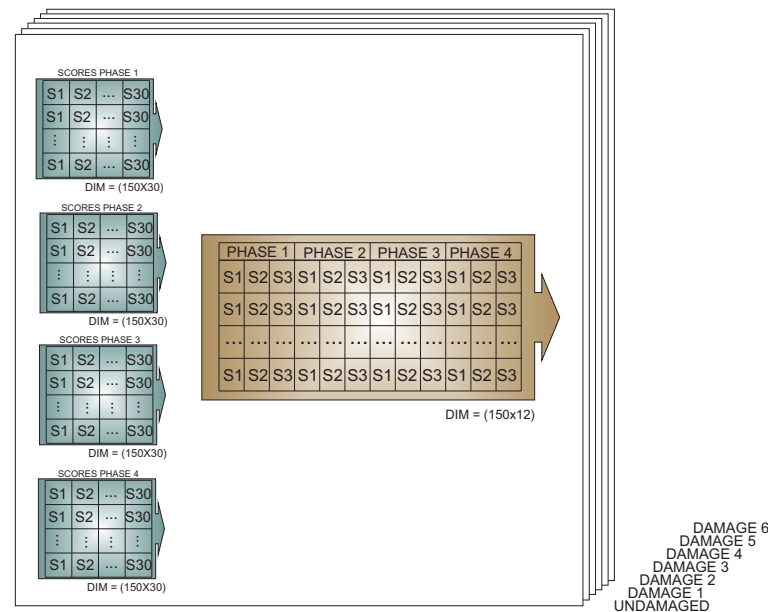
FIGURE 4.7: Assembled training vector.

4.4.2 Specimen 1: CFRP sandwich structure

The first structure corresponds to a CRFP sandwich structure (Figure 4.8), where the damages are intentionally produced to simulate different damage mechanisms, i.e. delamination and cracking of the skin. These damage mechanisms are summarized in Table 1. The overall size of this structure is 217 mm x 217 mm x 31 mm and it is made of carbon/epoxy material with a 0.5 mm thickness. The stacking sequence is $[\,0° \; 90°\,]$ (Figure 4.9).
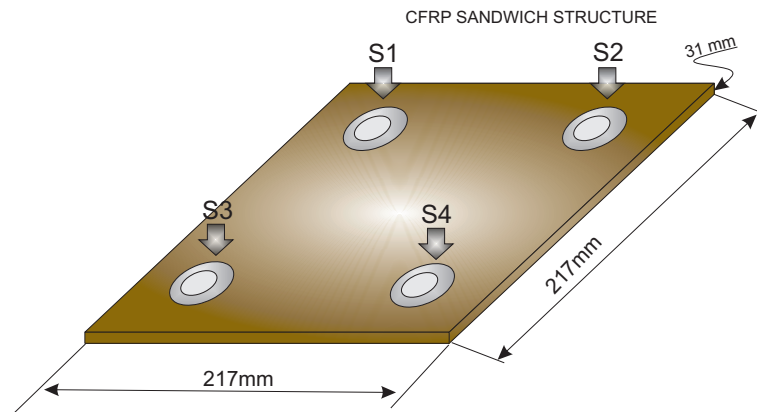
FIGURE 4.8: Specimen 1: CFRP sandwich structure and PZT distribution.

The core is made of polyetherimide foam with a 30 mm thickness. Four PIC-151 piezoelectric transducers from PI Ceramics are attached to the surface of the structure with equidistant spacing. Figure 4.9 shows a photo of the experiment.
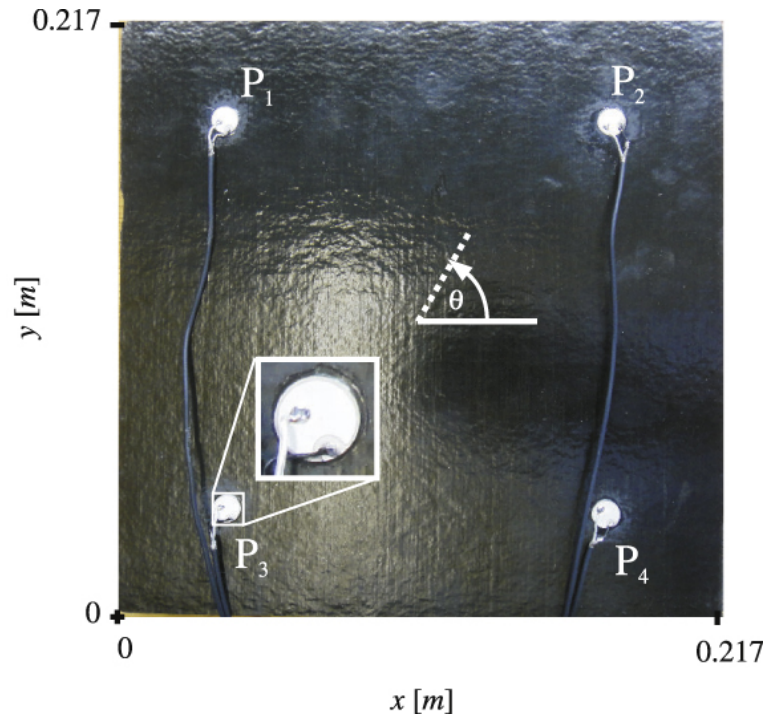
FIGURE 4.9: CRFP sandwich structure.

The scan frequency was a 50 kHz, with a peak voltage of 12 V, and Hamming windowed cosine form, with five cycles. Seven structural states were studied (healthy state and six damages) as it was previously explained. In each structural state 150 experiments were performed, according to the following distribution: 100 experiments were used for training and 50 experiments for testing. Data from each experiment was pre-processed by means of the DWT. The family Daubechies (db8) was chosen to obtain the approximation coefficients [4.46, 4.47]. This selection was applied since previous works demonstrated that this family contains most relevant information for this kind of applications. Coefficients are used to build the hierarchical non-linear PCA model for each actuation phase. The architecture of the h-NLPCA is a five layer nonlinear autoencoder network with 3-4-2-4-3 components as in [4.48]. As a result, three components by each actuation phase are used to build the feature vector that is used as the input for the training process to four different machines. For the training part, the MATLAB classification learner app was used.

Subsequently, testing is performed by using data from the structure in an unknown structural state and projecting the information to the non-linear components. The projected information, called scores, is used as the input to the trained machine to predict the kind of structural state. This procedure allows to detect and classify the structural state.

Several machines were trained to determine the elements in the feature vector, i.e. to determine the influence and the number of scores to use by actuation phase and the number of

experiments for an adequate training machine. Table 2 shows the results in the prediction process when two scores by each actuation phase and fifty experiments are used in the training step. During the prediction, one hundred experiments per damage are used. Twenty supervised learning machines were training using MATLAB's classification learner toolbox.

As it is possible to observe, all structural states are not properly predicted in all the trained machines, this means that a low number of scores affect the classification process. Table 3 shows the results when the number of scores per actuation phase are increased to five. As it is possible to observe, prediction improves in most of the machines, however, it is necessary to determine an adequate number of scores, because when it is increased could produce machine overfitting, and the learning may be poor. This is that the mistakes are added to others predictions and growing up the uncertainty.

Consistent with previous research, fine kNN and weighted kNN showed better results in the classification. However, when the number of scores is increased, other machines such as bagged trees and subspace kNN significantly improved their performance.

Some consideration about the algorithms can be summarized as follows, the k nearest neighbour (kNN) classifier is an algorithm recommended to work with low dimensional data. Particularly, in this kind of machine, the number of neighbours have an effect over the response so, in general, the use of a reduced number of neighbours improve the outcome. Decision trees (DT) is a different kind of machine. In this case, DT is a classification mechanism that allows to construct a predictive model where the value of splits can increase or decrease the flexibility of this algorithm, as well as the use of various trees (ensemble). Other kind of machine explored in this paper is the RUS (Random Under Sampling) algorithm in RUSBoost, which is a mechanism to eliminate data distribution imbalances.

TABLE 4.2: Behavior of machines with two scores per sensor (specimen 1, four sensors).

MACHINE NAME	UND	DMG1	DMG2	DMG3	DMG4	DMG5	DMG6
Complex Tree	90%	99%	13%	92%	100%	90%	100%
Medium Tree	90%	88%	13%	92%	100%	90%	100%
Simple Tree	90%	99%	0%	0%	100%	90%	100%
Linear SVM	96%	98%	81%	95%	99%	99%	100%
Quadratic SVM	96%	98%	96%	95%	99%	99%	100%
Cubic SVM	96%	99%	98%	95%	99%	99%	100%
Fine Gaussian SVM	68%	100%	57%	87%	79%	78%	99%
Medium Gaussian SVM	97%	100%	76%	100%	97%	98%	100%
Coarse Gaussian SVM	95%	98%	94%	96%	99%	99%	100%
Fine *k*-NN	97%	100%	96%	98%	99%	100%	100%
Medium *k*-NN	95%	100%	93%	94%	99%	100%	100%
Coarse *k*-NN	91%	100%	85%	80%	99%	100%	94%
Cosine *k*-NN	95%	100%	74%	89%	99%	100%	100%
Cubic *k*-NN	95%	99%	89%	93%	99%	99%	100%
Weighted *k*-NN	95%	100%	95%	97%	99%	100%	100%
Boosted Trees	90%	100%	20%	1%	100%	98%	100%
Bagged Trees	99%	100%	71%	95%	100%	100%	100%
Subspace Discriminant	97%	100%	64%	97%	100%	100%	100%
Subspace *k*-NN	97%	100%	82%	98%	100%	100%	100%
Rusboosted Trees	90%	100%	0%	0%	0%	0%	0%

TABLE 4.3: Behavior of machines with five scores per sensor (specimen 1, four sensors).

MACHINE NAME	UND	DMG1	DMG2	DMG3	DMG4	DMG5	DMG6
Complex Tree	90%	99%	18%	99%	99%	97%	100%
Medium Tree	90%	99%	18%	99%	99%	97%	100%
Simple Tree	90%	99%	0%	100%	0%	97%	100%
Linear SVM	97%	100%	100%	99%	99%	99%	100%
Quadratic SVM	97%	100%	100%	99%	99%	99%	100%
Cubic SVM	97%	100%	100%	99%	99%	99%	100%
Fine Gaussian SVM	100%	9%	8%	28%	8%	30%	56%
Medium Gaussian SVM	99%	100%	98%	99%	99%	98%	100%
Coarse Gaussian SVM	98%	100%	100%	100%	99%	100%	100%
Fine *k*-NN	97%	100%	100%	100%	99%	100%	100%
Medium *k*-NN	97%	100%	100%	100%	99%	100%	100%
Coarse *k*-NN	93%	100%	100%	99%	97%	100%	100%
Cosine *k*-NN	96%	100%	100%	100%	99%	100%	100%
Cubic *k*-NN	95%	100%	100%	100%	99%	99%	100%
Weighted *k*-NN	97%	100%	100%	100%	99%	100%	100%
Boosted Trees	90%	100%	0%	100%	0%	100%	100%
Bagged Trees	99%	100%	100%	100%	100%	100%	100%
Subspace Discriminant	98%	100%	100%	100%	99%	100%	100%
Subspace *k*-NN	98%	100%	100%	100%	99%	100%	100%
Rusboosted Trees	90%	100%	0%	0%	0%	0%	0%

Figure 4.10 and Figure 4.11 show the results in the damage classification process for fine kNN, weighted kNN, simple tree and rusboosted trees. Detailed information about the definition of these machines can be found in [4.7, 4.44, 4.49]. As it is possible to observe in Figure 10, both fine kNN and weighted kNN presented some of the best results since, in most of the experiments, the classification was properly performed, verifying its good behaviour like a statistical classifier [4.50]. For instance, in the fine kNN classifier, 348 cases have been correctly classified out of 350 cases. This magnitude represents 99,4% of correct decisions. It is worth noting that the specimen with damage is never confused with the healthy state of the structure thus leading to an absence of missing faults. The only misclassification between damages occurs with a sample corresponding to damage 2 that is classified as damage 3. Similar results are obtained when the weighted kNN is considered as the classifier. In this case, 348 cases have been correctly classified out of 350 cases, which represents 99,4% of correct decisions, too. However, in this case, all the damages are perfectly classified. The number of false alarms is

quite reduced in both cases: 1 out of 50 (2%) and 2 out of 50 (4%), with respect to fine kNN and weighted kNN, respectively.
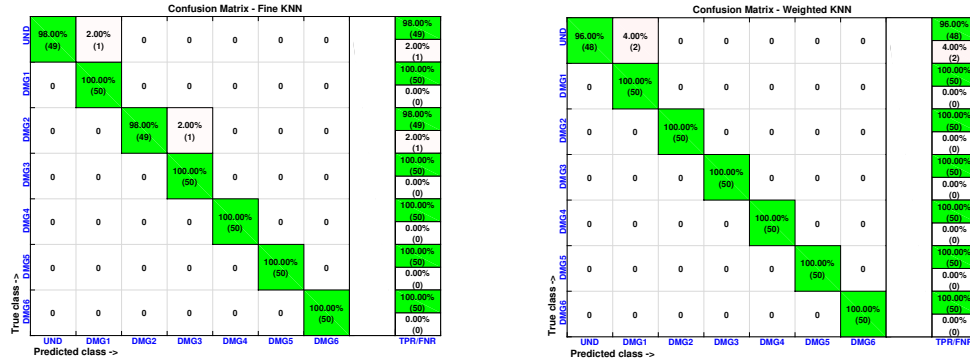
FIGURE 4.10: Confusion matrices for fine kNN (left) and weighted kNN (right) machines.

Worst results in the classification are obtained when rusboosted trees and simple tree machines are used. These results are summarized through the corresponding confusion matrices in Figure 4.11. The overall accuracy is 26,3% and 88,9%, in the case of rusboosted trees and simple tree machines, respectively. The classification is especially unacceptable in the case of rusboosted trees where damages 2 to 6 are all misclassified.

FIGURE 4.11: Confusion matrices for rusboosted trees (left) and simple tree (right) machines.

4.4.3 Specimen 2: CFRP composite plate

The second structure, shown in Figure 12 and Figure 13, corresponds to a CFRP plate made of 4 equal layers and stacking of $[0° \ 90° \ 90° \ 0°]$. Dimensions are 200 mm x 250 mm with a thickness of 1.7 mm and a density of 1.700 kg/m3. Nominal material parameters of the unidirectional (UD) layers are E1 =122 GPa, E2 = 10 GPa, ν12= 0.33,ν13=0.3, ν23=0.34, G12=G13=7.4 GPa and G23=5.4 GPa.
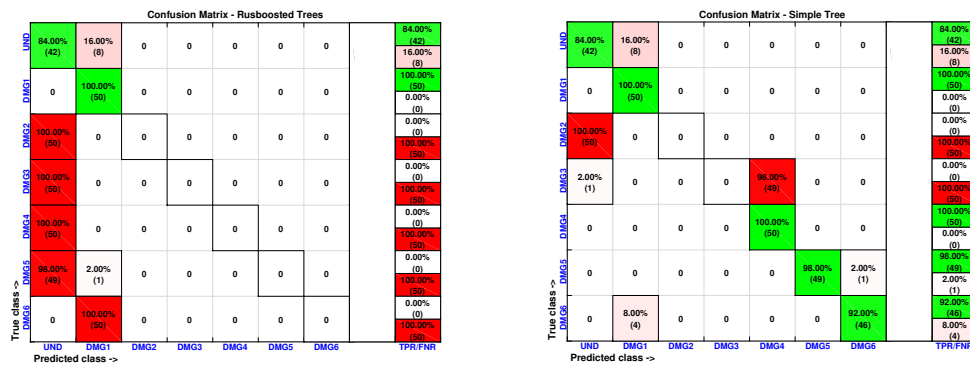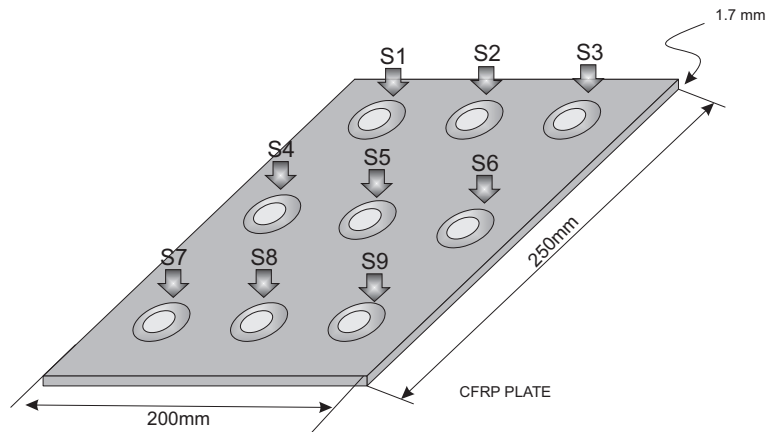

FIGURE 4.12: Specimen 2 - CFRP composite plate, sensors distribution.

This structure was instrumented with nine piezoelectric transducers PIC-151 from PI Ceramics which are attached to the surface of the structure as it is shown in Figure 4.12. Damage on the tested composite was simulated by localizing masses at different positions as described in Table 4.

TABLE 4.4: Damages in the CFRP composite plate.

Damage number	Damage location between sensors	X position [mm]	Y position [mm]
1	Sensors 1-2	65	220
2	Sensors 2-3	135	220
3	Sensors 3-6	170	172.5
4	Sensors 6-9	170	66.5
5	Sensors 5-8	100	66.5
6	Sensors 5-4	65	125

FIGURE 4.13: CFRP composite plate.

The excitation signal is a 12 V Hamming windowed cosine train signal with 5 cycles, 150 experiments have been performed and signals from sensors have been also recorded per sensor–actuator configuration. To determine the carrier central frequency for the actuation signal in each structure, a frequency sweep was performed and spectral analysis of each signal was analysed. The carrier frequency was found to be 30 kH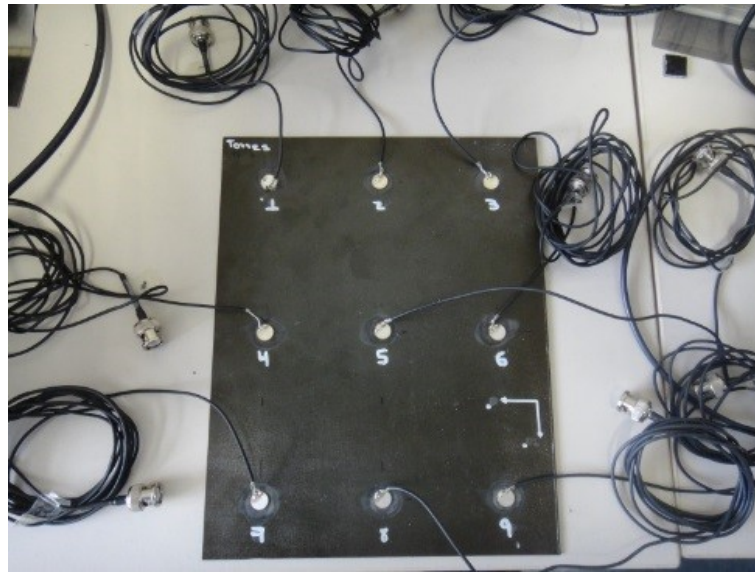z. A photo of this second specimen can be found in Figure 13. As with the previous specimen, several machines were trained and three scores were used per actuation phase. For this second experiment, and for the case of fine kNN and weighted kNN, the result are even better (Figure 14). More precisely, in the fine kNN classifier, 349 cases have been correctly classified out of 350 cases. This magnitude represents 99,7% of correct decisions. It is worth noting that the specimen with damage is never confused with the healthy state of the structure thus leading to an absence of missing faults. The only misclassification between damages occurs with a sample corresponding to damage 1 that is classified as damage 2. A perfect classification is obtained when the weighted kNN is considered as the classifier. In this case, 350 cases have been correctly classified out of 350 cases, which represents 100% of correct decisions. With respect to this second specimen, false alarms are no longer present.
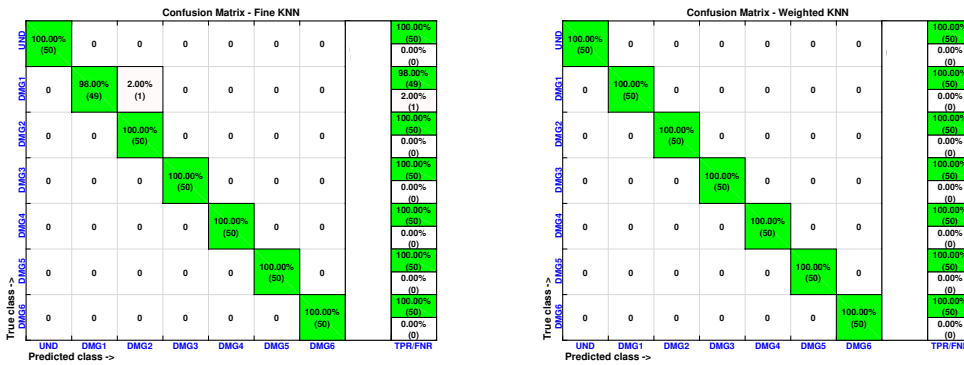
FIGURE 4.14: Confusion matrices for fine kNN (left) and weighted kNN (right) machines.

Worst results in the classification are obtained when rusboosted trees and simple tree machines are used. These results are summarized through the corresponding confusion matrices in Figure 15. The overall accuracy is 28,3% and 70,9%, in the case of rusboosted trees and simple tree machines, respectively. The classification is especially unacceptable in the case of rusboosted trees where damages 2 to 6 are all misclassified. Although the percentage of correct decisions fluctuates between 28,3% and 70,9%, both machines are able to accurately identify the structure with no damage. In general, the behaviour of these four machines in this paper with respect to both specimens is coherent with previous results in the literature. For instance, in the work of Vitola et al. [4.44, 4.49], a distributed sensor network is used to detect and classify structural changes with and without the influence of environmental conditions. Although in those papers how the data is collected and pre-processed differs significantly from the current work, the performance of both fine kNN and weighted kNN is similar.
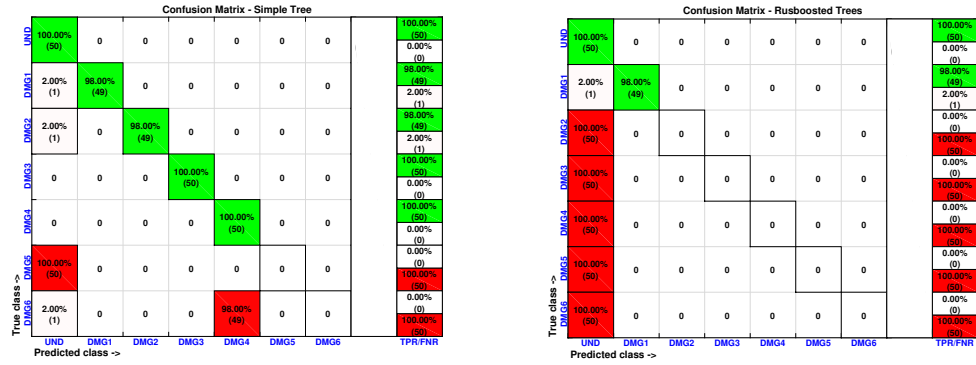
FIGURE 4.15: Confusion matrices for simple tree (left) and rusboosted trees (right) machines.

In this work, a damage classification methodology has been introduced. The proposed methodology includes the use of a piezoelectric sensor network, discrete wavelet transform, hierarchical non-linear PCA, and machine learning approaches. The methodology has been validated with excellent results showing its capability for damage classification tasks. Although different machines were trained, only the best two and the worst two of them were included in the paper, showing that the best results were obtained with fine kNN and weighted kNN machines and worst results are obtained by the use of trees. This is because the way as the data is organized by the different machines as was introduced along the paper.

In order to work with machine learning algorithms it is very important to select the training data in a proper way. Otherwise, results in the trained machine can be different to the system expectations. The non-linear scores demonstrated that the extracted information was very useful, since these scores reduced significantly the information by facilitating the training, and reducing the error possibilities in the predictions. In all studied cases, the use of three nonlinear scores demonstrates to be enough for building the featured vector by fusing data from all actuation phases. The k nearest neighbours algorithm has also shown to be an efficient and useful mechanism to applications in structural health monitoring. Results in this work also indicated its usefulness with the use of non-linear features.

The use of neural networks in this work is only considered to obtain the nonlinear components; however it is expected to work in a near future with different neural networks approaches for classification.

Although this work is not focused in the study of the relationship between the number and location of sensors but in the damage classification methodology, the inspected structures allow to extend the idea of the usefulness of this methodology by the following differences between the validations:

1. Different structures with different materials and configurations.

2. Structures with real (delamination and cracks) and simulated damage (added mass in different locations).

3. Progressive damage.

4. Structures with different sizes.

5. Structures are inspected with a different number of sensors at different locations. In the case of the first structure only four sensors were used and the second structure was inspected with nine sensors.

Future work will involve the influence of the number of sensors and location. However this study allows to observe that the methodology can be used with similar results in different structures with different number and position of the sensors and with different kind of damages.

Acknowledgments

Conflict of interests

The authors declare no conflict of interest. The founding sponsors had no role in the design of the study; in the collection, analyses, or interpretation of data; in the writing of the manuscript, and in the decision to publish the results.

Abbreviations

The following abbreviations are used in this manuscript:

CFRP	Carbon fibre-reinforced plastic.
db8	Daubechies.
DWT	discrete wavelet transform.
h-NLPCA	Hierarchical non-linear principal component analysis.
*k*NN	*k*-Nearest Neighbours.
ML	Machine learning.
MLP	Multilayered perceptron.
mm	Millimetres.
MSE	Mean square error.
PCA	Principal component analysis.
PZT	Piezoelectric sensor.
SHM	Structural Health Monitoring.

Bibliography

[4.1] K. V. Buren, J. Reilly, K. Neal, H. Edwards, and F. Hemez, "Guaranteeing robustness of structural condition monitoring to environmental variability," *Journal of Sound and Vibration*, vol. 386, pp. 134–148, 2017.

[4.2] K. Worden and C. R. Farrar, *Structural Health Monitoring: a machine learning perspective*. 2013.

[4.3] D. Balageas, C.-P. F. D., and A. Güemes, *Structural Health Monitoring*. Hermes Science Publishing, 2006.

[4.4] M. T. Yarnold and F. L. Moon, "Temperature-based structural health monitoring baseline for long-span bridges," *Engineering Structures*, vol. 86, pp. 157 – 167, 2015.

[4.5] M. M. Alamdari, T. Rakotoarivelo, and N. L. D. Khoa, "A spectral-based clustering for structural health monitoring of the Sydney Harbour Bridge," *Mechanical Systems and Signal Processing*, vol. 87, Part A, pp. 384–400, 2017.

[4.6] J. J. McCullagh, T. Galchev, R. L. Peterson, R. Gordenker, Y. Zhang, J. Lynch, and K. Najafi, "Long-term testing of a vibration harvesting system for the structural health monitoring of bridges," *Sensors and Actuators A: Physical*, vol. 217, pp. 139–150, 2014.

[4.7] D. A. T. Burgos, "Design and Validation of a Structural Health Monitoring System for Aeronautical Structures -," *PhD thesis*, vol. 1, 2012.

[4.8] R. K. Neerukatti, K. C. Liu, N. Kovvali, and A. Chattopadhyay, "Fatigue Life Prediction Using Hybrid Prognosis for Structural Health Monitoring," *Journal of Aerospace Information Systems*, vol. 11, pp. 211–232, apr 2014.

[4.9] V. Giurgiutiu, *Structural Health Monitoring of Aerospace Composites*. Academic Press - ELSEVIER, 2015.

[4.10] A. Korobenko, M. Pigazzini, V. Singh, H. Kim, D. L. Allaire, K. E. Willcox, A. Marsden, and Y. Bazilevs, "Dynamic-Data-Driven Damage Prediction in Aerospace Composite Structures," in *17th AIAA/ISSMO Multidisciplinary Analysis and Optimization Conference*, AIAA AVIATION Forum, American Institute of Aeronautics and Astronautics, jun 2016.

[4.11] I. Antoniadou, N. Dervilis, E. Papatheou, A. E. Maguire, and K. Worden, "Aspects of structural health and condition monitoring of offshore wind turbines," *Philosophical Transactions of the Royal Society of London A: Mathematical, Physical and Engineering Sciences*, vol. 373, no. 2035, 2015.

[4.12] S. Bogoevska, M. Spiridonakos, E. Chatzi, E. Dumova-Jovanoska, and R. Höffer, "A Data-Driven Diagnostic Framework for Wind Turbine Structures: A Holistic Approach," *Sensors*, vol. 17, no. 4, 2017.

[4.13] F. Pozo and Y. Vidal, "Wind Turbine Fault Detection through Principal Component Analysis and Statistical Hypothesis Testing," *Energies*, vol. 9, no. 1, p. 3, 2015.

[4.14] M. Anaya, D. Tibaduiza, and F. Pozo, "Detection and classification of structural changes using artificial immune systems and fuzzy clustering," *International Journal of Bio-Inspired Computation*, vol. 9, no. 1, 2017.

[4.15] M. Angel and T. Arredondo, "Acoustic Emission Testing and Acousto-Ultrasonics for Structural Health Monitoring," 2014.

[4.16] M. J. Shensa, "The Discrete Wavelet Transform: Wedding the À Trous and Mallat Algorithms," *IEEE Transactions on Signal Processing*, vol. 40, no. 10, pp. 2464–2482, 1992.

[4.17] A. Graps, "An introduction to wavelets," *IEEE Computational Science and Engineering*, vol. 2, no. 2, pp. 50–61, 1995.

[4.18] H. Z. Hosseinabadi, B. Nazari, R. Amirfattahi, H. R. Mirdamadi, and A. R. Sadri, "Wavelet network approach for structural damage identification using guided ultrasonic waves," *IEEE Transactions on Instrumentation and Measurement*, vol. 63, no. 7, pp. 1680–1692, 2014.

[4.19] X. Chen, X. Li, S. Wang, Z. Yang, B. Chen, and Z. He, "Composite damage detection based on redundant second-generation wavelet transform and fractal dimension tomography algorithm of lamb wave," *IEEE Transactions on Instrumentation and Measurement*, vol. 62, no. 5, pp. 1354–1363, 2013.

[4.20] A. Medda, E. Chicken, and V. DeBrunner, "Sigma-Sampling Wavelet Denoising for Structural Health Monitoring," in *Statistical Signal Processing, 2007. SSP '07. IEEE/SP 14th Workshop on*, pp. 119–122, 2007.

[4.21] M. V. Golub, A. N. Shpak, I. Buethe, C.-P. Fritzen, H. Jung, and J. Moll, "Continuous wavelet transform application in diagnostics of piezoelectric wafer active sensors," in *Days on Diffraction (DD), 2013*, pp. 59–64, may 2013.

[4.22] H. Jeong, "Analysis of plate wave propagation in anisotropic laminates using a wavelet transform," *Ndt & E International*, vol. 34, no. 3, pp. 185–190, 2001.

[4.23] M. A. Torres-Arredondo, I. Buethe, D. A. Tibaduiza, J. Rodellar, and C.-P. Fritzen, "Damage detection and classification in pipework using acousto-ultrasonics and non-linear data-driven modelling," *Journal of Civil Structural Health Monitoring*, vol. 3, no. 4, pp. 297–306, 2013.

[4.24] M. Scholz, F. Kaplan, C. L. Guy, J. Kopka, and J. Selbig, "Non-linear PCA: a missing data approach.," *Bioinformatics (Oxford, England)*, vol. 21, pp. 3887–95, oct 2005.

[4.25] A. D. F. Santos, M. F. M. Silva, C. S. Sales, J. Costa, and E. Figueiredo, "Applicability of linear and nonlinear principal component analysis for damage detection," in *Instrumentation and Measurement Technology Conference (I2MTC), 2015 IEEE International*, pp. 869–874, may 2015.

[4.26] M. Scholz, *Approaches to Analyse and Interpret Biological Profile Data*. PhD thesis, Max Planck Institute of Molecular Plant Physiology, Potsdam University, 2006.

[4.27] M. A. Kramer, "Nonlinear principal component analysis using autoassociative neural networks," *AIChE Journal*, vol. 37, no. 2, pp. 233–243, 1991.

[4.28] M. A. Torres, D. A. Tibaduiza, L. E. Mujica, J. Rodellar, and C. P. Fritzen, "Damage Assessment in a Stiffened Composite Panel using Non-Linear Data-Driven Modelling and Ultrasonic Guided Waves," in *4 th International Symposium on NDT in Aerospace. Ausburg, Germany*, 2012.

[4.29] Z. Liu and N. Mrad, "Validation of Strain Gauges for Structural Health Monitoring With Bayesian Belief Networks," *Sensors Journal, IEEE*, vol. 13, no. 1, pp. 400–407, 2013.

[4.30] H. Hothu and A. Mita, "Damage Detection Method Using Support Vector Machine and First Three Natural Frequencies for Shear Structures," vol. 2013, no. June, pp. 104–112, 2013.

[4.31] J. Zhang and S. Zhou, "Structure Health Monitoring in Extreme Events From Machine Learning Perspective,"

[4.32] J. Zhang and Z. Hou, "Application of Artificial Immune System in Structural Health Monitoring," vol. 2014, no. 2, 2014.

[4.33] K. P. Murphy, *Machine Learning: A Probabilistic Perspective*. 1991.

[4.34] C. M. Bishop, *Pattern Recognition and Machine Learning*, vol. 4. 2006.

[4.35] W. Nick, J. Shelton, K. Asamene, and A. Esterline, "A study of supervised machine learning techniques for structural health monitoring," *CEUR Workshop Proceedings*, vol. 1353, pp. 133–138, 2015.

[4.36] D. Charles, C. Fyfe, D. Livingstone, and S. Mcglinchey, *Biologically Inspired Artificial Intelligence for Computer Games*. 2008.

[4.37] W. Nick, K. Asamene, G. Bullock, A. Esterline, and M. Sundaresan, "A Study of Machine Learning Techniques for Detecting and Classifying Structural Damage," *International Journal of Machine Learning and Computing*, vol. 5, no. 4, pp. 313–318, 2015.

[4.38] B. Clarke, E. Fokoue, and H. H. Zhang, *Principles and theory for data mining and machine learning*. Springer Science & Business Media, 2009.

[4.39] K. R. Mulligan, C. Yang, N. Quaegebeur, and P. Masson, "A data-driven method for predicting structural degradation using a piezoceramic array," *Internation Journal of Prognostics and Health Management*, vol. 4, no. 2, p. 37, 2013.

[4.40] F. G. Baptista and J. V. Filho, "Transducer loading effect on the performance of PZT-based SHM systems," *Ultrasonics, Ferroelectrics, and Frequency Control, IEEE Transactions on*, vol. 57, no. 4, pp. 933–941, 2010.

[4.41] F. G. Baptista and J. V. Filho, "Optimal Frequency Range Selection for PZT Transducers in Impedance-Based SHM Systems," *Sensors Journal, IEEE*, vol. 10, no. 8, pp. 1297–1303, 2010.

[4.42] M.-A. Torres-Arredondo, D.-A. Tibaduiza, M. McGugan, H. Toftegaard, K.-K. Borum, L. E. Mujica, J. Rodellar, and C.-P. Fritzen, "Multivariate data-driven modelling and pattern recognition for damage detection and identification for acoustic emission and acousto-ultrasonics," *Smart Materials and Structures*, vol. 22, no. 10, p. 105023, 2013.

[4.43] L. E. Mujica, D. A. Tibaduiza, and J. Rodellar, "Data-Driven Multiactuator Piezoelectric System for Structural Damage Localization," in *Fifth World Conference on Structural Control and Monitoring. Tokio-Japan*, 2010.

[4.44] J. Vitola, F. Pozo, D. Tibaduiza, and M. Anaya, "A Sensor Data Fusion System Based on k-Nearest Neighbor Pattern Classification for Structural Health Monitoring Applications," *Sensors*, vol. 17, no. 2, pp. 1–26, 2017.

[4.45] D. Tibaduiza, M. Torres, J. Vitola, M. Anaya, and F. Pozo, "Non-linear damage classification based on machine learning and damage indices," in *Structural Health Monitoring 2017: Real-Time Material State Awareness and Data-Driven Safety Assurance - Proceedings of the 11th International Workshop on Structural Health Monitoring, IWSHM 2017*, vol. 2, 2017.

[4.46] M. Scholz and R. Vigário, "Nonlinear PCA: a new hierarchical approach," *Proceedings of the 10th European Symposium on Artificial Neural Networks (ESANN)*, pp. 439–444, 2002.

[4.47] J. Vitola, F. Pozo, D. Tibaduiza, and M. Anaya, "Distributed piezoelectric sensor system for damage identification in structures subjected to temperature changes," *Sensors (Switzerland)*, vol. 17, no. 6, 2017.

[4.48] L. Holmstrom, P. Koistinen, J. Laaksonen, and E. Oja, "Neural and statistical classifiers-taxonomy and two case studies," *IEEE Transactions on Neural Networks*, vol. 8, no. 1, pp. 5–17, 1997.

[4.49] M. Anaya, D. A. Tibaduiza, and F. Pozo, "A bioinspired methodology based on an artificial immune system for damage detection in structural health monitoring," *Shock and Vibration*, vol. 501, p. 648097, 2015.

[4.50] M. A. Torres-Arredondo and D. A. Tibaduiza-Burgos, "An acousto-ultrasonics approach for probabilistic modelling and inference based on Gaussian processes," *Structural Control and Health Monitoring*, vol. 25, p. e2178, jun 2018.

Chapter 5

Conclusions and further work

Contents

5.1 Concluding remarks

The current work shows the machine learning algorithms used in the field of structural health monitoring to detection, classification, and localization of damages in metallic and composed structures, including bioinspired algorithms like artificial neural networks, all using data-driven approaches. The mechanism that explores the structure was the lamb waves produced by piezoelectric transducers attached to them. The interaction between the wave with the damages was detected using the approximation discussed using pattern recognition starting to the behavior of the piece without damages. In this search were involved a variety of machine learning algorithms; in particular, the supervised learning strategy was effectively to resolve the problem. Classification algorithms like K-Nearest Neighbor, decision tree machine, support vector machine SVM, and ensemble classifiers shown its performance, standing out the first of them.

5.2 Considerations about data acquisition

The exploration using lamb wave is convenient thanks to easy installation, inexpensive sensors; in general, You can use this technique in different structures, including new and old ones. The piezoelectric transducers are easy acquisition, and the digitalization system does not need to be high-frequency, which is one of the parameters that make these modules more expensive.

One of the elements that can make this equipment more expensive is the number of acquisition channels required; these are associated with the number of transducers attached to the structure and the number of stimulus circuits. A multiplexing system can reduce this cost; this fulfills the function of the route the stimulus signal to the transducers. The same way can be introduced in the acquisition system to use one digitalization unit but have the disadvantage of an increase in the exploration time.

The acquisition signal system includes a multiplexing module. Designed with analog relays, using these devices can be very convenient thanks to low impedance and high bandwidth; however, it also has weaknesses like the response velocity and noise in its commutation. In developing an upgrade, a solid-state version can improve the system. Design can be adjusted to one type of stimulus signal exclusively, to reduce the exploration time and make more economical it's building.

The acquisition process follows the previous works developed in the CoDAlab group, given the relevant results obtained for them, uses an exploration system that applied superficial lamb waves using attached piezoelectric transductors to Metallic and composed material structures.

The strategy use data from the structure collected by a piezoelectric sensor network in several actuation phases and involves data fusion technique. These characteristics allow the accumulation of a sufficient amount of information from different points of view, guaranteeing an informed evaluation.

5.3   Machine learning and bio-inspired algorithms

The machine learning is a recognized mechanism used in complex problems resolution. Some of its strategies imitate a natural process, like an artificial neural network that is a mathematical version of the biological system. The first step is to digitalize the interaction between the lamb waves and the superficial damages in the structures. Following these signals are pre-processed and stored. A pre-processing includes the use of digital filters that seek to eliminate signals that reduce the effectiveness of the detection, classification, or location procedure.

Before training the machines, it is necessary to extract characteristic values that allow the damages to be distinguished and its features.

The preprocessing stage seeks to combat these effects; in the first case, the digital low-pass filters reduce the high-frequency components. The second effect usually happens by elements within the acquisition, such as impedance of the channels, quality, and length of the connection cables, welds, and others; normalization processes are carried out to reduce this effect.

The preprocessing also introduces the discrete wavelet transform (DWT) technique is a handy tool, used in an increasingly broad horizon, that allows representing the variability of a given function through coefficients at a specified time and scale.

The digitized information resulting from the exploration is extensive, and it is necessary to extract characteristics from them that allow determining the health of the structure. The current work includes the use and development of multivariate analysis techniques, such as linear principal component analysis (PCA) and non-linear PCA. It is necessary to highlight that PCA is not invariant to scale, so the data under study must be normalized.

The methodology also implies applying data-driven algorithms for SHM; this means the process is not oriented by mathematical models but by data analysis.

All machines explored they are part of a group of supervised learning. For this type of machine, the data input and data target are necessary; the knowledge will obtain training the machine using both types of information; the result can be a classification or a regression.

In general, the work uses the classification model, but the regression model took part in the location methodology in which the output was continuous, indicating the distance at which the damage was and neural networks and trees, showing both good behavior.

Different types of classification machines were used, such as Trees, close neighbors, vector support machines, and classifiers assembled in each of them; it was deepened by varying parameters searching for the best performance machine.

In the trees, the branching complexity was varied, in the K-Nearest Neighbor, the distance equation, and the number of neighbors, in the vector support machines, the representation kernel. Finally, the original data set was subdivided into groups and used various trees in the ensemble machines.

5.4 Structural damage detection, classification and localization

The original proposal of Rytter established four levels for identifying damage in structures; the first is the detection, the second the location, the third that classification, and the last determination of severity. The current work focuses on the first three, offering essential information for structural health monitoring.

The SHM methodology includes the use of a piezoelectric sensor network to excite the structure and collect the measured dynamic response in several actuation phases, folowing to data organization and using a tool of multivariate analysis like principal components analisys to define the feature vectors to training the machines.

Using machine learning algorithms, the different models extract the relation between inputs and outputs to solve the problem and give the user's answers about health conditions. However, it is crucial to do training with the most relevant information possible. The current work focusses on PSA to build the characterization vectors to training the machines. If the data without the extraction process training the machines, the search algorithm has a vast search space, and it is possible that a solution will not be found or at least not one of good behavior and that meets the expectations that the user has.

Were tested different types of machines, not all of them offered the same behavior, the types KNN and assembled classifiers standing for its good behavior, and machines like trees and support vector have in general less performance.

5.5 Temperature considerations

Since the structures are subject to temperature changes by the direct action of the environment, determining the methodologies' behavior to these conditions is very important because, in real conditions, it is impossible to prevent these changes.

Temperature changes affect the signals that propagate over the structures and the methodologies that use them for damages detection; These changes in the signals, induced for the temperature changes are present in metallic and composed structures. Therefore, it is necessary to fix these procedures to mitigate these effects not to generate errors.

To test the methodologies behavior to the temperature changes, the pieces understudy were placed in a climatic chamber with temperature changes in steps of five Celcius degrees, verifying that the flexibility of the algorithms used in the current work.

According to the experimental results, the subspace k-NN and weighted k-NN algorithms have presented the most accurate results in aluminum and composite plate.

It is necessary training the classifiers with a significant quantity of examples since if the classifiers are not trained with the changes produced by temperature, the answers offered are erratic.

5.6 Further research

- Subdivide the sensors' information into groups depending on damage localization and training independent classifiers; the sensors closed to damages can better the behavior and converge faster. Also, it can be an alternative solution in the chase of high attenuation like composed materials.

- Using the methodology described in terms of forming the characterization vectors and the organization of data to carry out training of unsupervised learning machines can provide additional information on new strategies that provide greater accuracy or reducing the number of examples for training.

- Compare other learning techniques such as deep learning to verify if the learning segmentation process offers better behaviors in the trained machine and how it responds to situations such as damage to sensors or abrupt temperature changes can broaden the horizon of application of SHM techniques.

- Verify if the methodology is applicable in the last level of damage information, that is, indicate the severity of the same, in addition to being able to predict if the operability time of the structure would be interesting even more because of the implications it would have for issues such as maintenance and security.

- Replace in the methodology another type of multivariate processing such as the analysis of independent components with interest in comparing its behavior with the analysis of principal components used in this study and verifying how efficient the behavior of the algorithms is.

- Exploring the application of the algorithm for damage detection in rotating machines using ultrasound and vibrational analysis can have applications in industrial maintenance and much industrial equipment monitoring.

Appendix A

Complete list of publications

Contents

A.1 Journals

1. A sensor data fusion system based on k-nearest neighbor pattern classification for structural health monitoring applications Authors Jaime Vitola, Francesc Pozo, Diego Tibaduiza, Maribel Anaya, Publication date: 2017, Journal: Sensors MDPI, Volume: 17, Issue: 2, Pages 14 Publisher: Multidisciplinary Digital Publishing Institute.

2. Distributed piezoelectric sensor system for damage identification in structures subjected to temperature changes Authors Jaime Vitola, Francesc Pozo, Diego Tibaduiza, Maribel Anaya, Publication date: 2017, Journal: Sensors MDPI, Volume: 17, Issue: 6, Pages 18 Publisher: Multidisciplinary Digital Publishing Institute.

3. A damage classification approach for structural health monitoring using machine learning Authors Diego Tibaduiza, Miguel Ángel Torres-Arredondo, Jaime Vitola, Maribel Anaya, Francesc Pozo, Publication date: 2018, Journal: Complexity, Pages 18 Publisher: Hindawi.

A.2 Conferences

1. Damage Localization Methodology using Pattern Recognition and Machine Learning Approaches Authors: Maribel Anaya Vejar, Hernan Ceron, Jaime Vitola Oyaga, Diego Alexander Tibaduiza Burgos, Francesc Pozo Montero Publication date: 2017, Conference: IWSHM 2017: 11th International Workshop on Structural Health Monitoring: Stanford, California: September 12-14, 2017: proceedings book, Pages: 2042-2049.

2. Damage classification based on machine learning applications for an unmanned aerial vehicle Authors: Maribel Anaya Vejar, Hernan Ceron, Jaime Vitola Oyaga, Diego Alexander Tibaduiza Burgos, Francesc Pozo Montero Publication date: 2017, Conference: IWSHM 2017: 11th International Workshop on Structural Health Monitoring: Stanford, California: September 12-14, 2017: proceedings book, Pages: 2042-2049.

3. Non-linear damage classification based on machine learning and damage indices Authors: Diego Tibaduiza, Miguel Angel Torres, Jaime Vitola Oyaga, Maribel Anaya Vejar

and Francesc Pozo Montero Publication date: 2017, Conference: IWSHM 2017: 11th International Workshop on Structural Health Monitoring: Stanford, California: September 12-14, 2017: proceedings book, Pages: 2042-2049.

4. A machine learning methodology for structural damage classification in structural health monitoring Authors: Francesc Pozo Montero, Diego Alexander Tibaduiza Burgos, Maribel Anaya Vejar, Jaime Vitola Oyaga Publication date: 2017, Conference: SMART 2017: ECCOMAS Thematic Conference on Smart Structures and Materials: Madrid, Espanya: June 5-8, 2017: proceedings book. Pages: 698-708.

5. Structural Damage detection and classification based on Machine learning algorithms Authors: Jaime Vitola Oyaga, Diego Alexander Tibaduiza Burgos, Maribel Anaya Vejar, Francesc Pozo Montero Publication date: 2016, Conference: Proceedings of the 8th European Workshop on Structural Health Monitoring

A.3 Chapter book

1. Data-Driven Methodologies for Structural Damage Detection Based on Machine Learning Applications Authors: Jaime Vitola, Maribel Anaya Vejar, Diego Alexander Tibaduiza Burgos, Francesc Pozo Publication date: 2016/12/14, Book: Pattern Recognition-Analysis and Applications: Publisher: IntechOpen

multiplexor board-photograh I

Appendix B

Multiplexing system

Contents
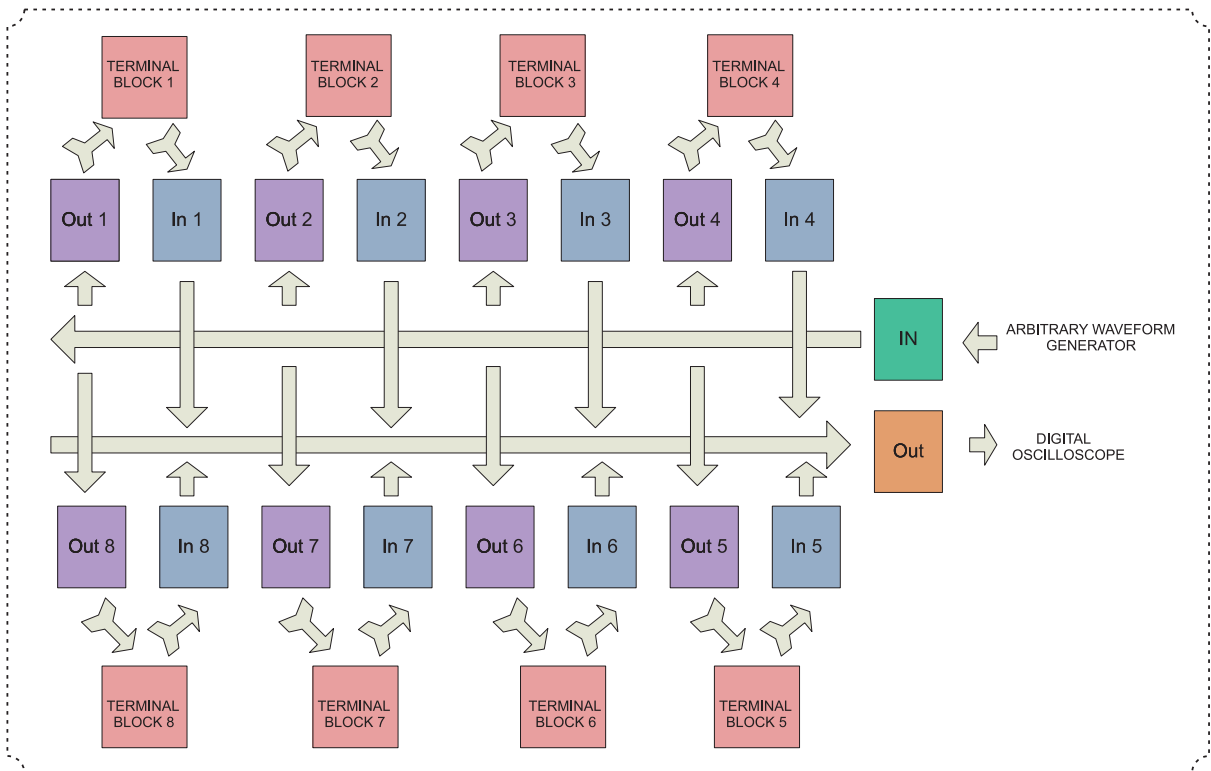
B.1   Multiplexing system block diagram

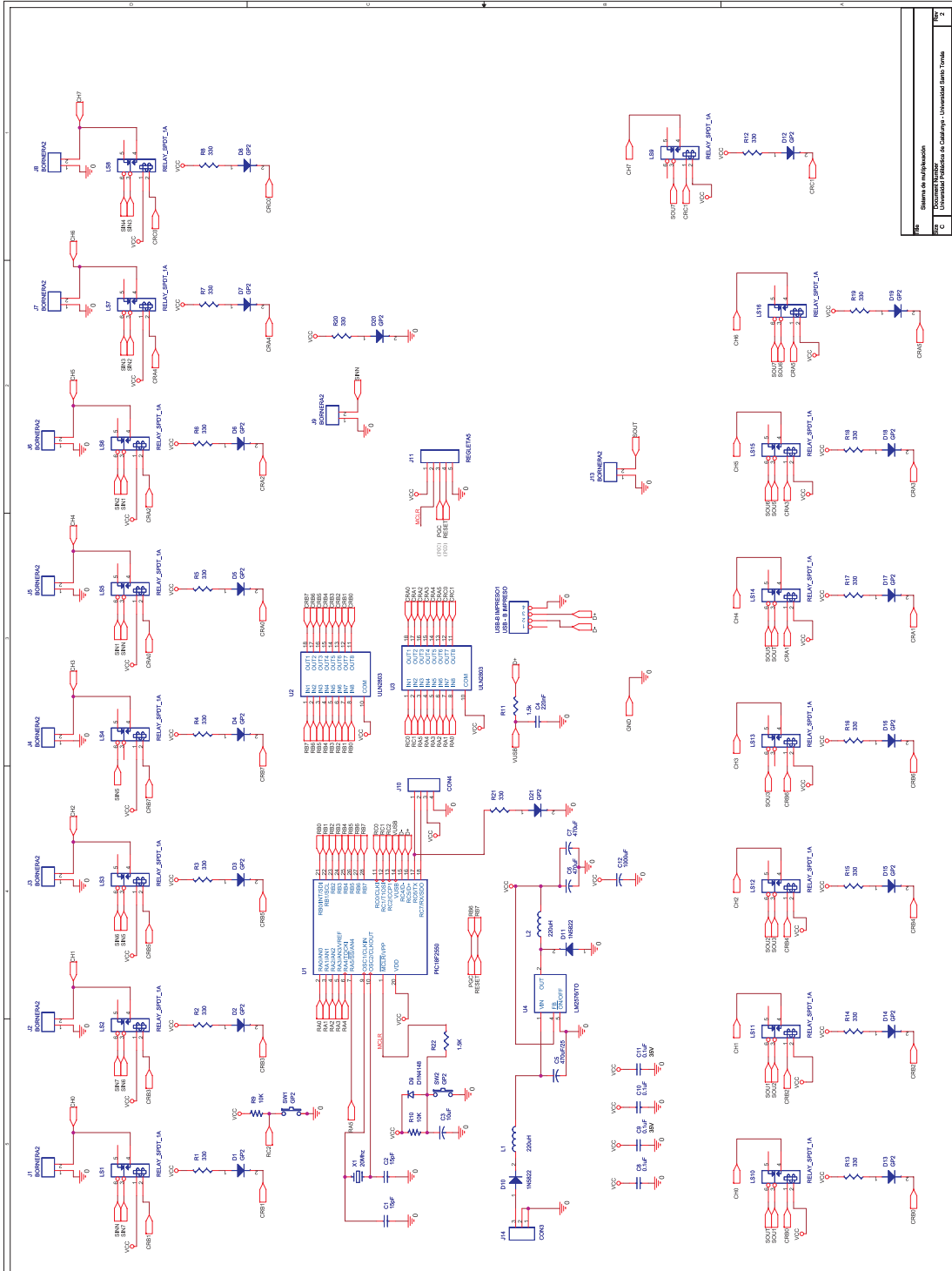FIGURE B.1: Multiplexing block diagram

B.2 Electronic scheme

FIGURE B.2: Schematic diagram

B.3   Multiplexor board photograph

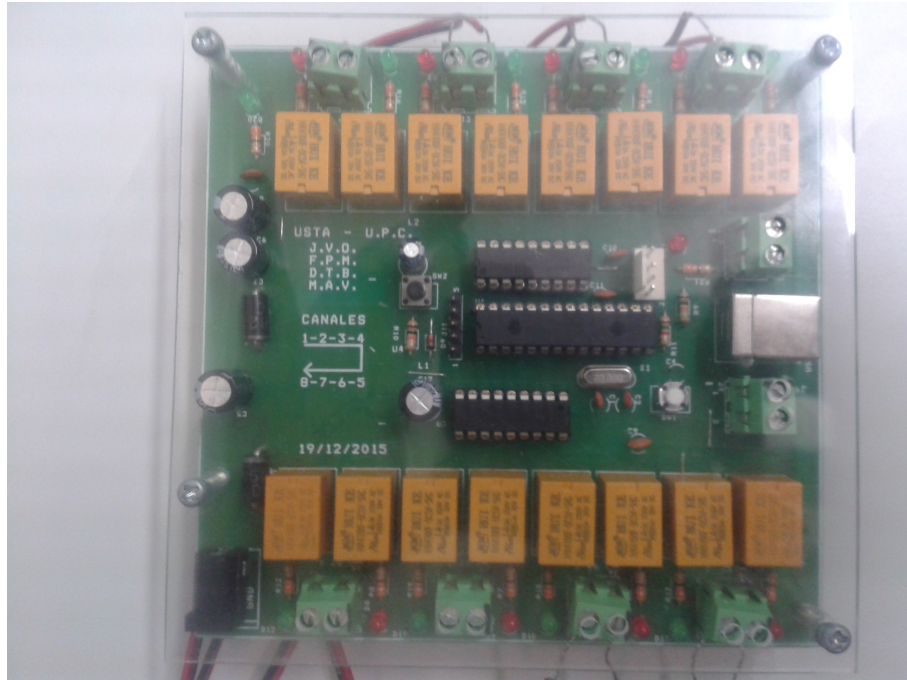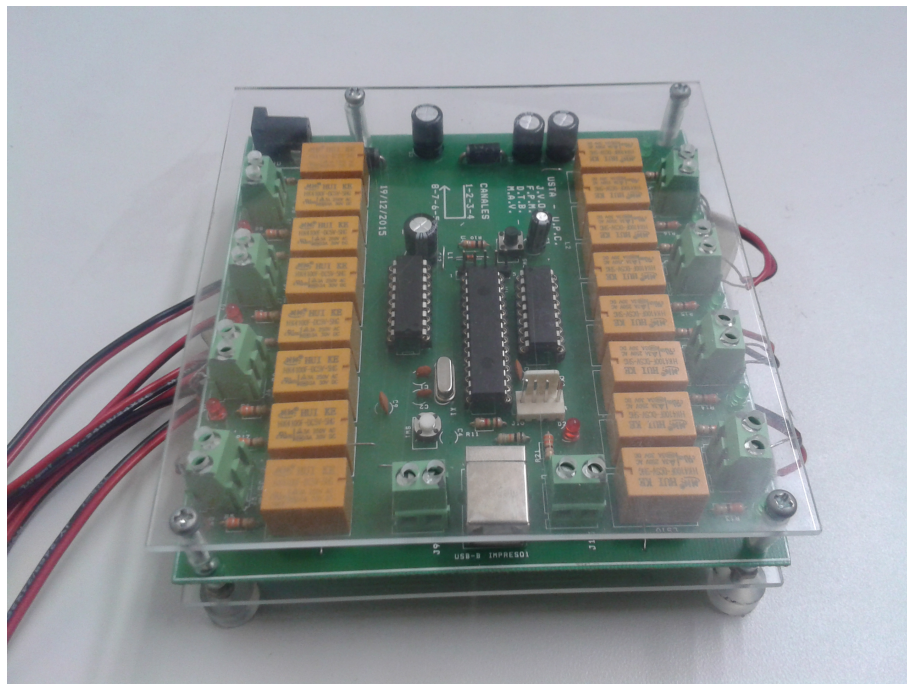

FIGURE B.3: Multiplexor board photograph I
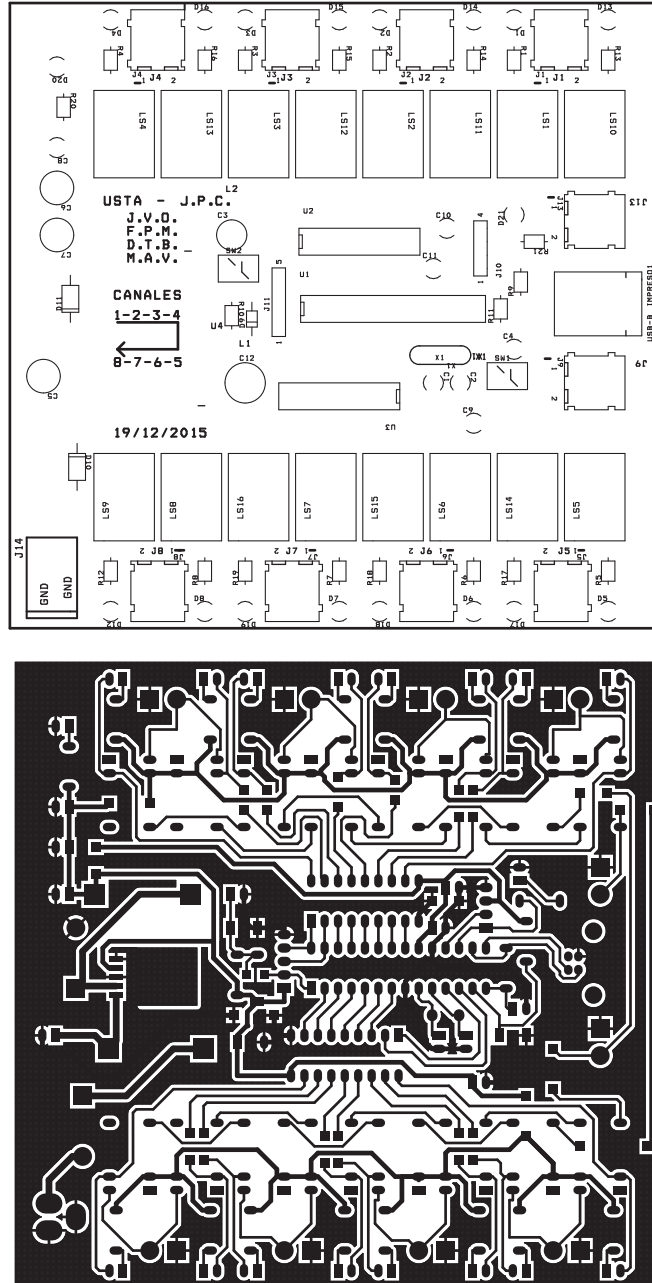

FIGURE B.4: Multiplexor board photograph II

B.4 Multiplexor printed circuit board

FIGURE B.5: Multiplexor printed circuit board